UNIVERSITÀ DEGLI STUDI DI MILANO

FACOLTÀ DI MEDICINA E CHIRURGIA

PhD Course in Translational Medicine

PhD Thesis

Novel strategies to implement extracorporeal life support techniques

PhD Tutors:
Prof. Antonio Pesenti
Prof. Giacomo Grasselli

PhD Coordinator:
Ch.ma Prof.ssa Chiarella Sforza

PhD Student:
Luigi Vivona
Matr.R12215

XXXIV Cycle

Academic year: 2020/2021

Index

Introduction

To understand the reason that made us implement the respiratory extracorporeal technique on which the present study is focused, it is necessary to describe the relevance of extracorporeal life support (ECLS) techniques and their differences when applied to the respiratory system.

The history of extracorporeal membrane oxygenation (ECMO) began in 1972 when Hill et al. described the use of this technique to support a post traumatic respiratory failure[1], but only with the H1N1 influenza A pandemic in 2009 the use of ECMO in clinical practice increased significantly[2]. In the same year, the CESAR trial by Peek et al. showed that, when ECMO was offered, patients had greater survival without disability and greater quality-adjusted life-years at 6 months[3]. Moreover, the EOLIA trial, the largest trial on ECMO to date, showed a clinically large reduction in mortality with ECMO[4]. Thus, ECMO represents a supporting treatment and a helpful bridge to allow natural organs to heal or to gain time while waiting for organ replacement with transplantation[5].

Extracorporeal techniques are the ultimate resources in critically ill patients with life threating respiratory or cardiac failure, maintaining tissue oxygenation for days to weeks by supporting the lungs, the heart, or both [6]. Due to ECLS different applications and configurations, in 2018 a position paper classified systems for ECLS nomenclature providing a standardized foundation for the description of ECLS application and decreasing ambiguity[7]. In this work, we will use the aforementioned classification, focusing on the two systems used to support patients with respiratory failure: extracorporeal membrane oxygenator (ECMO) and extracorporeal carbon dioxide removal ($ECCO_2R$) in veno-venous support mode.

ECMO and $ECCO_2R$

When mechanical ventilation is either unable to achieve sufficient gas exchange to meet metabolic demands or when it can only lead to injury, two modalities of ECLS can be used: extracorporeal membrane oxygenation (ECMO) and extracorporeal carbon dioxide removal ($ECCO_2R$). These two modalities of ECLS can substitute the gas exchange function of the native lung either entirely (ECMO) or only in part ($ECCO_2R$)[7]. When supplying the respiratory function only, both strategies require the cannulation of central veins. Deoxygenated blood is drained from a central vein, pumped through a hollow fibres gas exchanger, the “membrane lung” (ML), and then reinfused into a central vein. During veno-venous ECMO (VV-ECMO) the blood is fully oxygenated and decarboxylated. Fresh gas (sweep gas flow) flows through the fibres of the membrane lung, maintaining a favourable gradient for oxygenation and decarboxylation, while on the other side of the fibres the blood flows at a range between 3 and 7 L/min. To perform $ECCO_2R$, a lower blood flow is required, usually 0.5-1.5 L/min, allowing for the use of smaller vascular cannulas. Differently

from ECMO, $ECCO_2R$ cannot provide significant oxygenation, because of the relevant differences in CO_2 and oxygen kinetics

Physiology of ECMO and $ECCO_2R$

Oxygen

A healthy adult at rest has an oxygen consumption of about 250 mL/min (5–8 mL/kg/min). Oxygen consumption may vary according to the request of the mitochondrial activity. Oxygen is used in mitochondria to produce energy and carbon dioxide. This activity generates the partial pressure gradient that drives oxygen from the outer environment to the cells' mitochondria. The role of respiratory and cardiovascular systems is to provide oxygen to all organs and tissues[8]Partial pressure of inspired oxygen (pO_2insp) is determined by the inspired oxygen concentration (FiO_2) and the barometric pressure (pB). Oxygen partial pressure in the alveoli (pO_2alv) is lower, due to the added water vapour and the balance between oxygen removal by pulmonary capillaries and oxygen replacement by alveolar ventilation. Oxygen passes by a passive diffusion process from the alveolar gas into the blood, mainly into the erythrocytes. Oxygen solubility in plasma is minimal (coefficient of solubility = 0.003 mL/mmHg per 100 mL of blood), and haemoglobin plays a key role in raising blood oxygen exponentially. If fully saturated, haemoglobin binds 1.39 mL of oxygen per gram ($SatO_2$).

Oxygen content in the blood can be calculated as

$$O_2 content = (Hb * SatO_2 * 1.39) + (pO_2 * 0.0031)$$

Once the oxygen is loaded in the pulmonary capillary blood, the cardiac output (CO) is regulated so as to maintain a systemic oxygen delivery (DO_2) of four to five times the rate of consumption. Oxygen delivery is the arterial oxygen content times cardiac output, which is the oxygen delivered to the tissues each minute. DO_2 depends on cardiac output, haemoglobin concentration, haemoglobin saturation, and dissolved oxygen.

Haemoglobin releases oxygen in the peripheral capillaries. Following a pressure gradient, oxygen diffuses through the endothelium, the intracellular space, and the cellular membrane, reaching the mitochondria.

Capillary blood then flows into the venous district after having transferred oxygen to the tissues. The oxygen content in the venous district may be computed as

$$C_v O_2 = C_a\ O_2 - \left(\frac{VO_2 NL}{CO}\right)$$

Venous blood is then pumped into the pulmonary circulation by the right heart, and there it is loaded of an amount of oxygen which corresponds to that consumed by the tissues.

The most important cause of acute hypoxic respiratory failure is a ventilation (VA) / perfusion (Q) mismatch.

The lung can be imagined as divided in three functional units characterized by different VA/Q ratios according to the lung model developed by Riley [9]:

- An ideal lung, without any alteration of the natural coupling between ventilation and perfusion, having VA/Q ~ 1.
- The dead space, ventilated but not perfused, having VA/Q = ∞.
- An intrapulmonary shunt, perfused but not ventilated, having VA/Q = 0.

The blood flowing through pulmonary parenchyma with VA/Q = 0 does not participate in the gas exchange and is not oxygenated. Hence, part of the venous blood mixes with arterial oxygenated blood and determines hypoxemia. The shunt is usually characterized as the ratio (Qs/Qt) between the shunted blood (Qs) and the total pulmonary perfusion (Qt). If Qs/Qt is higher than 0.4, oxygenation provided by the native lung cannot sustain vital oxygen delivery. In these extreme clinical conditions, veno-venous ECMO (VV-ECMO) may prove to be the only clinical solution[10].

Oxygenation

When the respiratory system is not able to oxygenate the blood, a VV-ECMO may be employed.

A blood pump generates an extracorporeal blood flow (BF) by collecting part of the venous blood with its low oxygen content ($C_{in}O_2$) and directing it towards the ML. The ML loads the extracorporeal BF with oxygen (VO_2ML) and raises the oxygen content in the outlet blood ($C_{out}O_2$), as in the formula below:

$$VO_2ML = BF * (C_{out}O_2 - C_{in}O_2)$$

The blood returning to the right ventricle has mixed content of oxygen ($CvmixO_2$) deriving from the deoxygenated venous return and the well-oxygenated extracorporeal blood. The effect of VV-ECMO is the increase of oxygen content returning to the native lung. The venous content of oxygen may then be further increased to CaO_2 by the residual capacity in gas exchange of the natural lung (NL), this may be calculated as:

$$VO_2NL = CO * (C_aO_2 - C_{vmix}O_2)$$

The total oxygen (VO_2Tot) consumption of the patient is given by the sum of VO_2NL and VO_2ML.

Recirculation

In VV-ECMO the amount of oxygen entering the membrane lung ($BF * C_{in}O_2$) it is made up by two sources. The first one is given by the systemic venous blood from the tissues ($BF - Q_R) * C_{in}O_2$. The second one is constituted by recirculating blood flow, where Q_R is a variable amount of fully oxygenated blood recirculating ($Q_R * C_{out}O_2$), due to physical proximity of the two cannulas (a portion of blood ejected by the reinfusion cannula can be immediately re-drawn by the drainage cannula). Recirculation reduces the efficiency of the gas transfer by raising the oxygen content of the blood entering the membrane lung. The oxygen gradient across the membrane lung is thus reduced and the venous BF is given by BF – Q_R. Recirculation reduces the VO_2ML.

It is critical to detect and quantify the recirculation fraction (Q_R) to optimize VV-ECMO lung support[11]. The most commonly used method for quantifying recirculation is based on the computation of oxygen content in venous blood and blood drained by the ECMO (BF). If there is no recirculation, these two oxygen contents should be similar, while when recirculation occurs, the oxygen content of the ECMO inlet increases proportionally to the (Q_R). Unfortunately, under vv-ECMO, it is not possible to measure the real patient venous oxygen content. Therefore, an approximation is made with the theoretical venous oxygen content computed knowing the arterial oxygen content, total oxygen consumption, and cardiac output (CO)[12]. However, this calculation is inaccurate and may lead to a wrong estimation of the RF[13].

Carbon Dioxide

Carbon dioxide production is influenced by metabolic activity, core body temperature and caloric intake. It is the end product of aerobic metabolism and the production in an healthy man is 250 mL/min. Carbon dioxide generated in mitochondria leaves the cells and through the venous system and reaches the alveoli where it is released to the outer environment.

Carbon dioxide is carried in the venous blood in three different forms: dissolved, as bicarbonate ions (HCO_3^-), and in combination with proteins as carbamino compounds.

Dissolved form according to Henry's law

$$Dissolved\ CO_2 = pCO_2 * 0.03\ mmol/L * mmHg$$

Where 0.03 mmol/l*mmHg is the coefficient of solubility.

CO_2 dissolved in blood combines with water, forming carbonic acid (H_2CO_3), which in turn dissociates into hydrogen (H+) and bicarbonate ions (HCO_3^-). This reaction is catalysed by carbonic anhydrase (CA), an enzyme present within the red blood cell. Thanks to this enzyme, the conversion of CO_2 to H_2CO_3 requires less than 2 ms. As a result, most of the CO_2 is transported in blood as bicarbonate:

$$CO_2 + H_2O \leftrightarrow H_2CO_3 \leftrightarrow H^+ + HCO_3^-$$

Carbon dioxide also reacts with amino end groups of haemoglobin, forming carbaminic compounds. Haemoglobin plays an important role in the transport of CO_2, as deoxyhaemoglobin increases the amount of carbon dioxide carried in venous blood by acting as a proton recipient as follows

$$HbNH_2 + CO_2 \leftrightarrow HbNHCOOH$$

Carbon dioxide in pulmonary capillaries readily diffuses to the alveolar space. Due to the alveolar-capillary membrane efficiency, it is possible to consider pulmonary end-capillary blood (ven pCO_2) usually equal to alveolar partial pressure of carbon dioxide (alv pCO_2).

Alveolar ventilation removes the carbon dioxide constantly added to alveolar gas by venous circulation according to the formula:

$$alv\ pCO_2 = \frac{VCO_2NL}{Alveolar\ Ventilation}$$

Alveolar ventilation is the only fraction of inspired tidal volume that participates to the gas exchange calculates as follows

$$\text{Respiratory rate} * (\text{Tidal volume} - \text{Dead space})$$

Dead space may be distinguished in anatomical (the upper airways do not take part in gas exchange) and alveolar dead space (the non-perfused alveoli, where part of the inspired volume cannot take part in gas exchange as a consequence of ventilation/perfusion mismatching).

Carbon Dioxide Removal

Carbon dioxide transfer across the membrane lung (ML) is dependent on blood flow, sweep gas flow and pCO_2 gradient between the blood entering the ML and the sweep gas flow [14,15].

The CO_2 content of the venous blood is approximately 500 mL/L, while the O_2 content is 150 mL/L. Sweep gas flow (SGF) is equivalent to native lung minute ventilation and its rate is used to adjust extracorporeal CO_2 clearance.

Considering our system to be perfectly efficient, when working at BF of 500 ml/min, it is possible to remove 250 mL/min of CO_2 production ($\dot{V}CO_2$), while the O_2 uptake of the same blood volume is only 25 mL/min. This makes the respiratory quotient ($\dot{V}CO_2$/ $\dot{V}O_2$) of the ML highly variable and dependent upon the extracorporeal blood [16,17]. For this reason, ECMO BF can remove all the metabolically produced CO_2 and therefore maintain $PaCO_2$ within normal range guaranteeing an adequate oxygenation, while the same oxygenation result is not achieved during $ECCO_2R$.

The total amount of removed CO_2 ($\dot{V}CO_2Tot$) is the sum of $\dot{V}CO_2$ML and $\dot{V}CO_2$NL. Increasing the $\dot{V}CO_2$ML will reduce alveolar ventilation and $\dot{V}CO_2$NL.

It is possible to calculate the membrane lung $\dot{V}CO_2$ with two methods. The first is by using the difference between the total content of carbon dioxide (TCO_2) entering and exiting the membrane lung with the formula:

$$\dot{V}CO_2ML = (TCO_{2PRE} - TCO_{2POST}) * BF * 25.45$$

Where the BF is measured in L/min and the correction factor (25.45) is in mL/mmol

The second way to calculate membrane lung $\dot{V}CO_2$ is by measuring the concentration of CO_2 from the sweep gas outlet:

$$\dot{V}CO_2ML = pCO_2ML_{exp} * \left(\frac{7.5}{713}\right) * SGF * 1000$$

Using 7.5 mm Hg/kPa and 713 mm Hg (barometric pressure at the sea level minus vapour pressure) as correction factors and the SGF is measured in L/min.

Coagulation and Anticoagulation

Using an extracorporeal circuit, blood is exposed to multiple non-biological surfaces. When blood interacts with non-endothelial surfaces, there is a widespread inflammatory and prothrombotic response. Bennet et al. showed that, in patients on ECMO, platelets adhered to surface fibrinogen, causing platelet activation and aggregation, resulting in thrombocytopenia. Moreover, blood passing through non-biological surfaces leads to protein accumulation, upregulation of pro-inflammatory pathways and coagulation dysfunction[18]. Pro-coagulant stimuli and inflammatory response mediated by macrophages and cytokines increase tissue factor expression, causing platelets activation and thrombin generation[19,20]. Therefore, anticoagulation is crucial to prevent thrombosis and device failure [21].

The continuous administration of heparin is the mainstay of systemic anticoagulation during ECMO [22]. Heparin enhances the activity of antithrombin, resulting in downregulation of thrombin and Factor Xa. Heparin activity is correlated to two main risks: decreased antitrhombin concentration

within the extracorporeal device due to consumption, and binding to non-specific acute phase reactants causing apoptosis. Furthermore, antithrombin may interfere with biologic functions outside of coagulation, including pro- and anti-inflammatory pathways[23,24]

However, there is promising evidence that biocompatible circuitry or heparin-coated circuits may allow anticoagulant-free interventions in the future.

Heparin-coated circuits have been associated with reduced red blood cell trauma and decreased activation of complement and granulocytes[25,26] during cardiopulmonary bypass, but surface leaching of heparin from these circuits may limit this effect during ECMO.

Other kinds of extracorporeal circuits, such as continuous renal replacement therapy, have seen broader success with regional anticoagulation strategies by using citrate for circuit anticoagulation. Its successful use is due in part to the time course and the lower blood flow necessary those settings. Citrate chelates ionized calcium, which is necessary for the proper functioning of the coagulation cascade and for platelet aggregation. The effects of circuit-administered citrate remain largely local, due to the rapid physiologic metabolism of citrate to sodium bicarbonate[27]. Blood is generally recalcified as it exits the device; however, small amounts of free citrate do enter the systemic circulation and can determine symptomatic hypocalcemia. To mitigate these risks, some centers prophylactically administer oral or parenteral calcium to patients. Intravenous calcium may be more effective in the prevention of hypocalcaemia, even though its use may lead to vasodilation, cardiac arrhythmias, and hemodynamic instability[28]. Citrate is metabolized by the liver metabolizes and its elimination can lead to metabolic alkalosis, which limits the use of citrate to blood flows higher than 200 mL/min.

The engineering of the various extracorporeal circulation devices makes anticoagulation a critical factor in the prevention of pathologic thrombosis. However, anticoagulant agents are not solely benign, and their individual risk-benefit profiles must be taken into consideration. Close monitoring of coagulation status is therefore necessary to avoid both thrombosis and bleedings. Despite the ubiquitous use of extracorporeal devices and the above-mentioned risks associated with anticoagulation, there is a scarcity of evidence with respect to type of anticoagulant agent, dose, route of administration, and monitoring scheme across all devices. While there have been several small studies attempting to evaluate the safety and efficacy of various strategies, institutions around the world still use independently developed approaches, as evidence-based guidelines are lacking[29].

Aims that will be discussed

Starting from the main issues described in the chapter "Physiology of ECMO an $ECCO_2R$", we focused our interest on novel strategies to implement this technology in order to guarantee safer and more efficient extracorporeal techniques.

The works that will be presented in the following four chapters are the result of in vivo and in vitro experiments performed in the last three years of activity.

1 We point our attention to a novel regional anticoagulation strategy to reduce the risks of systemic anticoagulation using a system of ion exchange resins reaching an extracorporeal blood flow of 500ml/min.
2 Using a thermo dilution technique, we have been able to quantify recirculation flow, a phenomenon that must not be underestimated during extracorporeal setting in the veno-venous configuration.
3 Sodium hydroxide solution has been tested in an in-vitro experimental setting as an alternative medium to fresh gas flow to clear CO_2 in a membrane lung.
4 The last experiment of this period of activity underlines the relevance of haematocrit during extracorporeal CO_2 removal; we set up a closed loop in-vitro extracorporeal system where we measured the $\dot{V}CO_2$ according to different haematocrit concentrations.

A novel technique for regional anticoagulation in Extracorporeal life support: Ion Exchange Resins increase citrate removal and allow high blood flow.

Background

As described in the paragraph *Coagulation and Anticoagulation,* one of the main challenges of extracorporeal circulation is to reach an adequate anticoagulation setting. A recent study published on JAMA [30], which aimed at evaluating 90-day mortality in patients treated with ventilation + $ECCO_2R$ versus ventilation alone, had to be stopped by the ethical committee. Data monitoring highlighted severe adverse events, mainly haemorrhagic in nature, in the $ECCO_2R$ group. Citrate regional anticoagulation is the most widespread alternative to systemic anticoagulation[31]. Sodium citrate is able to chelate calcium, causing an interruption in the clotting cascade at the levels of thrombin generation[32] and platelet activation[33]. The limitation of this technique is the scant clearance of citrate, which requires flows within 200 ml/min. With the current technology, the use of citrate at higher blood flows would lead to risks of inadequate anticoagulation[34] or systemic complications[35].

In 2016, our group presented a novel technique based on ion exchange resins (i-ERs)[36]. Resins are insoluble polymers with acid or basic functional groups that are able to exchange cations or anions in aqueous solutions. The results of our previous study showed that the i-ERA system could be used as a regional anticoagulation strategy, as it allowed to reduce the calcium concentration in the extracorporeal circulation without infusing citrate.

The model used in 2016 had some limitations related to low blood flow, electrolyte balance (need to replace or remove molecules to maintain stability) and risk of clotting in the extracorporeal circuit upstream of the i-ERs. The current study is a proof of concept work aimed at showing the feasibility of regional anticoagulation in the whole extracorporeal circuit, avoiding the risk of excess electrolytes release by the resins by using a high blood flow (500mL/min).

Materials and methods

Animal preparation

This study was approved and conducted according to the Institutional Guidelines for the Care and Use of Laboratory Animals (Università degli Studi di Milano, Milan, Italy) under the supervision of a veterinarian, responsible for laboratory animal welfare. This study was performed using six healthy fasted female swines (41±3.4 Kg). After a 12-hour fasting period, the animals were sedated with an intramuscular injection of medetomidine (0.03 mg/kg) (Domitor, Orion corporation, Espoo, Finland) and tiletamine-zolazepam (4 mg/kg) (Zoletil, Virbac Srl, Milano, Italy). After catheterization of an

ear vein, anesthesia was induced with propofol (2 to 2.5 mg/kg) (Propofol, Fresenius Kabi, Verona, Italy), Tramadol (2mg/Kg) (Tramadolo Hexal AG, Hexal AG, Holzkirchen, Germany), and Pancuronium (0,1mg/Kg) (Pancuronium Inresa, Inresa Arzneimittel GmbH, Freiburg, Germany) to allow endotracheal intubation. Anesthesia was then maintained with a continuous infusion of propofol (6-8mg/Kg/h), medetomidine (0,025-0,05 mcg/kg/min) and pancuronium(0,3mg/Kg/h). Animals were mechanically ventilated (Servo 900C, Siemens-Elema AB, Sweden) with tidal volume at 10 mL/kg, inspiratory time to expiratory time ratio at 1:2, positive end-expiratory pressure at 5 cm H_2O and inspired oxygen fraction of 40%. Respiratory rate was kept fixed starting from a value $PaCO_2$ of 40 mmHg at baseline. After administration of antibiotic prophylaxis with cefazolin (2 g) (Cefazolina, Pfizer Italia Srl, Roma, Italy), a catheter (Seldicath 5 Fr, 8 cm, Prodimed, Le Plessis Bouchard, France) was surgically introduced into the right carotid artery for pressure monitoring and blood gas analyses. The right internal jugular vein was surgically cannulated (Triple-Lumen, 7 Fr, 20 cm, Arrow, Reading, PA, US) for drug infusion. Surgical cystostomy was carried out to introduce a 18Fr Foley catheter into the bladder of animals. Following a parenteral injection of 150 IU/kg of unfractionated heparin (UFH) (Sodium Heparin, Mayne Pharma, Napoli, Italy), the internal iliac vein and right external jugular vein were cannulated (18 Fr, N.G.C. Medical S.p.A., Novedrate (CO), Italy) and connected to a custom-made extracorporeal circuit optimized for i-ERA. A continuous infusion of UFH was provided targeting an activated clotting time (Hemocron, ITC, Edison, NJ) twice the baseline. Arterial pressure, electrocardiography, and core temperature were continuously monitored. Throughout the experiment, arterial ionized calcium (iCa) and ionized potassium were kept within the physiological range of 1.2 - 1.3 mmol/L and 3.5-4.5 mml/L by a parenteral infusion of calcium-chloride 1,36 mEq/ml (Calcio Cloruro Bioindustria L.I.M., Bioindustria L.I.M., Novi Ligure (AL), Italy) and potassium-chloride 2 mEq/mL (Potassio Cloruro, Fresenius Kabi Italia S.r.l., Isola della Scala (VR) Italy). At the end of the experiment, animals were euthanized, while still under deep sedation, with an injection of 40 mEq of potassium chloride. Throughout the whole experiment, Ringer's lactate was infused at 3 mL/kg/h.

Exchange Resin Processing

The resins used in our study are high-capacity mixed bed ion exchange resins consisting of a mixture of a strong base anionioic resin (60%) and a strong acid cationic resin (40%) (PMB 101-3 Pure Resin HSEDA Shangyu, Zhejiang, China). The treatment process started with the separation of the anionic component from the cationic one using a solution of NaCl 9%, whcih according to the different density allows d the separation of the two resins. The anionic resins were divided in half and charged with Cl^- or with HCO_3^-. The charging process of the anionic resin with Cl^- started with 10 litres of NaCl 9% solution, which was then rinsed with 10 litres of distilled water and finally with 10

litres of Bicarbonate Buffered Haemofiltration Solution 4mmol/L potassium (MultiBic, Fresenius Medical Care, Bad Homburg, Germany). The other half of the anionic resins were charged with HCO_3^- using 20 litres of $NaHCO_3$ 1M solution, and then rinsed with 10 litres of distilled water and finally with 10 litres of $NaHCO_3$ 140mM solution.

The cationic one were divided in half to be charged as well. One half was charged with Na^+ and K^+ using 10 litres of Na^+ 1.4M, K^+ 0.04M and Cl^- 1.44M, and then rinsing with 10 litres of distilled water and finally with 5 litres of Bicarbonate Buffered Haemofiltration Solution 4mmol/L potassium (MultiBic, Fresenius Medical Care, Bad Homburg, Germany). The other part was charged with H^+ using 10 litres of HCl 0.8M, and then rinsed with 10 litres of distilled water and finally with 5 litres of 0.1 M HCl solution.

Extracorporeal circuit

A scheme of the extracorporeal circuit is shown in Figure 1. The circuit was composed by a blood circuit and an hemodiafiltrate circuit. Blood was drained from the internal iliac vein with a peristaltic pump (Multiflow Roller Pump Module H10 series, Stöckert Shiley, München, Germany) called blood pump, and a withdrawal port was arranged in the blood circuit at the beginning of the extracorporeal circulation (P0). Through a second peristaltic pump (Volumat MC Agila I, Fresenius Kabi, Le Grand Chemin, France) a solution of Sodium Citrate (Sodium Citrate 4%, Fresenius Kabi AG, Bad Homburg, Germany) was continuously infused to obtain a final concentration of 5 mmol/L. A second withdrawal port was arranged after the point of infusion of Sodium Citrate (P1). From there, the blood flowed through two hemodiafilters (FX800, Fresenius Medical Care, Bad Homburg, Germany) and was then reinfused into the external jugular vein. The two hemodiafilters were connected in series and the pressure pre and post filter were continuously monitored. A third withdrawal port was arranged at the end of the circuit before the reinfusion in the jugular vein (P9).

In the hemodiafiltrate circuit, the outlet and inlet ports of the hemodiafilters were connected to create a closed-loop circuit. By means of a peristaltic pump (Multiflow Roller Pump Module H10 series, Stöckert Shiley, München, Germany), called hemodiafiltrate pump, the hemodiafiltrate was directed through the resins, which were set in series in three cartridges (FCR 35, Nobel, Segrate, Italy), two containing anionic i-ER charged with Cl^- and one containing cationic i-ER charged with Na^+ and K^+.

Upstream of the i-ERs, a portion of the hemodiafiltrate (waste flow) was diverted and discarded by a peristaltic pump (Volumat MC Agila I, Fresenius Kabi, Le Grand Chemin, France), called waste pump. The waste flow was necessary to balance the continuous infusion of citrate.

The flow of hemodiafiltrate was then split in three parallel branches, one main branch and two minor ones, drained by two peristaltic pumps (PD 5206 Pump Drive, Heidolph Instruments GmbH and Co, Schwabach, Germany). The flow of each minor branch was directed through a cartridge (FCR 35, Nobel, Segrate, Italy) containing anionic i-ER charged with HCO_3^- on one side, and with H^+ on the other.

After the passage through the cartridges, the flows of two minor branches were reuinited to allow for the release of CO_2 before reunification to the main branch. Upstream of the inlet port of the hemodiafilter, the hemodiafiltrate went through a hollow-fiber oxygenator (Quadrox-iD Adult, Maquet Cardiopulmunary GmbH, Rastatt, Germany) to be oxygenated with a constant flow of 10L/min and warmed to a temperature of 38° C.

A withdrawal port was arranged in the hemodiafiltrate side of the extracorporeal circuit, downstream every i-ER cartridge series. Two other withdrawal ports were arranged pre- and post-the oxygenator.

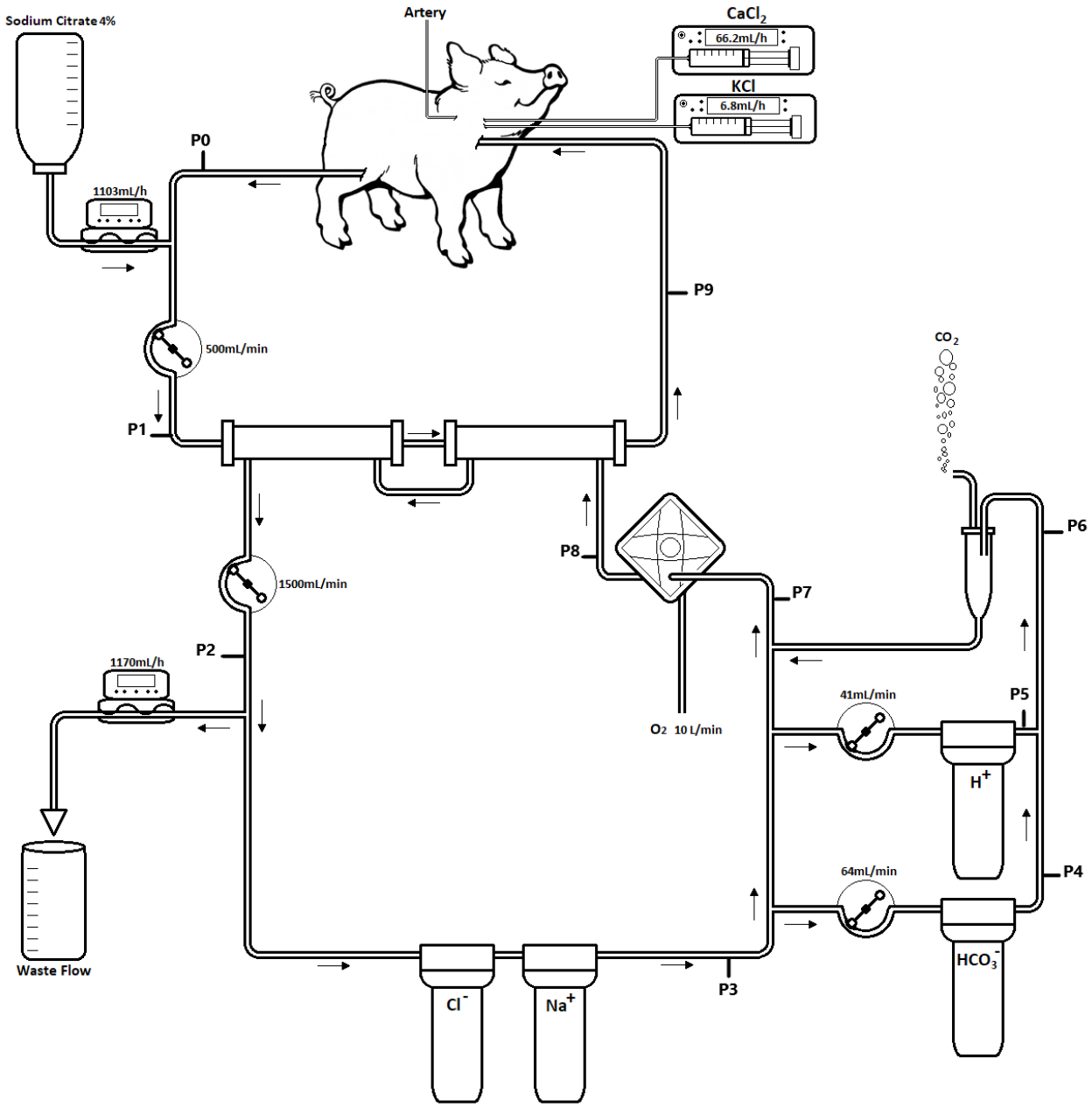

Figure1: Schematic representation of the circuit: Ions reported on the cartridge are exchanged during the dialysate passage; P are the withdrawal ports with the numeration as described in the text.

Ionic exchange along the circuit

As described above, two cationic i-ERs and two anionic i-ERs were present in the extracorporeal hemodiafiltrate circuit. A solution of Sodium Citrate was infused in the extracorporeal blood flow to avoid clotting. Citrate and ions passed through the two hemodiafilters FX800 at a blood flow of 500 mL/min with a dialysate flow of 1500mL/min. A first series of anionic and cationic i-ERs charged with Cl^- and Na^+ was placed in the extracorporeal hemodiafiltrate circuit. When the solution containing calcium citrate passed through the anionic i-ER charged with chloride, Cl^- was released by the i-ER in exchange for Citrate and Calcium crossed the cationic i-ER and was exchanged with

sodium. The salty solution obtained from the release of Na^+ and Cl^- needed to be treated/balanced before returning in the hemodiafilter, to remove the excess chloride and sodium coming from our treatment. The two collateral branches of our circuit played this role, a part of the solution was pumped through an anionic i-ER charged with HCO_3^- in order to exchange Chloride with HCO_3^-, the other part flowed through a cationic i-ER charged with H^+ exchanging Na^+ for H^+. When the two secondary branches reunified a high concentration of H^+ met HCO_3^-, producing H_2O and CO_2. Two collateral branches were necessary to balance the solution in order to obtain a final physiological range. Electrolyte balance was achieved both with the i-ERs and thanks to the different speed of the peristaltic pumps (Figure 1).

Experimental design and measurements

After animal preparation, the efficacy of the four i-ERs was evaluated for 120 minutes during a continuous infusion of citrate. Blood flow (BF) was set at 500 mL/min and dialysis flow at 1500 mL/min. Hemodynamics (i.e. heart rate, arterial pressures, core temperature) and ventilatory parameters (i.e. minute ventilation, respiratory rate, tidal volume, peak pressure, plateau pressure) were recorded. Samples were collected as shown in Table 1. A nine-step protocol for sample collection was carried out, from baseline, when only the extracorporeal blood flow pump was running, to 120 minutes of regional anticoagulation at 500 mL/min. Samples were withdrawn from arterial and circuit ports for gas analyses and ions concentrations (ABL 800 gas analyzer; Radiometer, Copenhagen, Denmark), as well as total calcium and magnesium concentrations (ADVIA Chemistry, Siemens Healthcare Diagnostics Inc, Tarrytown, NY). Blood was sampled at arterial line, and downstream the hemodiafilter for Kaolin Heparinase-Thromboelastography (KH-TEG)(TEG 5000, Haemonetics Corporation, Braintree, MA, USA). The KH-TEG technique was used to evaluate coagulation independently from the level of systemic anticoagulation.

The following TEG parameters were studied: reaction time (R), kinetics time (K), α angle, maximum amplitude (MA), and clot elasticity (G). Samples with R>60 min were deemed not clotted, and thus the TEG tests were interrupted. In these cases, values of 60 min for R and K, and of 0 for α angle, MA and G were assigned arbitrarily.

Citrate quantification was obtained with a citrate assay kit (Citrate Assay Kit, Sigma Aldrich, St. Louis, MO, USA). The measurement of citrate was performed according to the timeline (Table1) on the venous blood inlet, up and downstream of citrate infusion, on the venous blood outlet and on the arterial blood. In the hemodiafiltrate, citrate was measured after passage through the i-ERs, and in the waste flow.

Finally, at the end of the study, arterial blood was sampled for complete blood count and to measure fibrinogen, total proteins, lactate dehydrogenase (ADVIA Chemistry, Siemens Healthcare Diagnostics Inc) and concentration of plasma-free haemoglobin by spectrophotometric analysis.

Timing	Baseline	T2	T8	T15	T30	T45	T60	T90	T120
Step	Step1	Step2	Step3	Step4	Step5	Step6	Step7	Step8	Step9
BGA									
Artery	✓	✓	✓	✓	✓	✓	✓	✓	✓
P0	-	✓	✓	✓	✓	✓	✓	✓	✓
P1	-	✓	✓	✓	✓	✓	✓	✓	✓
P2	-	✓	✓	✓	✓	✓	✓	✓	✓
P3	-	✓	✓	✓	✓	✓	✓	✓	✓
P4	-	-	-	-	-	-	-	-	-
P5	-	-	-	-	-	-	-	-	-
P6	-	✓	✓	✓	✓	✓	✓	✓	✓
P7	-	✓	✓	✓	✓	✓	✓	✓	✓
P8	-	✓	✓	✓	✓	✓	✓	✓	✓
P9	✓	✓	✓	✓	✓	✓	✓	✓	✓
Citrate									
Artery	✓	✓	✓	✓	✓	✓	✓	✓	✓
P1	✓	✓	✓	✓	✓	✓	✓	✓	✓
P3	-	✓	✓	✓	✓	✓	✓	✓	✓
P9	✓	✓	✓	✓	✓	✓	✓	✓	✓
TEG									
Artery	✓	✓	-	-	✓	-	✓	-	✓
P9	-	✓	-	-	✓	-	✓	-	✓

Table 1: Timeline for sample collection. BGA, blood gas analysis; P, withdrawal port according to Figure 1; TEG, Thromboelastography; T(n), time plus minutes according to the steps of the experiment.

Statistical analysis

Data are reported as mean and standard deviation (SD) or median and interquartile range (IQR), as appropriate. One-way ANOVA for repeated measures was used, post-hoc analyses were performed with Tukey corrections to compare values at different time points (steps). Statistical significance was defined as $p < 0.05$. Analysis was performed with JMP 14 Pro Statistical Software (SAS Institute, Inc., Cary, NC, USA) and SigmaPlot v.11.0 (Systat Software Inc, San Jose, CA, USA).

Results

The aims set in order to validate this new technique for regional anti-coagulation were three:

1. To achieve regional anticoagulation while keeping a high blood flow (BF 500 ml / min);

2. To evaluate and manage electrolyte imbalances in the blood portion of extracorporeal circuit;
3. To evaluate the systemic impact of the proposed treatment by keeping stable both hemodynamic parameters and acid-base balance in the animal.

Regional anticoagulation at high blood flow

To validate our objective, the main outcomes evaluated were: (1) the concentration of citrate in the circuit and in the arterial blood, (2), the concentration of ionized calcium along the circuit (3) the TEG-R value and (4) the efficiency of the ion exchange resins.

Evaluation of citrate in circuit and in the arterial blood

The application of the ion exchange resin resulted in a significant reduction of citrate during its passage through the blood circuit (Figure 2). The high values recorded in P1, the sampling point immediately downstream of citrate infusion, underwent a drastic reduction during the passage in the haemodiafilters, with a value < 3 mmol / L in P9 at 60 minutes. The level of citratemia in the artery was also significantly lower at 60 minutes. A subsequent increase in values was noted at the end of the experiment (120 minutes) in all sampling points, due to the exhaustion of the exchange power of the resins.

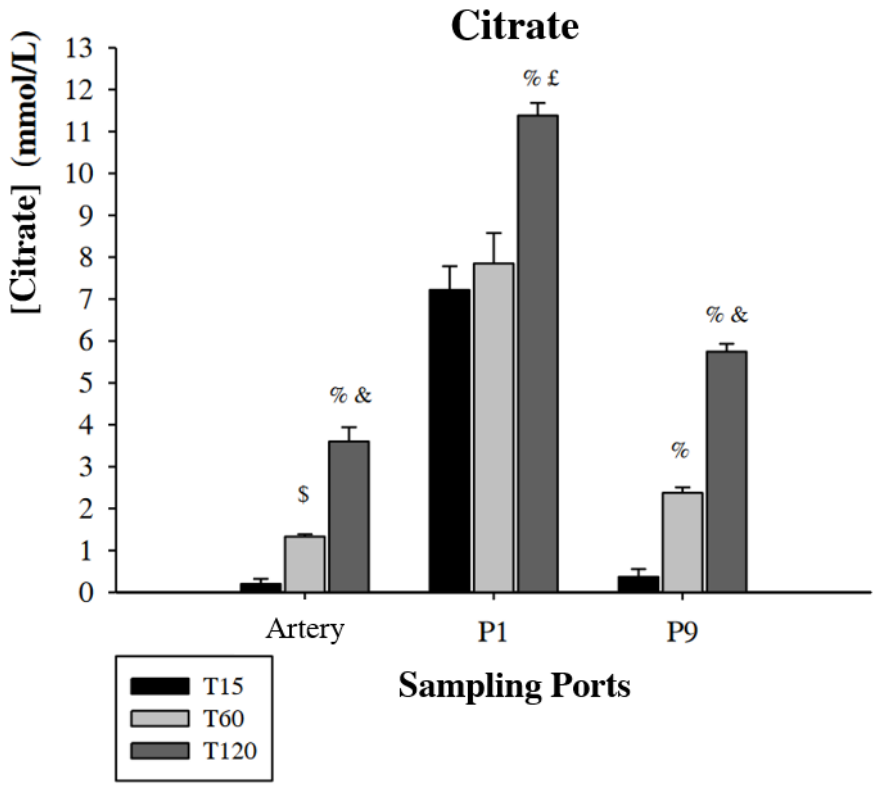

Figure 2: Trend of citrate (mmol/L) along the extracorporeal circuit over time (median and IQR). %) p < 0,0001 vs T15; &) p < 0,0001 vs T60; $) p < 0,05 vs T15; £) p < 0,05 vs T60

Figure 3 shows the detail of the arterial sampling timeline while considering arterial concentration of citrate only. The regional coagulation system proved effective and efficient in maintaining a citrate concentration <1 mmol/L for up to 45 minutes. Subsequently, citrate increased, until reaching maximum average (3.60 mmol/L) at T120. This variation is related to the exhaustion of ion exchange resins.

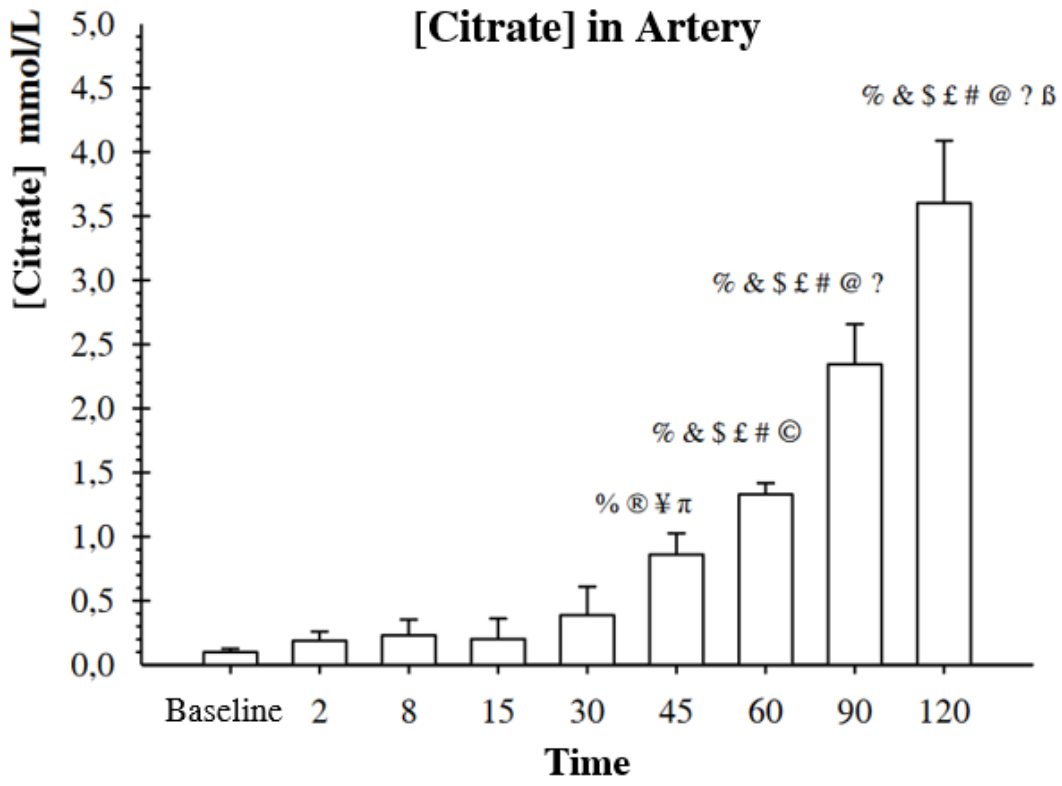

Figure 3: Trend of citrate (mmol/L) in artery over time (median and IQR). %) p < 0,0001 vs Baseline; &) p < 0,0001 vs T2; $) p <0,0001 vs T8; £) p < 0,0001 vs T15; #) p < 0,0001 vs T30; @) p < 0,0001 vs T45; ?) p < 0,0001 vs T60; ß) p < 0,0001 vs T90; ®) p<0,05 vs T2 ¥) p < 0,05 vs T8; π) p<0,05 vs T15; ©) p < 0,05 vs T45

Evaluation of ionized calcium and total calcium

The application of ion exchange resins resulted in a significant reduction of the Ionized Calcium (Ca^{++}) along the blood circuit, Figure 4.

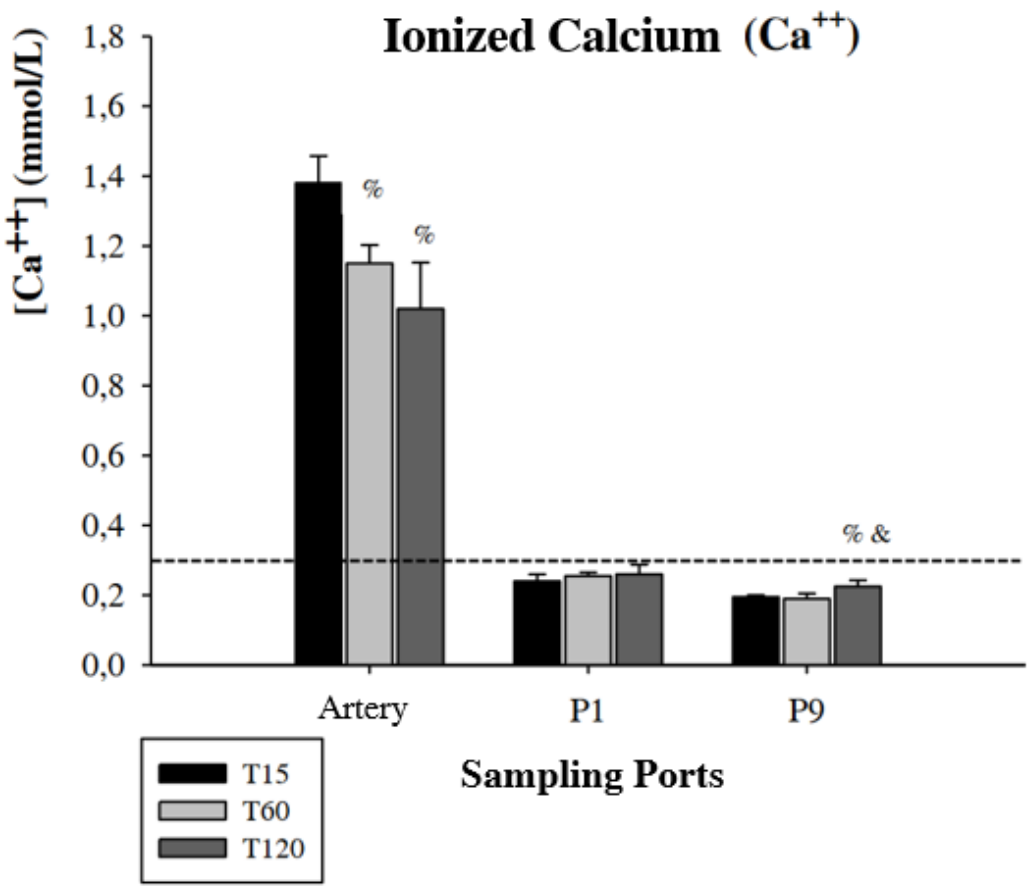

Figure 4: Trend of ionized calcium (mmol/L) along the extracorporeal circuit and in Artery over time (median and IQR). The black line shows the limit value of 0.3 mmol/L. %) p <0.05 vs T15; &) p <0.05 vs T60

The ionized calcium values refer to samples analyzed on a blood gas analyzer. The dotted line indicates the value of 0.3 mmol/L, the limit under which activation of the coagulation cascade with ionized calcium as a cofactor is avoided. Although there was a statistically significant increase (p-Value <0.05) observed in P9 between T15 - T120 and T60 - T120, the median value in P9 at the end of the treatment was 0.23 [0.22 - 0.24] mmol/L, therefore below the activation threshold. The graph also shows the value of Ionized Calcium in the Artery. Here, we observed a trend opposite to that found in withdrawal ports P1 and P9, with a statistically significant decrease in ionized Calcium (p-Value <0.05) between T15 - T60, T60 - T120 and T15 - T120. This is linked to the increase in serum citrate, which, as shown above, decreases the value of Ca^{++} by creating Citrate-Calcium complexes.

In addition to ionized calcium, the value of Total Calcium (Ca Tot) was measured in artery, at drainage point P0 and at reinfusion point P9 (Figure 5). The trend for total calcium (= free ionic form + component-linked; e.g. to albumin or, in this context, citrate) reflects the one of ionized calcium, with a significant increase between the analyzed points of the circuit. Over time, a statistically

significant increase is observed (p-Value <0.05) between T15 - T60, T15 - T120 and T60 - T120, at both withdrawal points.

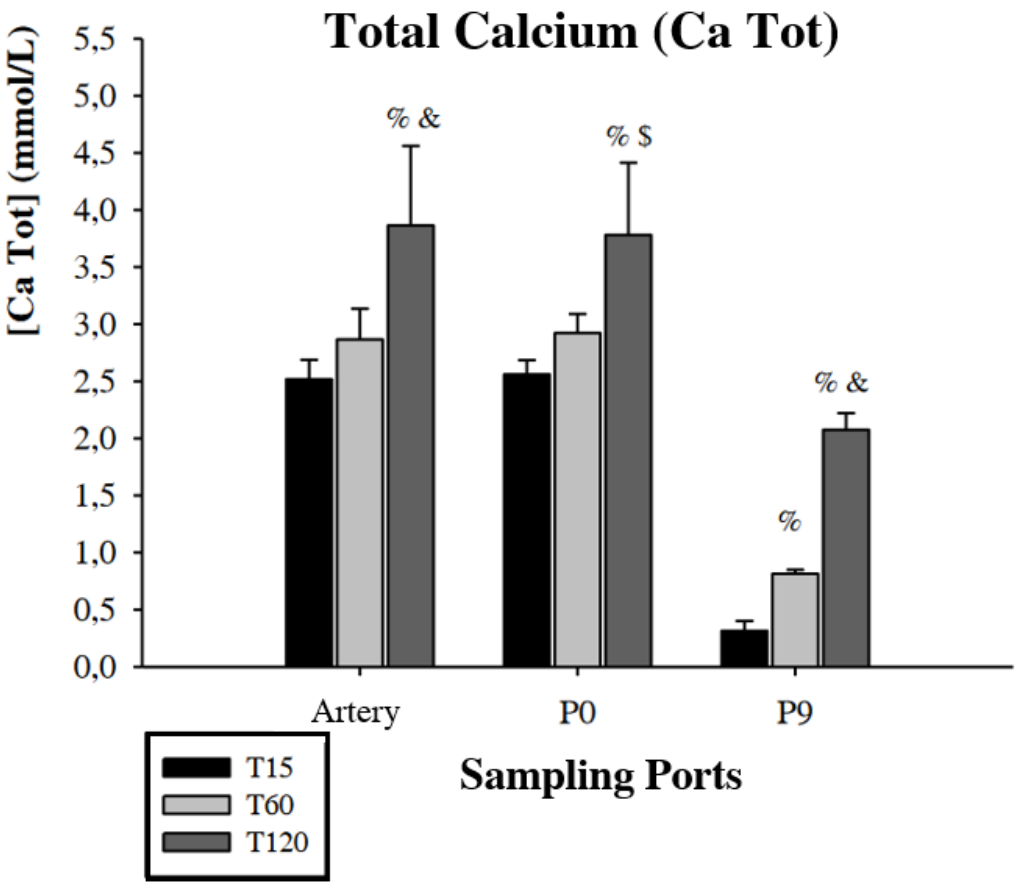

Figure 5: Total Calcium Trend (mmol/L) along the extracorporeal circuit and in Artery over time (median and IQR). %) p <0.0001 vs T15; &) p <0.0001 vs T60; $) p <0.05 vs T60

Ca Tot undergoes a constant increase in all the points examined throughout the duration of the experiment. In artery at T15 there is a median value of 2.44 mmol/L, within the normal range (2.12 - 2.62 mmol/L), while at the end of the treatment (T120) there is a value above the cut off of normality, reaching a value of 3.87 [3.78 - 4.56] mmol/L.

The ratio of Total Calcium and Ionized Calcium was thus calculated to understand this growing trend in the circuit. It is known that the CaTot/Ca^{++} ratio is an important parameter for estimating the accumulation of citrate above the acceptability threshold. A limit value of 2.5 is generally recognized as indicative of a significant accumulation of citrate, with an increase in total calcium compared to ionized calcium[37] (Figure 6). Of note, ionized calcium is the only form of biologically active calcium in the circuit.

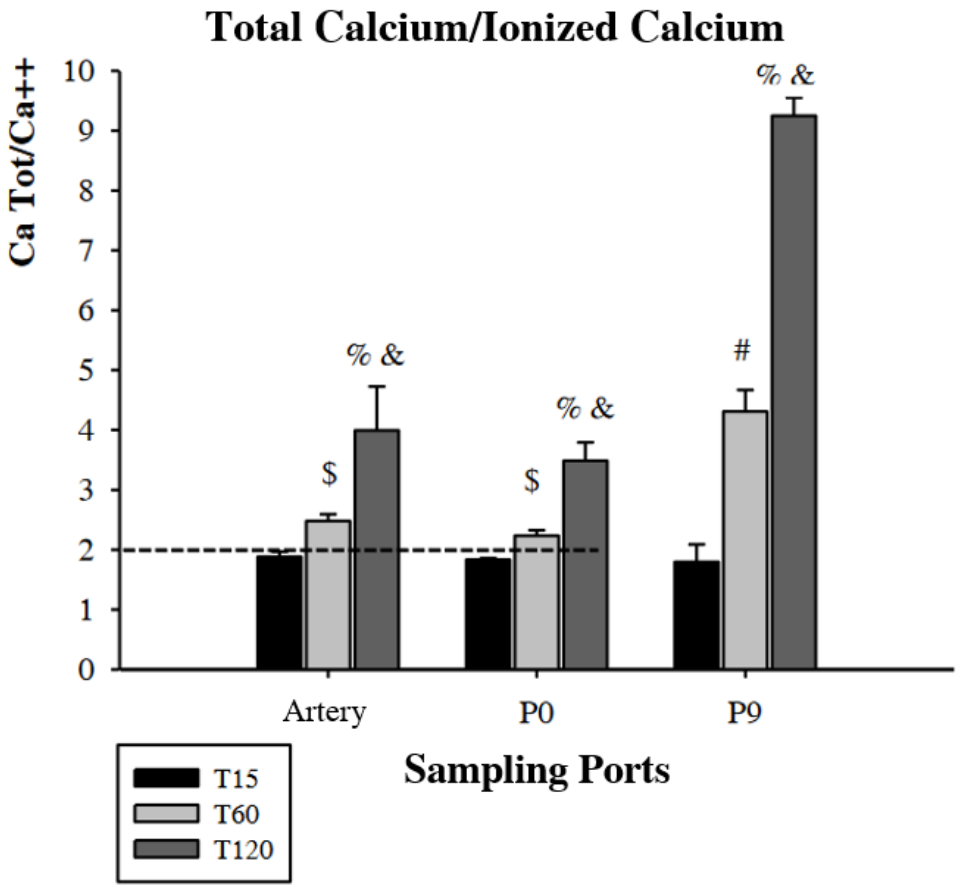

Figure 6: Trend of the Total Calcium/Ionized Calcium ratio along the extracorporeal circuit and in the Artery over time (median and IQR). The dotted line indicates the limit of 2 as the maximum clinically acceptable value. %) p <0.0001 vs T15; &) p <0.0001 vs T60; $) p <0.05 vs T15; #) p <0.0001 vs T15

Figure 6 shows that the CaTot/Ca^{++} ratio increased at all points in time. For what concerns the values calculated in Artery, the starting median ratio value in T15 was 1.88, arriving at 3.99 at T120. The ratio evaluated in P0 underwent the same increase, from 1.83 to 3.88. The greatest increase in the ratio between Total Calcium and Ionized Calcium was observed in P9, where it went from 1.80 at T15, to 4.31 at T60, and reached 9.25 at the end experiment at T120.

Thromboelastography (TEG) results

Thromboelastographic parameters (TEG) highlighted normal clotting in the arterial sample. During the whole experiment, the HK-TEG performed on samples collected in Artery (Table2) presented the following values: a mean reaction time (R) of 8.6 ± 1.3 minutes and a maximum amplitude (MA) of 72.2 ± 6.2 mm; while in the samples coming from the circuit (P9) no activation of coagulation was seen for the entire duration of the process. The main parameter to evaluate the activation of

coagulation was the value of TEG_R, the clot reaction time: this was shown to be constant in P9 at 60 minutes. The TEG examination was conducted with heparinase, in order to remove the confounding effect of UFH in continuous infusion, as described in "Materials and Methods", and was stopped at 60 minutes.

	Baseline	T2	T30	T60	T120	p-Value
TEG_R	9,1 [6,35 - 10,13]	11,95 [7,8 - 16,1]	8,9 [6,9 - 10,35]	8,2 [6,3 - 10,45]	8,1 [6,25 - 10,8]	0,9898
TEG_K	2,3 [1,55 - 3,25]	4,2 [1,8 - 6,6]	2,3 [1,95 - 3,3]	2,1 [1,7 - 3,7]	2,3 [1,55 - 3,4]	0,9449
TEG_alpha	64,8 [52,25 - 73,80]	50,65 [32 - 69,3]	61,4 [55,2 - 66,6]	65,8 [49,65 - 69]	62,4 [41,1 - 65,2]	0,6540
TEG_MA	73,4 [68,33 - 80,13]	66,25 [56,5 - 76]	71,7 [62,85 - 75,5]	69 [63,4 - 76,15]	72,1 [70,75 - 77,3]	0,4812
TEG_Ly30	1,5 [0,45 - 26,9]	0 [0 - 0]	0,4 [0,1 - 0,7]	0,2 [0,05 - 3,2]	1,7 [0,8 - 3,2]	0,6149
Platelets (10^3/uL)	316 ± 137,4	-	-	-	348,2 ± 141,18	0,7030
Fibrinogeno (mg/dL)	111 [92,5 - 135,5]	-	-	-	114 [107,5 - 149]	0,1899

Table 2: Values of TEG_R, TEG_K, TEG_ alpha, TEG_MA, TEG Ly30, Platelets (10^3/uL) and Fibrinogen (mg/dL) in Artery during the experiment. The data are reported as median [IQR] or mean ± SD when normally distributed.

Efficiency of Ion Exchange Resins

As stated in previous chapters, the removal of both citrate and calcium was allowed and achieved by the new extracorporeal circuit system with hemodiafilters and i-ERs. The resins favored greater efficiency and effectiveness of removal of ionic forms compared to normal hemodialysis, functioning as an "artificial liver" and permitting the reestablishment of ion concentrations in the hemodiafiltrate at the end of the circuit. However, the system suffered a loss of efficiency during the 120 minutes. This loss was highlighted by the high levels of serum citrate which were found. We thus calculated the efficiency of the resins. The calculation is based on the increase in citratemia and the difference between pre- and post-filter concentrations according to the formula:

$$\frac{([\text{Prefilter Citrate}] - [\text{Postfilter Citrate}])}{[\text{Prefilter Citrate}]} * 100$$

In figure 7, each line represents the efficiency of the resins for the six experiments performed. The resins proved to be very efficient and effective in removing citrate in the first steps. Effectiveness indicates the ability of the resins to achieve a set goal, which is to be able to remove ions through

ionic exchange. Efficiency, on the other hand, is the ability to fulfill the intended purpose in the best possible way, in the shortest time and with the maximum yield. From our assessments, both effectiveness and efficiency turned out to be very high in the first few minutes, with an average efficiency (represented by the small red line in the graph) of 92% at 2 minutes, and of 96% at 8 minutes, with the circuit at full speed. At 15 minutes, average efficiency was 93% and it slightly decreased at 30 minutes, reaching 88%. The true drop in efficiency was observed at 45 minutes, with an average efficiency of 77%, due to exhaustion of the resins. This datum further decreased from 70% at 60 minutes, to 58% at 90 minutes, and up to 48% at the end of the study (120 minutes) due the exhaustion of absorbent materials.

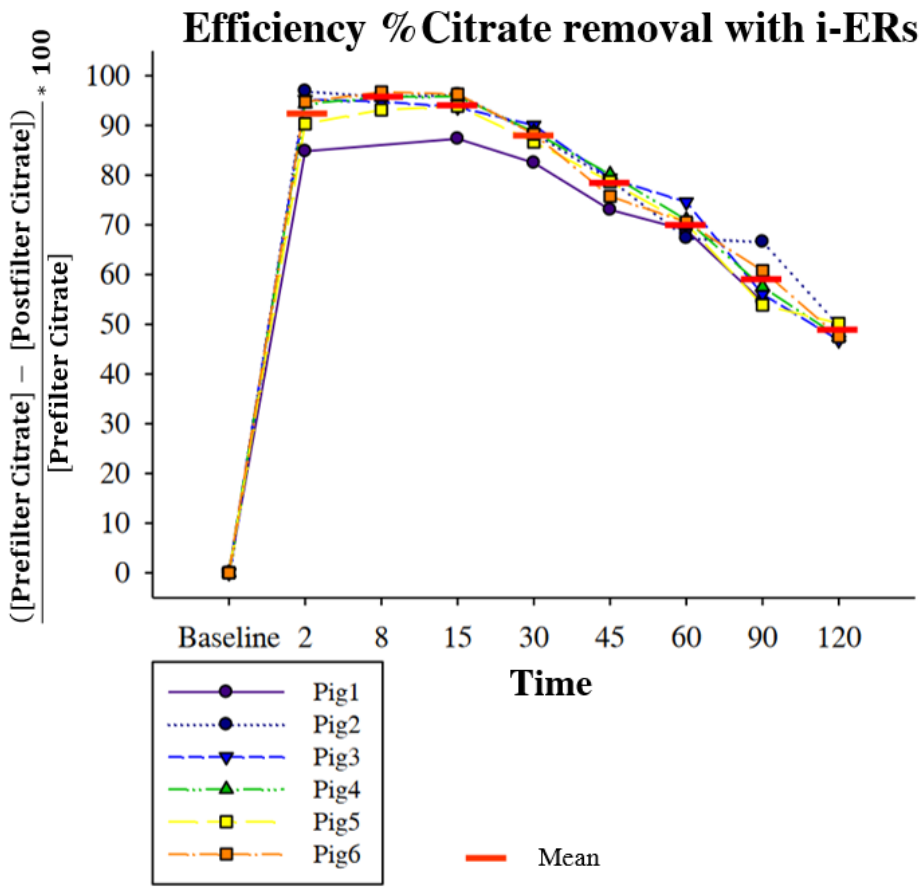

Figure 7: Comparison of the efficiency of ion exchange resins over time in the six pigs treated.

Evaluation of electrolyte variation in the blood portion of the extracorporeal circuit

Considering the overall effect of the application of ion exchange resins, the concentration of Potassium (K^+) decreased in the sample in P1 from 3.70 ± 0.32 mmol/L at T15, to 3.44 ± 0.40 mmol/L at T120 minutes, and this difference was statistically significant. Similar variations were identified

for the concentration of K^+ in P9, where average concentration was 3.55 ± 0.12 mmol/L at T15 and 3.27 ± 0.31 at T120. On the contrary, the potassium concentrations in P0 were found to be stable and within the normal range, without any statistically significant variations.

The cationic resins aimed at exchanging and removing Sodium, which was infused together with citrate as sodium citrate. Na^+ remained clinically in the range of normality in P0 and in P1 (135 - 145 mmol/L). A slight decrease in the values was recorded at the end of the treatment (T120 - step 9), at sampling port P9 the average concentration of Na^+ was 129 mmol/L, and this decrement was statistically significant.

A statistically significant progressive decrease was also recorded for Chloride along the extracorporeal circuit. At P0, the average starting value at T15 was 104.84 ± 4.83 mmol/L, while it dropped to 93.5 ± 6.41 mmol/L at T120. The trend in P1 was similar, with a T15 value of 97.84 ± 2.93 mmol/L, and one of 89 ± 7.67 mmol/L at 120 minutes L. The most significant decrease was at withdrawal port P9, where the average starting value at T15 of 103.84 ± 4.97 mmol/L dropped to 85.83 ± 8.66 mmol/L at the end of the experiment. To restore chloride concentration to normal range in the artery, an infusion of KCl and $CaCl_2$ was performed (see "Materials and methods") to avoid excessive ion imbalances for the animal.

Although the electrolytes evaluated with the blood gas analyzer were found within the clinical range, magnesium and phosphorus underwent an important decrease along the passage through the extracorporeal circuit. This may be attributable to the effect of the cation exchange resins, which unselectively removed these electrolytes as well. Further reasons for this decrease are the ability of the citrate to bind the ion Mg^{++} [38] and the lack of adequate correction of these electrolytes during the experiment. Over time, the observed values increase thanks to the loss of efficiency of our circuit, even if the Mg^{++} level is still lower than the normal range adjusted for the increase in citrate. The magnesium in P0 was constant, without significant variations. On the other hand, in P9, with the circuit highly performing at 15 minutes, there is a drastic impact on the magnesemia, with a value of 0.45 mg/dL. Eventually this increased to 0.96 mg/dL at 120 minutes due to the loss of ion exchange efficiency.

The same imbalance was also reported for phosphorus. At T15, in P0, this ion was relatively stable and recorded values were 3.34 ± 0.54 mg/dL. At T120 there was a statistically significant slight increase (5.34 ± 0.29 mg/dL), due to the reduction of the ion exchange capacity of the resins. On the other hand, we found phosphorus to be significantly reduced in P9.

The values of the blood gas analysis parameters collected at withdrawal ports P0, P1 and P9 along the blood circuit at different time points are reported in detail in the following tables (Table 3, 4, 5).

	Baseline	T15	T 30	T 60	T 120	p - Value
pH	7,40 ± 0,001	7,40 ± 0,07	7,43 ± 0,06	7,43 ± 0,05	7,46 ± 0,06 % &	0,0029
pCO_2 (mmHg)	50,1 ± 0,14	49,47 ± 13,06	47,23 ± 10,46	47,47 ± 9,68	45,37 ± 7,87	0,1940
pO_2 (mmHg)	41,55 ± 1,91	39,76 ± 2,36	37,01 ± 2,77 %	34,5 ± 4,20 % &	32,5 ± 4,06 ¥ $ @	<,0001
K^+ (mmol/L)	3,95 ± 0,35	3,94 ± 0,31	3,95 ± 0,40	3,95 ± 0,50	3,8 ± 0,48	0,0540
Na^{++} (mmol/L)	139,5 [136 – 143]	137 [135,8 – 138,2]	137,5 [136,3 - 140,8]	137,5 [135,8 - 141,2]	134 [132,5 - 136] % @ €	0,0088
Cl^- (mmol/L)	94 ± 5,65	104,84 ± 4,83 %	103,67 ± 4,59 %	99,34 ± 5,01 $ @	93,5 ± 6,41 % $ £ #	<,0001
HCO_3^- (mmol/L)	30,45 [30,4 – 30,5]	32 [27,20 - 32,25]	33,1 [29 - 33,5] %	33,45 [29,35 - 34,08] % &	35,05 [30,43 - 35, 73] ¥ $ @	<,0001
Lac (mmol/L)	2,05 ± 0,07	2,65 ± 0,53	2,38 ± 0,45 %	2,72 ± 0,60 %	2,87 ± 0,63 % @	0,0013
Glu (mg/dL)	137,5 [137 – 138]	128 [106 – 139,25]	129 [116,8 – 142,8]	126,5 [108 – 134,25]	123 [99,7 – 132,5] @	0,0091
BE (mmol/L)	5,8 [5,6 – 5,9]	7,4 [-1,75 - 8,2]	8,7 [0,35 - 9]	8,6 [1,3 - 9,4]	11,1 [1,55 - 11,7] % &	0,0014
Phosphorus (mg/dl)	-	6,3 ± 0,49	6,27 ± 0,54	6,25 ± 0,54	6,82 ± 0,45 & @ €	0,0004
Magnesium (mg/dl)	-	1,30 ± 0,07	1,20 ±0,09	1,23 ± 0,08	1,33 ± 0,09	0,0576

Table 3: Blood gas analysis values and electrolyte concentrations in P0 over time. The data are reported as median [IQR] or mean ± SD when normally distributed. Bicarbonate ion (HCO_3^-), base excess (BE), sodium (Na^{++}), chloride (Cl^-), potassium (K^+), ionized calcium (Ca^{++}), lactate (Lac), and glucose (Glu). %) p <0.05 vs Baseline; ¥) p <0.0001 vs Baseline; &) p <0.05 vs T15; $) p <0.0001 vs T15; @) p <0.05 vs T30; £) p <0.0001 vs T30; €) p <0.05 vs T60; #) p <0.0001 vs. T60

	Baseline	T 15	T 30	T 60	T120	p - Value
pH	-	7,37 ± 0,06	7,40 ± 0,05	7,41 ± 0,05 &	7,43 ± 0,06 &	0,0012
pCO_2 (mmHg)	-	49,52 ± 12,21	48,13 ± 10,3	47,38 ± 9,89	45,92 ± 9,25	0,0871
pO_2 (mmHg)	-	41,2 ± 3,57	37,44 ± 2,89 &	35,91 ± 4,22 &	32,51 ± 3,34 $ @ €	<,0001
K^+ (mmol/L)	-	3,7 ± 0,32	3,67 ± 0,33	3,65 ± 0,42	3,44 ± 0,40 & @ €	0,0106
Na^+ (mmol/L)	-	142,5 [140,7 – 145]	144 [142 - 147]	143 [141 – 145,8]	141 [139 - 141,2]	0,0570
Cl^- (mmol/L)	-	97,84 ± 2,93	99,17 ± 6,37	96,17 ± 5,49	89 ± 7,67 & $ €	<,0001
HCO_3^- (mmol/L)	-	29,9 [26,1 - 30,9]	31,5 [27,5 - 32,2]	32,2 [27,8 - 32,8] &	33,2 [28,9 - 33,7] &	0,0005
Lac (mmol/L)	-	2,45 ± 0,41	2,22 ± 0,38	2,5 ± 0,54	2,68 ± 0,63 @	0,0258
Glu (mg/dL)	-	116,5 ± 14,04	115,5 ± 15,10	121 ± 16,41	111,5 ± 14,31 €	0,0444
BE (mmol/L)	-	5,1 [-2,5 - 6,15]	6,4 [-0,7 - 7,4]	7,2 [0 - 8,1] %	8,6 [-0,1 - 10,05] %	0,0030
Phosphorus (mg/dl)	-	-	-	-	-	-
Magnesium (mg/dl)	-	-	-	-	-	-

Table 4: Blood gas analysis values and electrolyte concentrations in P1 over time. The data are reported as median [IQR] or mean ± SD when normally distributed. Bicarbonate ion (HCO_3^-), base excess (BE), sodium (Na^{++}), chloride (Cl^-), potassium (K^+), ionized calcium (Ca^{++}), lactate (Lac), and glucose (Glu). %) p <0.05 vs Baseline; ¥) p <0.0001 vs Baseline; &) p <0.05 vs T15; $) p <0.0001 vs T15; @) p <0.05 vs T30; £) p <0.0001 vs T30; €) p <0.05 vs T60; #) p <0.0001 vs. T60

	Baseline	T15	T 30	T 60	T 120	p – Value
pH	-	7,56 [7,38 - 7,60]	7,5 [7,54 – 7,60]	7,59 [7,55 – 7,61]	7,59 [7,53 – 7,63]	0,2710
pCO_2 (mmHg)	-	35,00 [31,90 - 64,35]	33,95 [33,1 - 37,55]	33,15 [31,55 - 35,75]	32 [30,80 –36,21]	0,3821
pO_2 (mmHg)	-	129,5 [71,1 - 170,75]	105,4 [65,85 - 140,2]	83,85 [66 - 156]	63,7 [54,1 - 108] &	0,0124
K^+ (mmol/L)	-	3,55 ± 0,12	3,42 ± 0,16	3,38 ± 0,26	3,27 ± 0,31&	0,0183
Na^+ (mmol/L)	-	140,50 ± 3,94	136,16 ± 2,04	135,17 ± 4,84 &	129,67 ± 1,97 $ @ €	<,0001
Cl^- (mmol/L)	-	103,34 ± 4,97	99,17 ± 4,26 &	94,17 ± 5,41 $ @	85,83 ± 8,66 $ £ #	<,0001
HCO_3^- (mmol/L)	-	32,9 [30,18 - 34,5]	33,2 [31,08 - 33,83]	32,65 [30,35 - 33,43]	33,3 [30,03 - 34,38]	0,9481
Lac (mmol/L)	-	1,77 ± 0,36	2 ± 0,35	2,15 ± 0,37 &	2,62 ± 0,63 $ @ €	<,0001
Glu (mg/dL)	-	92,34 ± 8,82	102,17 ± 12,58 &	113,5 ± 10,13 $ £	111,17 ± 13,53 $ £	<,0001
BE (mmol/L)	-	9,7 [2,35 - 9,8]	10,2 [6,2 - 10,55]	9,2 [6,5 - 10,3]	10,2 [5,00 - 11,45]	0,1470
Phosphorus (mg/dl)	-	3,34 ± 0,54	3,98 ± 0,46 $	4,75 ± 0,42 $ £	5,34 ± 0,29 $ £ €	<,0001
Magnesium (mg/dl)	-	0,45 [0,42 - 0,47]	0,56 [0,49 - 0,65] &	0,87 [0,79 – 0,97] $ £	0,96 [0,92 – 0,99] $ £ €	<,0001

Table 5: Blood gas values and electrolyte concentrations in P9 over time. The data are reported as median [IQR] or mean ± SD when normally distributed. Bicarbonate ion (HCO_3^-), base excess (BE), sodium (Na^{++}), chloride (Cl^-), potassium (K^+), ionized calcium (Ca^{++}), lactate (Lac), and glucose (Glu). %) p <0.05 vs Baseline; ¥) p <0.0001 vs Baseline; &) p <0.05 vs T15; $) p <0.0001 vs T15; @) p <0.05 vs T30; £) p <0.0001 vs T30; €) p <0.05 vs T60; #) p <0.0001 vs. T60

Assessment of the systemic impact of animal treatment

To ensure the safety on the animal of the regional anticoagulation treatment through the infusion of sodium citrate and its selective extracorporeal removal with ion exchange resins, hemodynamics and blood gas analysis have been evaluated.

Hemodynamic parameters

The hemodynamic parameters recorded did not undergo important changes and no pharmacological support was necessary. A slight drop in systolic pressure values was observed at the end of treatment together with a slight increase in temperature (Table 6)

	Baseline	**T15**	**T30**	**T60**	**T120**	**p-Value**
HR (bpm)	106 [95,5 - 123]	114,5 [82 - 125,25]	115 [80,5 - 128]	118,5 [90,25 - 127,5]	118,5 [103 - 124,5]	0,3187
SAP (mmHg)	108,5 [99,75 - 125]	100 [94 - 111,25]	91 [88,75 -102,25] %	93,5 [90,75 - 103]	92 [87 - 97,5] %	0,0127
DAP (mmHg)	70 [67,75 - 97,5]	72,5 [57,25 - 80]	59,5 [55,25 - 76]	63 [58 - 71,75]	60 [56,5 - 74,5]	0,0975
MAP (mmHg)	84 [83 - 99]	83 [67,5 - 90,9]	71 [66 -82]	75 [69 - 78]	71 [66 - 79,5]	0,1046
SpO_2 (%)	100 [100 - 100]	100 [100 - 100]	100 [99 - 100]	100 [99 - 100]	100 [99 - 100]	0,4307
T °C	36,8 ± 0,52	37,3 ± 0,67 %	37,4 ± 0,54 %	37,6 ± 0,52%	37,9 ± 0,31 & $ £	<,0001

Table 6: Trend of hemodynamic parameters throughout the treatment. The data are reported as median and [IQR] or mean ± SD if normally distributed. Heart rate (HR), Systolic arterial pressure (PAS), Diastolic arterial pressure (PAD), Mean arterial pressure (PAM), O_2 saturation (SpO2), Temperature (T ° C). %) p <0.05 vs Baseline; &) p <0.0001 vs Baseline; $) p <0.05 vs T15; £) p <0.05 vs T30

Analysis of blood and blood gas tests in animals

Blood samples from the arterial catheter were analyzed with a gas analyzer to evaluate how the extracorporeal system affected the electrolytes and hemo-components of the animals (Table 7). At the end of the treatment, the result was a mild increase in the pH: from a baseline value of 7.45 ± 0.03 mmol/L to 7.55 ± 0.04 mmol/L after 120 minutes. This event is hypothetically related to the presence of the citrate accumulated at 120 minutes, and linked to a decrease in pCO_2. A decrease

in sodium and chloride values was also observed over time, due to the loss of efficiency of the system and the lack of correction through systemic infusions.

At 120 minutes there was a statistically significant difference between the value recorded last (for Sodium, 132.67 ± 4.08 mmol/L; for Chloride 94.16 ± 8.61 mmol/L, below the minimum normal cut-off) and the values collected at 90 minutes. Potassium remained stable throughout the circuit and adequately within the normal range, thanks to the systemic infusion of KCl. On the contrary, Magnesium values decreased over time. This was due to two mechanisms: the increase of Citrate, which chelates magnesium in the ionic form, and the non selectivity for ions of cationic resins.

Therefore, Magnesium needed to be supplemented, but was not adequately corrected. Its final value was 1.28 (1.18-1.36) mg/dL. Phosphorus had a similar decrease in progressive values over time, resulting 6.45 mg/dL at T120. The blood gas values obtained from the arterial sample as oxygen partial pressure (pO_2), Hemoglobin (Hb), Oxygen saturation of hemoglobin ($O_2Hb\%$), Hematocrit (Hct), Bicarbonate ion (HCO_3^-), Glucose (Glu), Lactate (Lac) and Base Excess (BE) were found stable and in the clinical normal range and did not show any statistically significant difference throughout the treatment with extracorporeal circuit.

	Baseline	T15	T30	T60	T120	p - Value
pH	7,45 ± 0,03	7,48 ± 0,07	7,52 ± 0,03 %	7,54 ± 0,03 % &	7,55 ± 0,04 % &	<,0001
pCO_2 (mmHg)	39,6 [39,08 – 43,3]	38,6 [37,2 – 43,03]	38,2 [35,78 – 39,5]	37,35 [35,75 – 38,8]	36,0 [33 – 38,37] % &	0,0152
pO_2 (mmHg)	187,5 [158,7 – 207]	183 [149,7 –193,5]	179 [167,5 –184,7]	179 [163,2 -189,5]	171,5 [156,5 -180,5]	0,3966
Hb	8,45 [7,2 – 8,8]	8,15 [7,1 – 9,0]	8,05 [7,45 – 9,35]	7,65 [7,05 – 8,88]	8,2 [6,35 – 9,3]	0,6513
O_2Hb	97,73 ± 0,35	97,6 ± 0,51	97,56 ± 0,31	97,56 ± 0,30	97,8 ± 0,71	0,3659
Hct (%)	26,3 [22,58 – 27]	25,45 [22,01 – 27,9]	25,15 [23,22 – 29]	23,85 [22,03 – 27,5]	25,6 [19,83 – 28,9]	0,6478
K^+ (mmol/L)	3,91 ± 0,27	4,1 ± 0,26	3,98 ± 0,26	3,95 ± 0,22	3,85 ± 0,21	0,0911
Na^+ (mmol/L)	138,16 ± 2,63	137,67± 2,33	136 ,5 ± 2,07	135,34 ± 1,86	132,67 ± 4,08 % &	0,0041
Cl^- (mmol/L)	100,8 ± 4,79	104,3± 3,38	102,84 ± 2,79	98,67 ± 2,25	94,16 ± 8,61 & $	0,0029
HCO_3^- (mmol/L)	28,65 ± 1,75	29,15 ± 1,12	30,9 ± 1,62	31,6 ± 1,31%	31,3± 4,26	0,0113
Lac (mmol/L)	2,13 ± 0,65	2,23 ± 0,30	1,95 ± 0,43	2,18 ± 0,43	2,5 ± 0,64	0,2112
Glu (mg/dL)	132,5 [111,8 – 140]	122,5 [91,2 – 136,5]	130 [107,2– 134,8]	128,5 [106,5 – 136]	120 [104 – 130,5]	0,5200
BE (mmol/L)	4,9 ± 2,01	5,32 ± 1,98	7,2 ± 1,62	8,12 ± 1,52	7,78 ± 4,61	0,0278
Phosphorus (mg/dl)	7,95 [7,4 – 8,7]	5,45 [5,01 – 6,03] #	5,8 [5,08 – 6,12] #	6 [5,52 – 6,43] #	6,45 [6,12 – 6,7] # & $	<,0001
Mg (mg/dl)	1,67 [1,58 – 1,74]	1,07 [1,04 – 1,16] #	1,04 [1,01 – 1,10] #	1,11 [1,09 – 1,18] #	1,28 [1,18 – 1,36] # & $ £	<,0001

Table 7: Blood gas analysis and electrolyte concentrations in artery during treatment. Data are reported as median and [IQR] or mean ± SD if normally distributed. Bicarbonate ion ($HCO3^-$), Base Excess (BE), Oxygen saturation of hemoglobin (O2Hb%), Hemoglobin (Hb), Hematocrit (Hct), Chloride (Cl^-), Potassium (K^+), Ionized Calcium (Ca^{++}), Lactate (LAC) and Glucose (GLU). %) p <0.05 vs Baseline; #) p <0.0001 vs Baseline; &) p <0.05 vs T15; $) p <0.05 vs T30; £) p <0.05 vs T60

The experiment did not lead to hemolysis. Lactate dehydrogenase (LDH) values and plasma free hemoglobin (plasmatic Hb) did not have statistically significant changes. No major complications happened during the experiment, however a slight, statistically significant rise in aspartate aminotransferase (AST or GOT) was found, yet this was clinically acceptable as it was within the normal range (<40 IU/L), Table 8.

	Baseline	**T120**	**p-Value**
Albumin (g/dL)	2,38 ± 0,26	2,36 ± 0,25	0,8220
AST – GOT (UI/L)	22,4 ± 5,03	29,5 ± 5,32	0,0121 %
ALT – GPT (UI/L)	48,5 ± 11,91	49,0 ± 11,40	0,6756
Bilirubin (mg/dL)	0,09 [0,08 - 0,11]	0,13 [0,07 - 0,28]	0,1271
CPK (U/L)	698,8 ± 310,79	585,75 ± 248,98	0,2285
Creatinine (mg/dL)	0,73 ± 0,06	0,67 ± 0,09	0,0895
D-dimer (mcg/L)	351,2 ± 253,6	314,25 ± 123,25	0,3460
Free plasmatic Hb	5,31 ± 2,42	6,58 ± 2,25	0,4034
LDH	401 ± 50,58	405,8 ± 79,22	0,8126
Total Protein (g/dL)	4,89 ± 0,52	4,80 ± 0,46	0,5467
Urea (mg /dL)	8 ± 2,53	9,4 ± 2,07	0,0905

Table 8: Biochemical blood samples collected in artery at the beginning and at the end of the treatment. The data are reported as median [IQR] or mean ± SD if normally distributed.

Discussion

The described system represents an innovative method of regional anticoagulation in extracorporeal circuits, obtained with ion exchange resins. The application of this method in the animal model proved to be effective and feasible at an extracorporeal blood flow greater than the one commonly used with citrate (200 ml / min): the circuit was set and maintained at 500 ml / min. No major systemic and / or circuit complications were recorded in the swine model analyzed. As described in the *coagulation and anticoagulation* paragraph, any treatment that involves extracorporeal blood circulation requires anticoagulation since the contact of the blood with non-biological artificial surfaces induces the activation of the coagulation cascade[39].

The methods of anticoagulation currently available consist of systemic or regional treatments. The systemic ones provide anticoagulation of the entire blood mass, performed directly in the patient.

On the other hand, the regional ones allow for exclusive anticoagulation of the blood flow in the extracorporeal circuit, without any theoretical direct effect on the patient's vascular system. Systemic anticoagulation is achieved using various anticoagulant medications: among these, the infusion of unfractionated heparin is the most used method as it is inexpensive and quick. The problem linked to this therapy is the possibility of bleeding[40]. On the other hand, regional anticoagulation is mostly applied in the course of extracorporeal circulation and at low flows, an example being continuous renal replacement therapy (CRRT)[41]. This technique instead is obtained by infusing citrate at the beginning of the extracorporeal circuit and represents the method currently most applied in the clinic.

The citrate infused in the first part of the circuit determines the chelation of ionized calcium present in the blood, reducing the concentration below 0.3 mmol/L[42] and guaranteeing complete anticoagulation of the circuit. A systemic infusion of calcium chloride normalizes the calcium ions restoring coagulation function[43]. A portion of citrate (estimated to be around 50%) is removed by the hemodiafilter, while the remaining amount is able to reach the systemic circulation, where it is metabolized by the liver[44]. Since the clearance of citrate is limited, this method cannot be applied to high extracorporeal blood flows as the limits of citratemia (<0.5 mmol/L)[37] would be exceeded, with subsequent accumulation and intoxication.

In order to avoid the complications described above and increase the blood flow in the extracorporeal circuit, we developed a technique that allows both regional anticoagulation with citrate infusion (to lower ionized calcium, essential in the coagulation cascade), and at the same time guarantees greater removal of citrate, maintaining the hydro-electrolytic balance of the system, using ion exchange resins.

The ion exchange resins used in this treatment are both cation and anion exchange resins. The ion exchange is regulated by a variety of factors, including the affinity of the resin for the specific ion, the speed of the haemodiafiltrate flow, the concentrations of the ions, the pH of the solution, the temperature, and the stoichiometry of reaction between substances. In our set up, there was a shift of ions, with liberation of the ions charged inside the resins and replacement by ions present at high concentrations in the hemodiafiltrate.

A total of seven resins were used for this treatment: two containing Cl^- to remove citrate, one Na^+ resin to remove Calcium, two containing H^+ and two HCO_3^- to restore electrolyte balance. This large number of resins managed to support the high flow set and ensured efficient ion exchange. The resin matrix does not have a surface compatible with direct blood contact, therefore it was

necessary to create a special circuit in which the cartridges were positioned along the hemodiafiltrate flow.

In the setup presented, it was necessary to use all these resins to maintain hydro-electrolytic balance, i.e. all the excess electrolytes introduced into the flow by the resins had to be adequately removed, and those discarded were replaced with adequate infusions. This treatment would have been possible at the same flow rate even without the H^+ and HCO_3^- resins for the removal of Na^+ and Cl^-, but this would have led to the creation of a massive waste flow, which would hace forced us to reintegrate the hemodiafiltrate liquid continuously. Using these resins, we ensured the lowest possible waste flow, so as to remove only the amount of liquid which we could re-infuse as KCl and $CaCl_2$. Based on the loss of calcium, chloride and potassium, corrective infusions with potassium chloride (KCl) and calcium chloride ($CaCl_2$) were administered. Our system proved to be effective in ensuring the removal of citrate and maintaining electrolyte stability, without a strong impact on the animal. As highlighted in the results section, the passage of haemodiafiltrate through the resins obtained a substantial reduction in the concentrations of calcium ions and citrate.

We observed that in the first 30 minutes the system proved to be effective and efficient in the removal of citrate, obtaining arterial values <0.5 mmol/L and P9 values (sampling point placed at the end of extracorporeal circuit) of 0.89 mmol/L. There was also a significant reduction in the concentrations of ionized calcium (Ca^{++}), recorded both in P1 (sampling point at the beginning of the circuit) and in P9. In particular, the passage of haemodiafiltrate along the haemodiafilter with counter-current flow made it possible to achieve a statistically significant reduction of ionized calcium (Ca^{++}) in the extracorporeal blood flow, reaching concentrations of 0.3 mmol/L, associated with a known anticoagulant effect[45]. For the first 30 minutes the arterial Ca^{++} remained stable within the normal range, thanks to the infusion of calcium chloride ($CaCl_2$). Similarly, the total calcium (CaTot) in the blood samples collected in P9, in the first 30 minutes, showed a significant decrease while no variation was recorded in the concentrations in the arterial sample. One of the most important and indicative parameters of accumulation and excess of citrate, as explained in results (*Evaluation of ionized calcium and total calcium)*, was the total calcium / ionized calcium ratio ($CaTot/Ca^{++}$)[37] which was shown to be <2 in the artery and in the blood samples collected in P0 for the first 30 minutes, demonstrating the efficiency of citrate removal. As shown in the results section, the efficiency of the resins was evaluated by observing the reduction of citratemia along the extracorporeal circuit and was calculated according to the ratio between pre-filter and post filter citratemia, which was 93% at 15 minutes and 88% at 30 minutes.

Our complicated system was not perfect in managing the electrolyte balance. In fact, for the first 30 minutes, the values of the main electrolytes (potassium, sodium and chloride) were adequately maintained in range, both in the samples collected in the artery and in the extracorporeal circuit; however, a loss of magnesium and phosphorus ions was immediately detected along the circuit. The loss of magnesium and phosphorus is attributable to four mechanisms: (1) the non-selectivity of the resins; (2) the bond with citrate (which can bind magnesium[38]); (3) the waste flow, while removing a portion of fluid, simultaneously allowed the loss of all electrolytes in the hemodiafiltrate; (4) failure to supply these electrolytes by systemic infusions.

A stable arterial concentration of potassium, sodium and chloride ions was recorded. The thromboelastographic analyses highlighted the "regional extracorporeal anticoagulation" capacity of the system, recording a complete absence of coagulation in the blood sample coming from the return catheter (P9) but, at the same time, a normal coagulation activity in the arterial sample. It is interesting to note how, with the passage of time, the efficiency of the system progressively reduced, as was shown in all the parameters recorded and analysed. Starting from serum citrate, a constant increase in the values in the artery was observed, with the achievement of an average value of 3.60 mmol/L at 120 minutes. This increase was also reported along the entire extracorporeal circuit: through the pre- and post-filter values of serum citrate (P1 and P9), we observed the decrease in the efficiency of the resins in the removal capacity, which was calculated to be 48% at 120 minutes. On the contrary, arterial Ca^{++} underwent an important decrease below the normal range, also due to lack of correction, since the rate of $CaCl_2$ infusion was increased, but not adequately enough to compensate for the loss of calcium. Despite this, at 120 minutes, the Ca^{++} values in the circuit proved to be stable <0.3 mmol/L, guaranteeing the non-coagulability of the extracorporeal system. This was further confirmed by the R parameter of the TEG, which remained > 60 minutes throughout the treatment. Consequently, an imbalance of the CaTot/Ca^{++} ratio was obtained in the artery: by decreasing ionized calcium and increasing calcium bound to the citrate, and thus total calcium as well, an increase of the ratio above the threshold of 2 was allowed. This is an indirect index of the increase of citrate in arterial blood.

Arterial blood gas analyses were performed throughout the study to monitor serum electrolyte concentrations. After the first 30 minutes, some alterations were present in the electrolytes most involved in the process: sodium, calcium, magnesium and phosphorus. Potassium, on the other hand, proved to be the only stable electrolyte, thanks to the adequate correction obtained by systemic infusion of KCl. The variations in the concentrations of the other electrolytes are substantially the result of an inadequate correction. A CaCl solution was infused to balance the Ca^{++} bound by resins and citrate, but was not sufficient. Sodium underwent a decrease during the

treatment, due to the creation of a waste flow, necessary to eliminate water overload. On the contrary, magnesium and phosphorus underwent an increase over time, after a significant initial decrease. We attributed this phenomenon to the loss of efficiency of the resins which, over time, lost their power on these electrolytes. Due to the rise during the experiment, the values of magnesium and phosphorus were statistically significantly higher at the end than at the start, and outside the expected normal range, as no corrective infusions were administered. Finally, the loss of the ability for citrate removal and its consequent increase determined a significant increase in pH, with the development of a mild metabolic alkalosis at the end of the treatment.

Despite some imperfections, the introduction of ion exchange resins made it possible to develop a substantially effective, simple and apparently free from serious complications regional anticoagulation technique. The thromboelastographic analyses carried out on the arterial sample showed a normal and unchanged coagulation profile throughout the experiment, indicating that the treatment with ion exchange resins did not alter systemic hemostasis, but acted exclusively with a regional mechanism along the circuit. This was further demonstrated by performing the thromboelastographic analyses on samples taken from the extracorporeal circuit before reinfusion (P9), which showed a reaction time R> 60 minutes for the entire duration of the experiment.

The application of an extracorporeal circuit with ion exchange resins did not result in hemolysis. Despite these results, we are aware that the systemic, long-term effects of this method have not been assessed in the least. Subsequent studies are certainly necessary in order to identify the safety profile of this technique and will allow to recognize any subhemolytic damage. This new technique, aimed at improving the extracorporeal removal of citrate with ion exchange resins and obtaining a regional coagulation at high flows, bases its main anticoagulant effect on the reduction of ionized calcium concentrations in the extracorporeal circuit and, at the same time, on a greater removal of the infused citrate. The treatment under study proved to be able to achieve the goal we set for citrate removal and regional anticoagulation, albeit for a limited time. The loss of efficiency of the ion exchange resins and the loss of effectiveness in the removal of citrate (which progressively increased) represents one of the limitations of this study. Further works will certainly be needed to promote the regeneration of the resin matrix during treatment, in order to ensure greater ion exchange efficiency and allow longer-lasting extracorporeal therapy. We are convinced that this study lays the foundations for a theoretical application of ion exchange resins in techniques that require high extracorporeal blood flows, effectively freeing them from systemic drugs such as unfractionated heparin. Among these we must certainly include chronic dialysis, plasmapheresis, and systems for the removal of CO_2 and blood oxygenation.

The major limitation of this study is the use of systemic anticoagulation with unfractionated heparin (UFH) during the entire experiment. In particular, the baseline activation clotting time (ACT) level was 133 ± 3 seconds, consequently the ACT level during the experiment was 265 ± 37 seconds obtained by mean infusion of heparin equal to 4800 ± 800 IU / h. The UFH infusion was carried out in order to prevent coagulation of the circuit during the initial stages of the experiment, in which the ion exchange resins were not connected to the circuit, and maintained for the duration of the experiment as a precaution in view of the possibility of the exhaustion of the resin matrices, as was actually recorded. However, the study was not influenced by this choice, as the thromboelastographic analyses for the evaluation of coagulation were conducted using heparinase-kaolin, to remove the anticoagulant effect induced byunfractionated heparin. In particular, the heparinase contained in the analytical cuvette is able to inhibit heparin concentrations much higher than those used in the present study[46]. Thromboelestographic analyses, thanks to the use of heparinase-kaolin, showed a normal systemic coagulation structure, validated by arterial TEG-R values indicative of a good coagulation profile.

A thermo dilution technique: an in vitro evaluation to quantify recirculation flow during extracorporeal setting in the veno-venous configuration.

Background

In 2020, our group developed an idea to detect recirculation flow during VV-ECMO[13] in collaboration with the University of Milano Bicocca. As described in the paragraph *Recirculation*, in VV-ECMO, blood drained from the central venous system is oxygenated and decarboxylated by a membrane oxygenator and then reinfused in the central venous system[47]. During VV-ECMO a certain amount of extracorporeal oxygenated blood can flow back from the reinfusion cannula into the drainage cannula without reaching the heart and the peripheral tissues. This dynamic phenomenon, which must not be underestimated, mainly depends on the cannulae position and the ECMO-patient hemodynamic interaction. Thus, a quantification is necessary to adjust cannulae position[48,49].

In 2000, a conventional thermodilution technique was employed by Sreenan et al.[50] in rabbits on VV-ECMO. Because of the specific experimental setting, the Canadian group was able to compute only 0% and 100% of recirculation flow (RF). Taking into account the need for an easily accessible technique able to identify recirculation in ECMO patients, we decided to further investigate this issue. The purpose of this in vitro study was to evaluate the feasibility of a thermodilution technique to compute RFs at different extracorporeal blood flows (BF) and cardiac outputs (CO). The results of this study have been published and the description of the methods and results and a brief discussion of this in vitro evaluation will be reported below[13].

Materials and Methods

In vitro circuit design

An in vitro setting was built to simulate a patient undergoing vv-ECMO. For this purpose, the circuit was primed with swine blood and MultiBic (Fresenius Medical Care Italia, Palazzo Pignano, Italy) solution. In compliance with CE (1069/2009) regulation for the use of animal-derived products, blood was collected at an abattoir during usual slaughtering process for food industry purposes. Using a 4 L reservoir (VHK 71000 venous hardshell cardiotomy reservoir; Getinge, Rastatt, Germany), blood was mixed with Sodium Heparin 25000 I.U. (Pfizer Italia S.r.l, Latina, Italy) and ACD 300ml (Fresenius Kabi Italia, Isola Della Scala, Italy) to avoid coagulation. Blood was then stored in a disposable parenteral bag (Bertoni Nello S.r.l., Modena, Italy) with cefazolin 1 g (Teva Italia, Milano, Italy). The circuit consisted of three sections: body, recirculation bridge, and ECMO as shown in Figure 1.

The body section representing the patient vascular system was assembled using 3/8 and 1/4 inch polyvinylchloride class VI medical tubes (Medtronic, Minneapolis, MN), a reservoir (VHK 71000 venous hardshell cardiotomy reservoir; Getinge), and two membrane oxygenators as heat exchangers (Quadrox-I adult HMO; Getinge). A centrifugal blood pump (BPX-80; Medtronic) mimicked CO, allowing blood to flow along the circuit passing through heat exchangers, from and back into the reservoir. Downstream the second heat exchanger, three Y connectors split BF into four different 1/4 inch tubes, 300 cm long, immersed in a thermostatic water bath, ensuring a stable temperature of 37°C. In addition, another short 1/4 inch circuit was used to remove exceeding volume due to repeated cold bolus injections, through an ultrafilter (FX 100 classix; Fresenius Helixone High-Flux; Fresenius Medical Care AG&Co. KGaA, Bad Homburg, Germany). A peristaltic pump (Volumat MC Agilia; Fresenius Kabi Italia; "Ultrafiltrate" in Figure 1), connected to the ultrafilter, removed ultrafiltrate to maintain a stable blood hematocrit during the entire experiment. Blood circulating volume in the body section was 4.5 L. The ECMO section, placed in between the two body heat exchangers, consisted of a drainage line (IN), a centrifugal pump (BPX-80), a membrane oxygenator (Quadrox-i small adult HMO; Getinge), and a reinfusion line (OUT). The bolus injection port, equipped with a temperature probe (Ti) to record the bolus injection temperature, was placed 20 cm downstream the membrane oxygenator. The length of this portion of circuit is 300 cm, with a volume of 460 ml. Thermocouple-OUT and thermocouple-IN were placed 150 cm downstream cold bolus injection port and 20cm downstream centrifugal pump, respectively. The recirculation bridge made of a 30cm long medical tube (3/8 inch) was placed in between ECMO drainage and reinfusion. Flowmeters (bio-probe flow transducer model TX40; Medtronic) placed along the circuit were used to monitor recirculation flow, ECMO flow, and CO. Recirculation fraction was set according to ECMO flow and recirculation flow, both measured by flowmeters. Two mechanical resistances (Hoffman clamps), placed on the recirculation bridge and drainage line, were adjusted to set recirculation flow at the desired target.

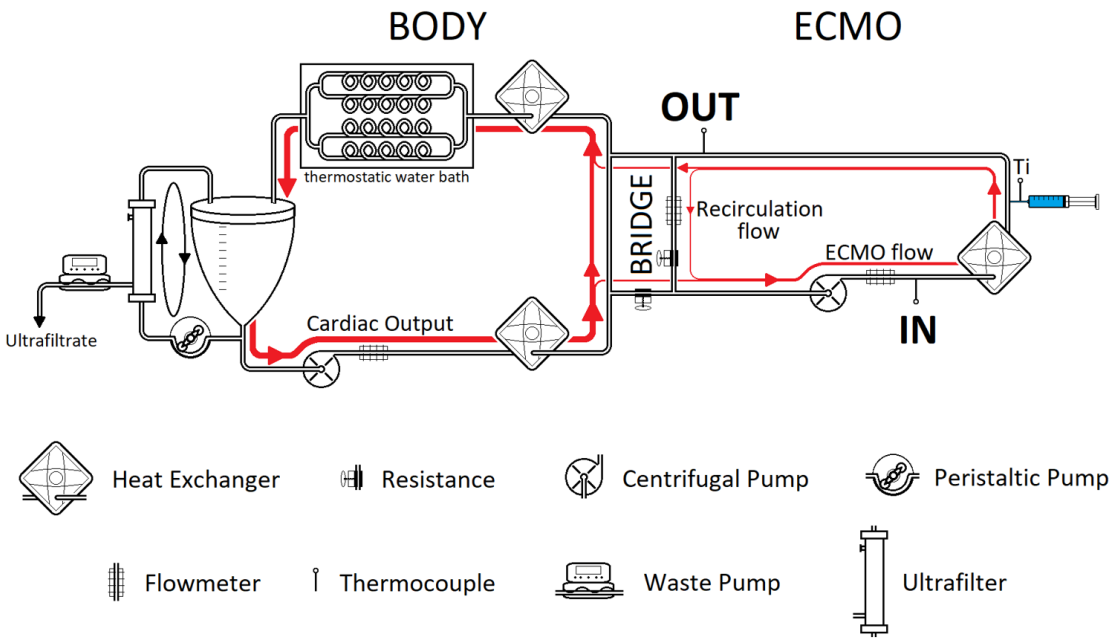

Figure 1: Schematic representation of the circuit.

Study Design

Experiments were performed injecting 10 ml cold bolus of saline solution at room temperature (23.5–26°C) to evaluate the RF through a thermodilution technique. Three ECMO BF (1.5, 3, and 4.5 L/min) were tested. For each ECMO flow, we evaluated seven RFs ranging from 0% to 50% (0%, 5%, 10%, 20%, 30%, 40%, and 50%). Zero RF was achieved by clamping the bridge line. Various combinations of CO and ECMO BF had been selected to verify whether or not CO influenced the thermodilution technique used to evaluate RF: 1.5 L/min BF has been tested at 3 and 5 L/min CO; 3 L/min BF at 4 and 5 L/min CO; 4.5 L/min BF at 5.5 L/min CO. For each RF, to minimize variability, we performed five bolus injections and acquired related thermodilution measurements.

Temperature Probe Recording

Temperatures were closely monitored using Powerlab 16/35 (ADInstruments, Dunedin, New Zealand) with temperature probes (MLT1405 T-type implantable thermocouple; ADInstruments) and temperature transducers (ML312 T-type Pod; ADInstruments). LabChart 8 pro (ADInstruments) software was used to collect data.

Recorded Variables

Injected bolus temperature (Ti—lowest registered temperature during bolus injection), temperature on reinfusion line (TOUT—thermocouple-OUT), temperature on drainage line (TIN—thermocouple-IN), and basal fluid temperature (T b—mean fluid temperature recorded before

bolus injection on thermocouple-IN over the first 200 frames) have been recorded for each thermodilution.

Computed Variables

Temperature curves acquired from the thermocouples were sampled at 100 Hz, then inverted with respect to the x-axis and downshifted of T b. Curves were then filtered with a sixthorder low-pass Butterworth filter with a cutoff frequency of 4 Hz for T OUT signal and 1 Hz for T IN signal (Matlab R2018b; The MathWorks, Inc, Natick, MA). Timespans of temperature variations ([t1 OUT–t2 OUT] and [t1 IN–t2 IN]) due to the bolus injection were selected at visual inspection, taking into account possible oscillation of the signal due to the activity of heat exchangers. After zeroing the selected timespan, traces were integrated over time (ratio of the area under temperature-time curves [AUC]).

The AUC thermocouple-OUT over the time range t1 OUT–t2 OUT:

$$AUC\ OUT = \int_{t1\ OUT}^{t2\ OUT} T_{OUT}\ dt$$

the AUC thermocouple-IN over the time range t1 IN–t2 IN:

$$AUC\ IN = \int_{t1\ IN}^{t2\ IN} T_{IN}\ dt$$

and the RF was computed as the ratio between AUC IN and OUT curves:

$$AUC\ ratio = \frac{AUC\ IN}{AUC\ OUT}$$

Statistical Analysis

Statistical analysis was performed with SAS 9.4 (SAS Institute Inc, Cary, NC), SigmaPlot (Systat Software, Inc, San Jose, CA) and STATASE 16 (StataCorp LP, College Station, TX). Intraclass correlation coefficients (ICC, single-measurement, absolute-agreement, 2-way mixed-effects model) were computed to assess the test-retest reliability of AUC and AUC ratio values computed by the thermodilution technique[51]. Reproducibility was calculated analyzing the percentage standard error of the mean (SEM%) of the replicated AUC determinations and AUC ratios at every ECMO flow–CO–set RF combination:

$$SEM\%_{ijk} = \frac{\overline{SD}_{ijk}}{\sqrt{N_{ijk}}} \Big/ \overline{AUC}_{ijk}$$

where SD_{ijk} represents the standard deviation of the N_{ijk} replicated AUC determinations at a given ECMO flow (i), CO (j), and RF (k) and $\overline{AUC}_{ijk} = mean\left(AUC_{ijk}\right)$. Moreover, in evaluating

reproducibility, ±2 × SEM% defines the 95% confidence limits of a determination[52]. The AUC ratio accuracy was assessed by a modified Bland–Altman analysis corrected for multiple replicates with no pairing of the measures and constant true values[53]. Analyses were performed for the overall data and for different ECMO flow and CO values[54]. A linear mixed model was used to assess the relationship of set RF on AUC ratio at different ECMO flow and CO combinations and for the overall data, including as covariates ECMO flow, CO, and interactions.

Results

We collected about 3L of swine blood and mixed it with 2L of MultiBic to fill the circuit. Hematocrit was 28.3% at baseline and remained stable throughout the experiment with an ending value of 28.1%. A total of 175 temperature traces were recorded after bolus injection. Bolus progression along the circuit is outlined in Figure 2, Panels A–E.

At zero set RF, no temperature variation on T IN curve was detected after bolus injection, therefore, the AUC ratio computed was zero These values were not included in test-retest reliability and Bland-Altman analyses.

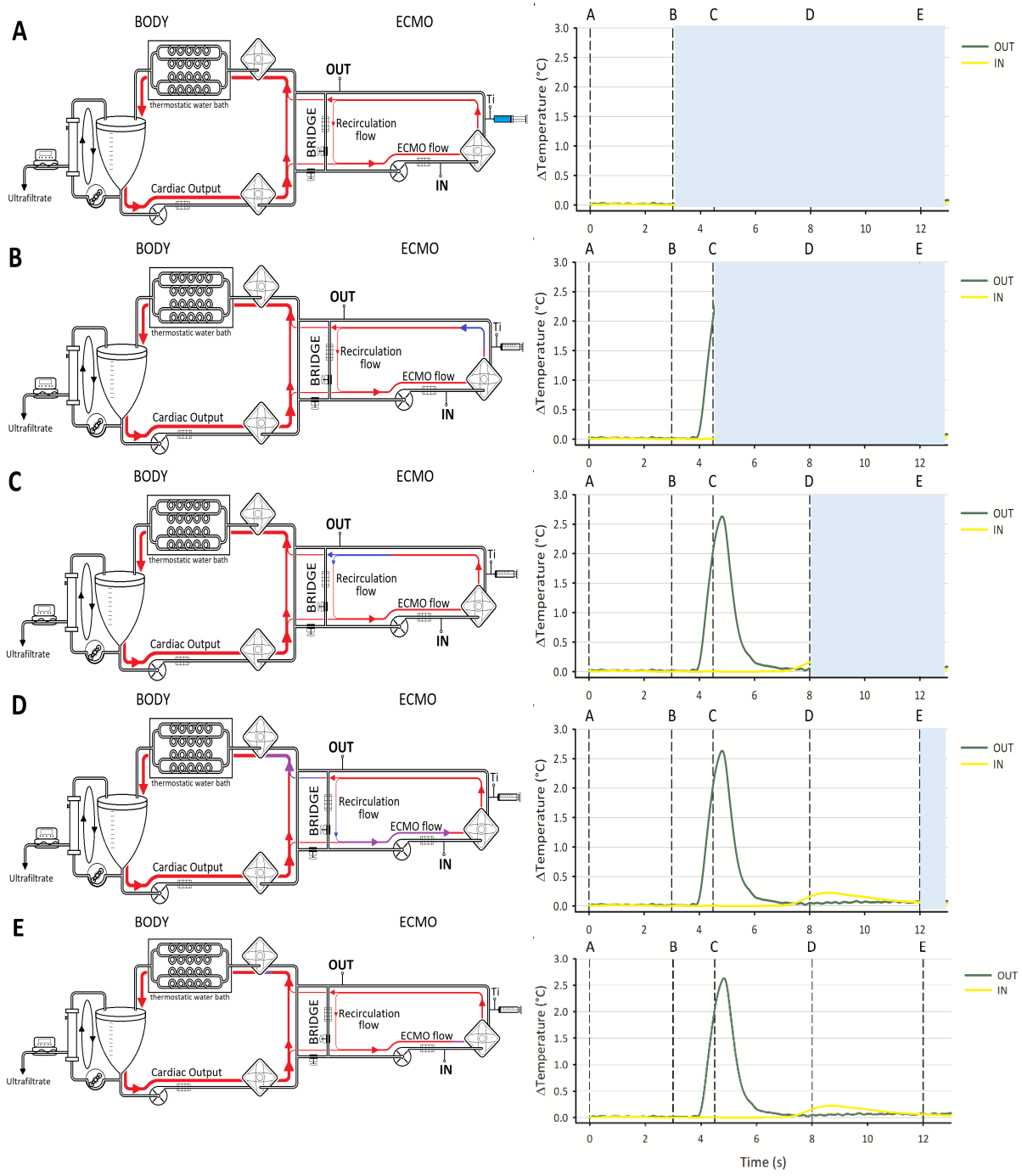

Figure 2: Schematic representation of the experimental setting. A–E: Cold bolus progression and temperature changes along the circuit at 5 L/min cardiac output, 3L/min ECMO flow, and 30% recirculation fraction. Lines and arrows represent flows and directions, while color suggests different temperatures (red: 37°C blood; blue: temperature reduction due to injected cold bolus; purple: rise of bolus temperature after recirculation). A: Baseline, before bolus injection (light blue). B: Bolus injection (blue). C: Bolus reaches the thermocouple-OUT and splits into two branches. D: The bolus (blue) passing through the bridge merges with the drainage flow (red), lowering blood temperature (purple), registered by thermocouple-IN. E: The entire cold bolus goes past the thermocouple-IN. On the right side: Temperature variation registered by thermocouple-OUT (green line) and thermocouple-IN (yellow line) over time, with dashed lines marking different time frames figured in (A–E).

Test-Retest Reliability of Thermodilution Technique

Intraclass correlation coefficient showed excellent (i.e. ICC>0.9) test-retest reliability of the overall data (0.983, 95% confidence interval [CI] 0.973–0.991 and 0.986, 95% CI 0.977–0.993, for AUC OUT and AUC IN, respectively). ICC for computed RF (AUC ratio) was 0.993 [95% CI 0.988-0.996]. Median SEM% for 5 measurements per AUC determination are 1.5% (interquartile range [IQR] 1.1–2.3%), 3.1% (2.0–5.1%), and 2.0% (1.2–4.5%) for AUC OUT, AUC IN, and AUC ratio, respectively. The median SEM% (IQR) values for each set ECMO flow and CO combinations are reported in the Table 1.

		SEM% (%)	
	AUC OUT	**AUC IN**	**AUC RATIO**
BF 1.5 L/min CO 3 L/min	1.55 [1.48-2.82]	4.1 [1.54-7.73]	3.59 [1.18-7.74]
BF 1.5 L/min CO 5 L/min	2.36 [1.89-2.45]	4.02 [3.11-5.03]	2.59 [1.88-4.09]
BF 3 L/min CO 4 L/min	1.14 [0.97-1.34]	2.68 [2.12-3.17]	1.79 [1.26-3.16]
BF 3 L/min CO 5 L/min	1.76 [1.08-2.1]	3.05 [2.72-5.87]	2.12 [1.44-5.51]
BF 4.5 L/min CO 5.5 L/min	1.17 [0.77-1.21]	1.69 [1.45-2.73]	1.72 [1.22-2.49]
Overall data	1.52 [1.11-2.27]	3.09 [1.98-5.13]	2.02 [1.23-4.53]

Table 1 reports the median [IQR] percentage standard errors of the mean (SEM%) of the AUC and AUC ratio determinations for the overall data and at each blood flow/cardiac output tested

SEM% values for AUC OUT ranged from a minimum of 0.2% to a maximum of 3.4% for the overall data, from 0.7% to 3.4% for ECMO flow = 1.5 L/min and CO = 3 L/min; from 1.4% to 2.7% for ECMO flow = 1.5 L/min and CO = 5 L/min; from 0.9% to 2.4% for ECMO flow = 3 L/min and CO = 4 L/min; from 0.2% to 2.3% for ECMO flow = 3 L/min and CO = 5 L/min; and from 0.4% to 1.5% for ECMO flow = 4.5 L/min and CO = 5.5 L/min.

SEM% for AUC IN, showed a higher maximum value, in fact for the overall values the range was from a minimum of 0.4% to a maximum of 10.7%, from 0.6% to 9.2% for ECMO flow = 1.5 L/min and CO = 3 L/min; from 2.6% to 5.2% for ECMO flow = 1.5L/min and CO = 5L/min; from 1.7% to 5.6% for ECMO flow = 3 L/min and CO = 4 L/min; from 0.4% to 10.7% for ECMO flow = 3 L/min and CO = 5 L/min; and from 0.6% to 5.5% for ECMO flow = 4.5L/min and CO = 5.5L/min.

However, values exceeding the 5% of SEM% (10% for 95% confidence limits of a determination) limit were nine (five values were below 6%): three at ECMO flow = 1.5 L/min and CO = 3 L/min (5–10–20% RF); two at for ECMO flow = 1.5 L/min and CO = 5 L/min (10–20%); one at ECMO flow = 3 L/min and CO = 4 L/min (5% RF); two at ECMO flow = 3 L/min and CO = 5L/min (5–10% RF); and one at ECMO flow = 4.5L/ min and CO = 5.5 L/min (5% RF), as reported in the figure 3.

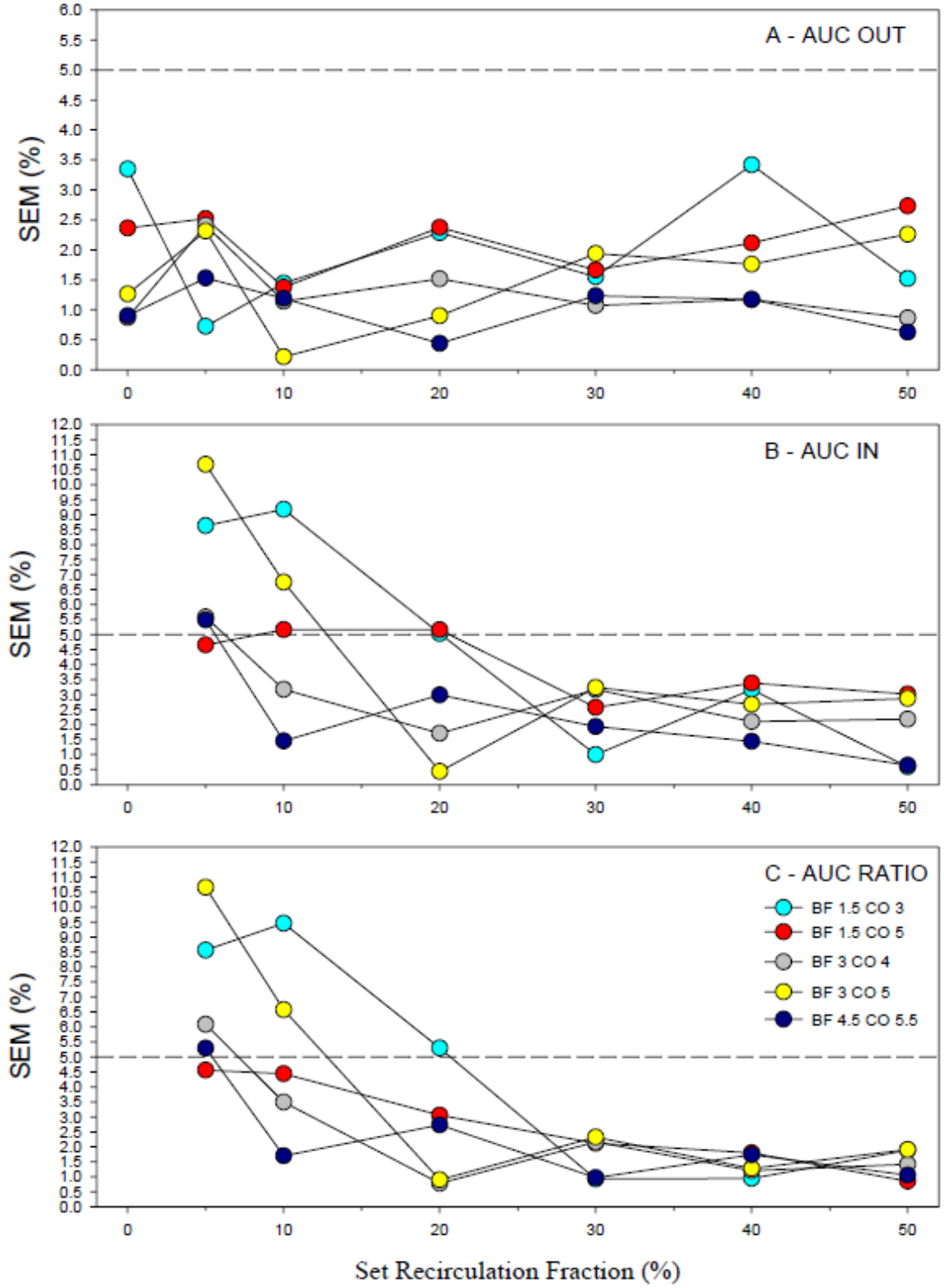

Figure 3: shows the percentage standard error of the mean (SEM%) of the replicated determinations of AUC OUT (panel A), AUC IN (panel B) and AUC ratio (panel C) at every ECMO flow-Cardiac Output combination as a function of set Recirculation Fraction. Colors represent different set of ECMO flow - Cardiac Output combinations. Dashed lines represent the 5% upper limit of SEM% found by Stetz at al.[52].

Higher SEM% values are mainly concentrated at low RF percentages, where a small difference (median 0.46 [IQR−0.18 to 1.02] at 5% and 0.14 [IQR −0.52 to 0.78] at 10%) between AUC ratio and RF represents SEM% values as high as 11%, as shown in the Bland–Altman analysis (Figure 4). SEM% values for AUC ratio ranged from a minimum of 0.8% to a maximum of 10.7% for the overall data and values at different ECMO flow and CO combinations resemble the one computed for AUC IN.

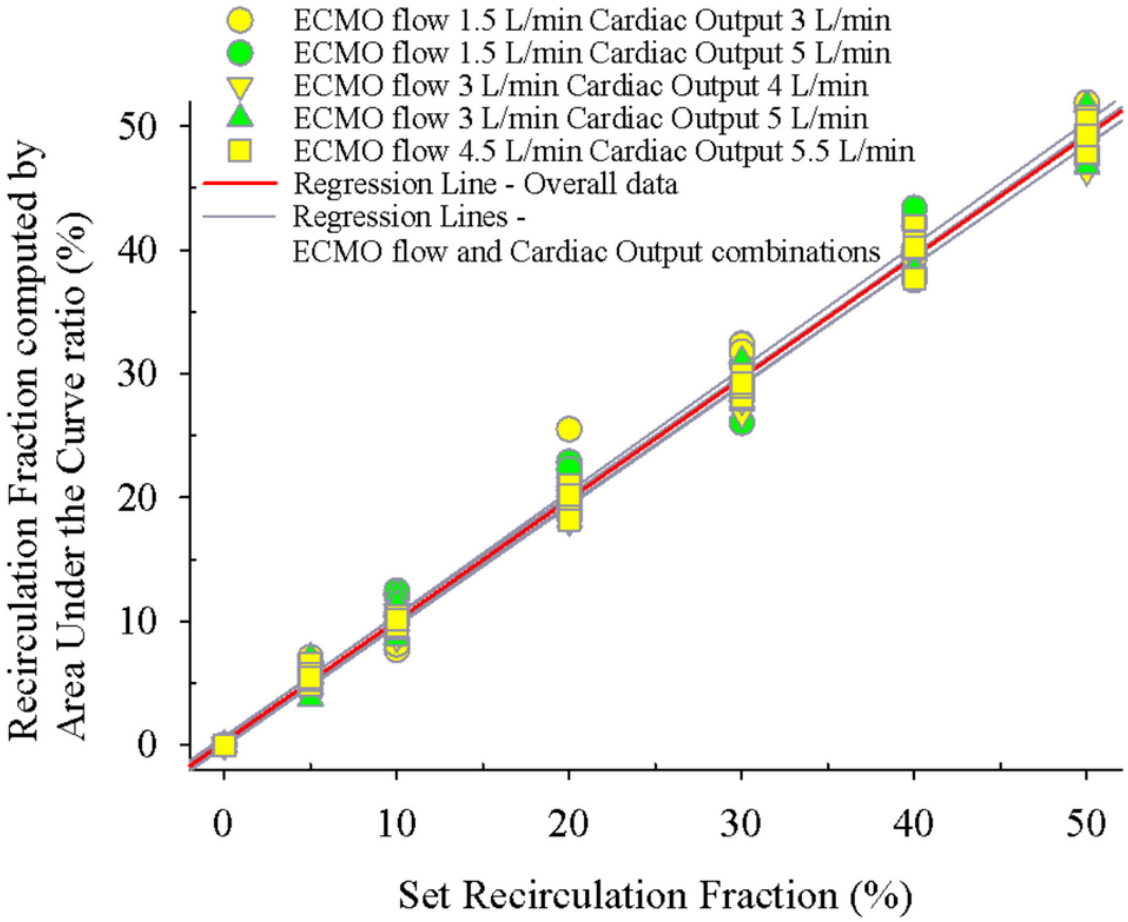

Figure 4: The figure represents the corrected Bland–Altman plot for repeated measurements comparing the experimental technique (thermodilution, AUC ratio) with the set recirculation fraction values for the overall data. The solid line represents the −0.21% bias, dashed lines with error bars represent the 95% limits of agreement (LOA −3.36% [CI −3.94% to −2.77%] to 2.94% [CI 2.36% to 3.53%]). CI, confidence interval; ECMO, extracorporeal membrane oxygenation

Accuracy and Precision of Area Under Temperature-Time Curves Ratio

A modified Bland–Altman analysis for repeated measurements was performed for the overall data points (Figure X4) and for the five different ECMO flows and CO combinations

The biases were:

1. −0.21% (limits of agreement [LOA] −3.36% [CI −3.94% to −2.77%] to 2.94% [CI 2.36% to 3.53%]), for the over-all data (Figure 4);

2. 0.57% (LOA −3.39% [CI −4.98% to −1.80%] to 4.52% [CI 2.93% to 6.11%]), at ECMO flow 1.5 L/min and CO 3 L/min (Figure 5 Panel A);

3. 0.12% (LOA −3.41% [CI −5.24% to −1.58%] to 3.66% [CI 1.83% to 5.48%]), at ECMO flow 1.5L/min and CO 5L/min (Figure 5 Panel B);

4. −0.87% (LOA −3.38% [CI −4.46% to −2.30%] to 1.65% [CI 0.57% to 2.72%]), at ECMO flow 3L/min and CO 4L/min (Figure 5 Panel C);

5. −0.69% (LOA −3.56% [CI −4.53% to −2.59%] to 2.18% [CI 1.21% to 3.15%]), at ECMO flow 3 L/min and CO 5 L/min (Figure 5 Panel D);

6. −0.17% (LOA −2.24% [CI −2.94% to −1.55%] to 1.90% [CI 1.20% to 2.59%]), at ECMO flow 4.5 L/min and CO 5.5 L/min (Figure 5 Panel E).

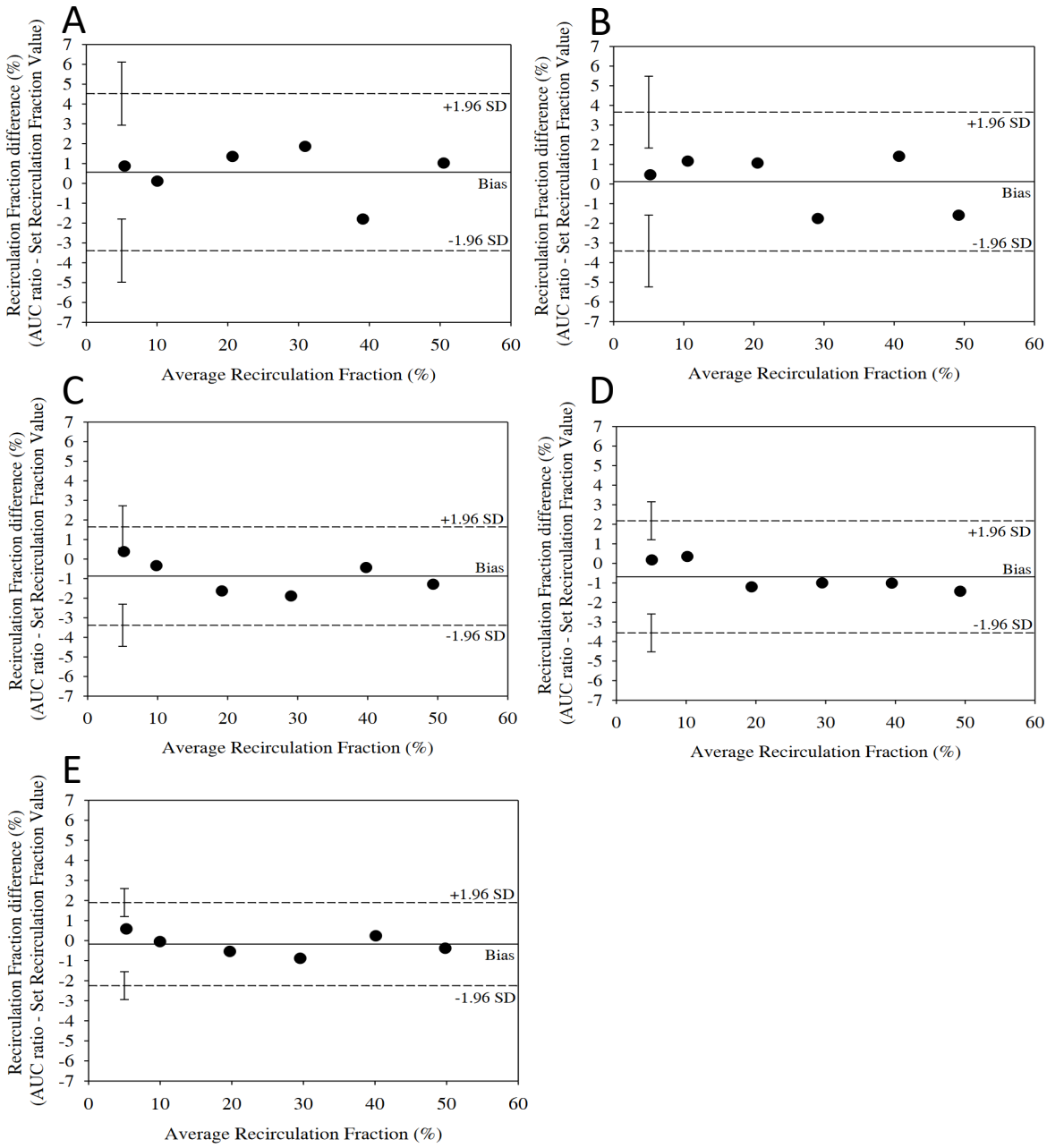

Figure 5 Panel A-D: the Bland-Altman analysis to compare the experimental technique (thermodilution, AUC ratio) with the referral method (set recirculation fraction). Panel A, ECMO flow 1.5 L/min and CO 3 L/min; Panel B, ECMO flow 1.5L/min and CO 5L/min: Panel C, ECMO flow 3L/min and CO 4L/min; Panel D; ECMO flow 3 L/min and CO 5 L/min; Panel E, ECMO flow 4.5 L/min and CO 5.5 L/min.

Linear Mixed Model

Data obtained from various combinations of ECMO flows and CO, well overlap at each RF. The linear mixed model tests the effect of set RF on AUC ratio. P values of set RF (fixed effect) are highly statistically significant ($p < 0.001$) for the overall data model and for models tested at each ECMO flow–CO combination (Table 2 for parameters). None of the covariates and interactions was

statistically significant in the overall data model, indicating that the relationship between set RF and AUC ratio is independent of ECMO flow, CO, and interactions (Table 3).

	Intercept %	Slope	p
BF 1.5 L/min – CO 3 L/min	0.574	0.996	<0.0001
BF 1.5 L/min – CO 5 L/min	0.715	0.973	<0.0001
BF 3 L/min – CO 4 L/min	−0.137	0.973	<0.0001
BF 3 L/min – CO 5 L/min	0.155	0.966	<0.0001
BF 4.5 L/min – CO 5.5 L/min	0.080	0.990	<0.0001
Overall data	0.277	0.979	<0.0001

Table 2: Models were computed at different ECMO flows (BF) and cardiac output (CO) combinations and for the overall data. Set recirculation fractions on AUC ratio were expressed as percentage values. AUC, area under temperature-time curves; BF, blood flows; ECMO, extracorporeal membrane oxygenation.

Effect on AUC ratio (%)	P value
Set Recirculation Fraction (%)	<.0001
ECMO flow (L/min)	0.362
Set Recirculation Fraction (%) x ECMO flow (L/min)	0.312
Cardiac Output (L/min)	0.693
Set Recirculation Fraction (%) x Cardiac Output (L/min)	0.185
ECMO flow (L/min) x Cardiac Output(L/min)	0.468
Set Recirculation Fraction (%) x ECMO flow (L/min) x Cardiac Output (L/min)	0.269

Table 3: P-values of type 3 test of fixed effects of the linear mixed models for the overall data testing the effect of Set Recirculation Fraction (%) on AUC ratio (%), including also the effects of set ECMO flow and Cardiac Output (and their interactions with set Recirculation Fraction)

Discussion

We built an in vitro setup mimicking a patient undergoing vv-ECMO to measure the RF. We used a thermodilution technique, positioning two thermocouples along the circuit: one on the ECMO reinfusion line (OUT), the other on the drainage line (IN). The RF was computed as the AUC ratio between temperature traces IN and OUT. We decided to test clinically relevant ECMO flows (1.5, 3, and 4.5 L/min) at different RFs ranging from 0% to 50%, also varying CO (3, 4, 5, and 5.5 L/min). The thermodilution technique (bias −0.21%) and test-retest reproducibility (ICC coefficient 0.993). We found that the measurement of RFs by the AUC ratio was not statistically dependent on tested ECMO flows and CO values. Quantification of the RF during vv-ECMO is extremely crucial in optimizing the extracorporeal oxygen delivery, allowing clinicians to decide whether it is appropriate to change the cannulae position or adjust patient hemodynamic[11]. Furthermore, if RF

becomes a known data, patient's real venous saturation can be estimated, a clinically relevant information otherwise incalculable during vv-ECMO[12]. Several techniques have been introduced to quantify the RF of veno-venous extracorporeal supports. The most commonly used estimates the RF comparing the oxygen content of venous blood, theoretically computed, and measured oxygen content of the ECMO inlet blood. In our in vitro setup, we tried to reproduce a physiologic setup, priming the circuit with blood and using a thermostatic water bath to maintain a stable temperature. As a cold bolus,we used 10 ml of saline solution at room temperature, easily accessible in ICU and commonly employed for CO measurement. Our setup still has limitations because vessels are simulated using PVC tubes and the recirculation bridge is exposed to room temperature (23–26°C), a nonexisting condition in vivo, where recirculation happens within the central venous system. Part of the AUC computation is still manual and may be affected by the noise of the heater activity on the temperature-curves, resulting in an additional limit of this study. Additional filtering of data and automatic timespan detection may fasten AUC computation and further increase accuracy and precision. The tested thermodilution technique provides a punctual measurement of the RF. In contrast, a continuous recirculation monitoring would be more beneficial in the clinical setting due to the dynamic nature of the machine–patient interaction. Finally, our experimental setup was representative of the adult population, with ECMO flows ranging from 1.5 to 4.5 L/min, and 10 ml saline as cold bolus.

Sodium hydroxide solution to clear CO_2 in a membrane lung: liquid ventilation an in-vitro experimental setting.

Background

The study here presented is a proof of concept of an experiment developed in our department and published by Vivona et al. in 2021[55].

$ECCO_2R$ devices are characterized by a low extracorporeal blood flow (i.e., <500 mL × min−1) to achieve minimally invasive approaches[56]. Indeed, although 500 mL of blood contain an amount of CO_2 comparable to that produced by the body in one minute ($\dot{V}CO_2$), the relatively low CO_2 transfer efficiency of conventional MLs significantly reduces the efficacy of these strategies[57]. The transmembrane gradient of pCO_2 is the driving force that moves CO_2 from blood to the sweeping gases. However, the use of high sweep gas flows, while maximizing the transmembrane gradient, does not increase CO_2 clearance significantly. To enhance the $ECCO_2R$ system, we hypothesized the use of a medium with high CO_2 absorbing capacity (sodium hydroxide -NaOH- solutions), thereby preserving the transmembrane CO_2 gradient.

When CO_2 is added to highly-concentrated NaOH solutions, sodium bicarbonate is formed directly, $NaOH + CO_2 \leftrightarrow NaHCO_3$, and sodium carbonate is generated subsequently, $NaHCO_3 + CO_2 \leftrightarrow Na_2CO_3 + H_2O$. Thus, highly concentrated NaOH solutions can absorb a conspicuous amount of CO_2 while keeping pCO_2 almost down to zero, although the elevated pH of the solution causes safety concerns.

The aim of our study was to evaluate the in-vitro the feasibility and the CO_2 transfer efficacy of membrane lung ventilation with a NaOH solution. This type of ventilation was named “alkaline liquid ventilation”. Different concentrations of NaOH were tested and the efficacy and efficiency in CO_2 removal of alkaline liquid ventilation were compared to conventional sweep gas flow.

Materials and methods

Circuit design

An in vitro setting (Figure 1) was built to simulate a patient undergoing extracorporeal CO_2 removal. A closed-loop circuit was assembled with 3/8 and 1/4 inch polyvinylchloride class IV medical tubes (Medtronic, Minneapolis, MN, USA), one 4 L reservoir (VHK 71000 venous hardshell cardiotomy reservoir, Getinge, Gothenburg, Sweden), two polypropylene oxygenators membrane gas exchangers (Quadrox-i Small adult HMO 50000, Getinge, Gothenburg, Sweden) and one peristaltic pump (Multiflow Roller Pump Module H10 series, Stöckert Shiley, München, Germany). The circuit

was primed with about 3 L of swine blood collected at a local abattoir during usual slaughtering processes in compliance with CE regulations (1069/2009), authorization number 0141051/19 provided by ATS Milano, Regione Lombardia. MultiBic® solution (Fresenius Medical Care Italia, Palazzo Pignano, Italy) was added to achieve a total volume of about 4 L. Sodium Heparin 25000 I.U. (Pfizer Italia S.r.l, Latina, Italy), anticoagulant-citrate-dextrose ACD 300 mL (Fresenius Kabi Italia, Isola Della Scala, Italy) and cefazolin 1 g (Teva Italia, Milano, Italy) were added to the blood. The first gas exchanger downstream the reservoir was ventilated with a gas mixture of air and CO_2 to maintain a constant pCO_2 of 60 ± 2 mmHg at the inlet of the second oxygenator throughout all experiments. The second oxygenator was employed to remove CO_2 through either ventilation with oxygen or a continuous infusion of sodium hydroxide (NaOH) solution, "alkaline liquid ventilation", into the gas side of the membrane lung. Circuit accesses for blood sampling were positioned upstream (PRE) and downstream (POST) of the second oxygenator.

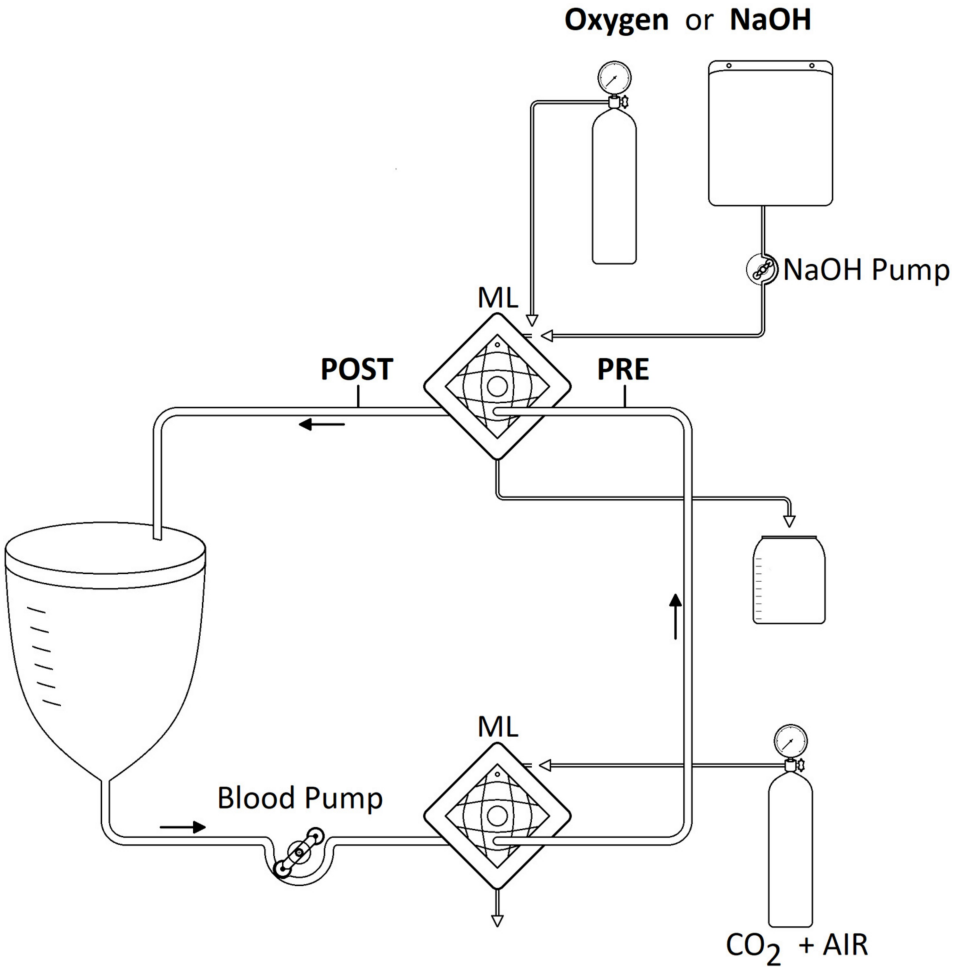

Figure 1: Schematic representation of the extracorporeal circuit. ML: membrane lung; PRE: blood sampling access upstream the ML for $ECCO_2R$; POST: blood sampling access downstream the ML for $ECCO_2R$.

NaOH pellets (Sigma-Aldrich, Merck KGaA, Saint Louis, MO, USA) were diluted in distilled water to achieve the required concentrations. NaOH solutions were stored in disposable parenteral bags (Bertoni Nello S.r.l. Modena, Italy) and infused into the gas inlet port in the gas exchanger using a peristaltic pump (Multiflow Roller Pump Module H10 series, Stöckert Shiley, München, Germany). NaOH exiting the oxygenator was discarded.

The blood temperature was kept stable at 37° C through heat exchangers connected to the membrane lungs.

The study was divided into three steps: (1) a safety and feasibility test to evaluate the effects of increasing NaOH concentrations on the membrane lung integrity and CO_2 removal; (2) an efficiency test to compare the CO_2 removal of similar sweep flows (up to 1 L/min) of oxygen vs. NaOH at the concentration selected following the feasibility test; (3) an efficacy test to compare the CO_2 removal of the best liquid ventilation flow, selected from the efficiency test, vs. 10 L/min of oxygen.

All the in-vitro tests were performed with 500 mL/min of blood flow.

Definitions and Calculations

Bicarbonate ion concentration ($[HCO_3^-]$) was calculated from pH and pCO_2 modifying the Henderson-Hasselbalch equation:

$$[HCO_3^-] = \alpha * pCO_2 * 10^{pH-pK}$$

where α = 0.0307 mmol/L * $mmHg^{-1}$ (solubility of CO2 in plasma)[58,59] and pK = 6.129 (negative logarithm of the equilibrium constant)[59–61].

Plasma carbon dioxide content PRE and POST membrane lung (expressed in mmol/L) was calculated according to the method published by Douglas et al.[62]:

$$[TCO_2] = \alpha * pCO_2 * (1 + 10^{pH-PK}$$

Carbon dioxide transfer across the membrane lung, $\dot{V}CO_2$ (in mL/min), was calculated from the transmembrane lung TCO_2 difference[63]:

$$\dot{V}CO_2 = ([TCO_{2PRE}] - [TCO_{2POST}]) * blood\ flow * 25.45$$

where TCO_{2PRE} represents CO_2 content before the membrane lung while TCO_{2POST} is the CO_2 content after the membrane lung, blood flow is measured in L/min, and the conversion factor is in mL/mmol.

Safety and Feasibility Test

Possible macroscopic detrimental effects on the membrane lung were evaluated. The effect on CO_2 removal of alkaline liquid ventilation at increasing concentrations of NaOH (10, 30, 60, 90, 100 mmol/L) and increasing ventilating flows (100, 250, 500, 1000 mL/min) was likewise evaluated. Each combination of NaOH concentration and sweep fluid flow was tested once and for 15 min. At the end of each step, PRE and POST blood samples were collected for blood gas analysis (BGA) (Radiometer abl800 flex, Copenhagen, Denmark). In addition, the integrity of the oxygenator was evaluated through visual inspection of the membrane lung, evaluation of the presence of blood in the NaOH solution exiting the oxygenator, and through analysis of blood sodium, potassium, and methemoglobin as indirect markers of hemolysis. The time-course of methemoglobin was evaluated at 4 time points (15, 30, 45, and 60 min) while testing aqueous NaOH at different sweep flows during the efficiency and efficacy tests.

The CO_2 removal efficiency was estimated by computing pCO_2 differences across the membrane lung and $\dot{V}CO_2$. At the end of the feasibility test, we selected the highest NaOH concentration endured by the membrane lung to perform the subsequent efficiency and efficacy tests.

Efficiency and Efficacy Tests

We performed six experiments with blood from 4 pigs. For each experiment, we tested, in random order, two different sweeping fluids, pure oxygen (FiO_2 equal to 1) and aqueous NaOH at 100 mmol/L (the concentration selected from the feasibility test). Four sweep flows (100, 250, 500, 1000 mL/min) for each fluid were randomly tested. We also randomized and tested 10 L/min of oxygen flow. Each combination of sweep fluid and flow was applied once during the single experiment. The target PRE pCO_2 was 60 ± 2 mmHg. At the end of each step lasting about 15 min, we collected PRE and POST blood samples for BGA. CO_2 removal efficiency and efficacy were evaluated from pCO_2 differences across the membrane lung and $\dot{V}CO_2$. The highest CO_2 removal achieved with alkaline liquid ventilation was compared with the CO_2 removal achieved with conventional gaseous ventilation performed with 10 L/min of oxygen.

Statistical Analysis

Data are reported as median and interquartile range (IQR). Two-way repeated measures ANOVA or two-way repeated measures ANOVA on ranks was used, as appropriate, to test safety, feasibility (PRE and POST values), and efficiency. One-way repeated measures or Friedman repeated measures was used, as appropriate, to test safety and feasibility (POST–PRE differences) and to compare methemoglobin values at different time points. Paired t-test or Wilcoxon signed rank test was used, as appropriate, to test efficacy. Post-hoc analyses were performed with Bonferroni or Tukey corrections. Statistical significance was defined as $p < 0.05$. Analysis was performed with SAS

software 9.4 (SAS Institute, Inc.,Cary, NC, USA) and SigmaPlot v.11.0 (Systat Software Inc, San Jose, CA, USA)

Results

Feasibility and Safety Test

No detectable damages to the membrane lung were observed. Moreover, no blood was found in the sweep fluid exiting the oxygenator.

Figure 2 and Table 1 report the BGAs of PRE and POST blood. pCO_{2PRE} was stable throughout the entire test, 59.0 (58.0–60.0) mmHg. Delta pCO_2 across the membrane lung was significantly lower at 10 mmol/L (−32.2 (−38.6–−23.1) mmHg). Other- wise, it showed small increases as NaOH concentration increases (−41.4 (−43.1–−36.8), −47.7 (−49.5–−44), −47.8 (−48.6–−47) and −48.2 (−48.4–−46.6) mmHg at 30, 60, 90, and 100 mmol/L respectively). pCO_{2POST} was reduced to about 12 mmHg with NaOH con- centration ≥ 60 mmol/L (12.0 (11.0–15.0), 11.4 (10.2–12.4) and 12.4 (11.3–13.1) mmHg at 60, 90, and 100 mmol/L respectively), subsequently pH_{POST} increased up to 7.913 (7.885–7.943) at NaOH concentration equal to 100 mmol/L. The lowest $\dot{V}CO_2$ was also recorded at the lowest NaOH concentration 73.9 (54.3–91.8) mL/min. PRE blood sodium and potassium concentration were stable. POST chloride concentrations were higher than PRE values while sodium concentrations were lower. Moreover, a simultaneous decrease in potassium and calcium POST concentrations was observed. Methemoglobin values were not different over the time during the experiments (median (IQR) values 1.100 (0.950–2.850) at 15 min, 1.100 (1.050–2.150) at 30 min, 1.100 (1.050–2.400) at 45 min, 1.200 (1.050–2.900) at 60 min; $p = 0.606$).

As the highest delta pCO_2 was observed when 100 mmol/L NaOH was used, this concentration was employed for the efficiency and efficacy tests.

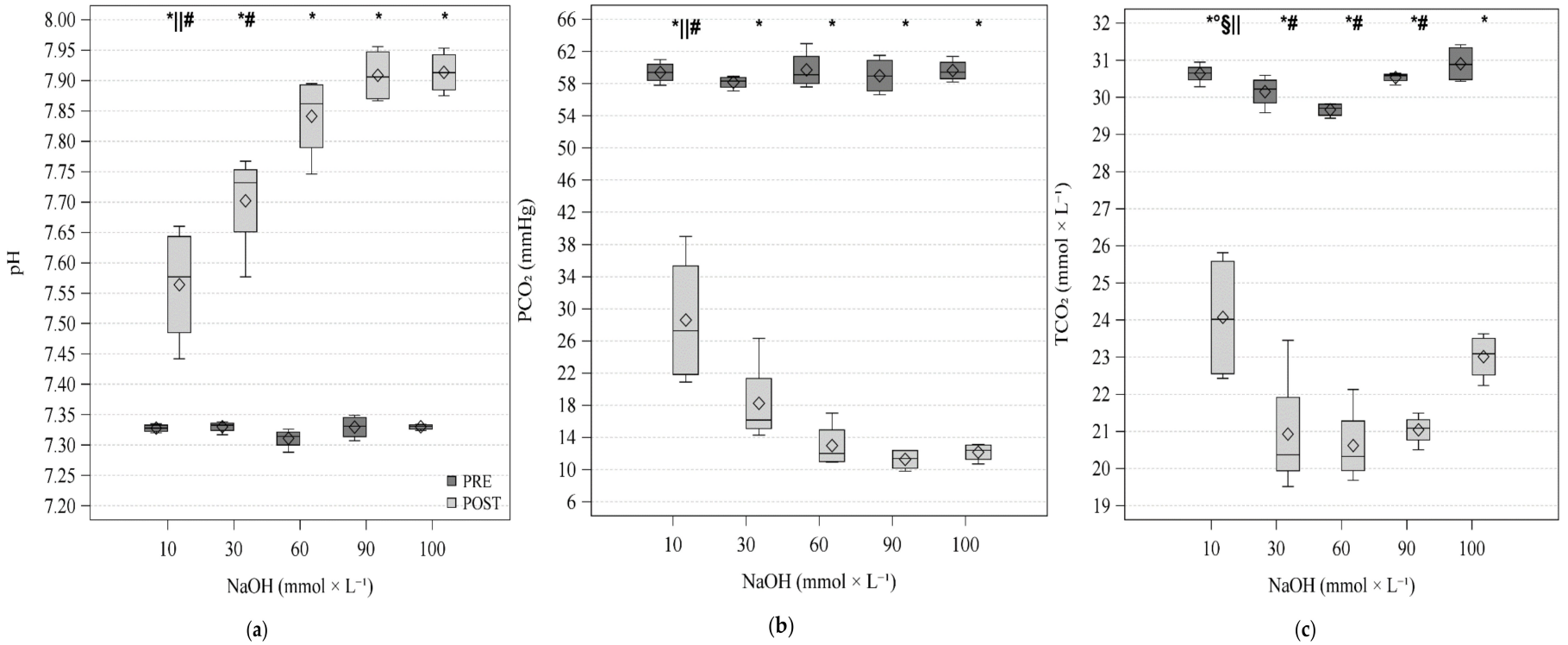

Figure 2: Figures display the distribution of data by using a rectangular box plot and whiskers, the bottom and top edges of the box indicate the intra-quartile range (QR) between the f rst and th rd quart es (the 25th and 75th percent es). The d amond marker ns de the box nd cates the mean va ue. The ne ns de the box nd cates the med an va ue. Wh skers nd cate the range of va ues outs de of the ntra-quart e range but at a d stance ower than the upper and ower fences (±1.5 × QR). Dark grey represents PRE b ood samp ng. L ght grey represents POST b ood samp ng. Stat st ca ana ys s Two-way ANOVA RM (TCO_2) or two-way ANOVA RM on ranks (pH and pCO_2). * $p < 0.05$ vs. PRE; ° $p < 0.05$ vs. 30; § $p < 0.05$ vs. 60; $p < 0.05$ vs. 90, # $p < 0.05$ vs. 100. (a) pH d str but on according at different NaOH concentrat ons,(b) pCO2 (part a pressure of carbon d ox de) d str but on at d fferent NaOH concentrat ons. (c) TCO2 (Carbon dioxide content) d str but on at d fferent NaOH concentrations.

Variable		Ventilation	Flow (L × min^{-1})				*p* Vent.	*p* Flow	*p* Int.
			100	250	500	1000			
pH	PRE $	NaOH	7.346 (7.337–7.374)	7.351 (7.333–7.359)	7.356 (7.333–7.363)	7.336 (7.334–7.366)	**0.027**	0.999	**0.020**
		O_2	7.325 (7.306–7.333) *	7.313 (7.311–7.349) *	7.321 (7.301–7.34) *	7.325 (7.318–7.346)			
	POST $	NaOH	7.972 (7.968–8.057) #	7.987 (7.977–8.077) §#	7.964 (7.932–8.040)	7.938 (7.902–8.008)	**<0.001**	**<0.001**	**<0.001**
		O_2	7.352 (7.333–7.379) *°§#	7.405 (7.374–7.439) *§#	7.481 (7.435–7.514) *#	7.616 (7.612–7.654) *			
	Difference $	NaOH	0.628 (0.597–0.683) #	0.643 (0.624–0.718) §#	0.606 (0.597–0.673)	0.591 (0.565–0.635)	**<0.001**	**<0.001**	**<0.001**
		O_2	0.028 (0.011–0.041) *°§#	0.094 (0.063–0.101) *§#	0.145 (0.124–0.186) *#	0.295 (0.268–0.326) *			
PCO_2 (mmHg)	PRE	NaOH	59.7 (59.2–60.1)	59.5 (59.0–59.7)	59.4 (58.4–60.2)	60.0 (59.2–60.4)	0.909	0.882	0.332
		O_2	59.0 (58.4–59.9)	59.0 (58.7–60.5)	60.6 (59.0–61.0)	59.7 (59.5–59.8)			
	POST	NaOH	11.2 (11.0–13.0)	10.5 (10.3–11.1)	11.7 (11.3–12.1)	13.1 (12.8–13.1)	**<0.001**	**<0.001**	**<0.001**
		O_2	54.6 (53.7–56.2) *°§#	46.2 (45.4–49.7) *§#	40.4 (39.0–41.6) *#	28.2 (26.9–29.1) *			
	Difference	NaOH	−48.3 (−48.9–−47.1)	−48.5 (−50.5–−48.3)	−47.5 (−49.0–−46.3)	−46.5 (−47.6–−45.3)	**<0.001**	**<0.001**	**<0.001**
		O_2	−4.4 (−6.2–−2.0) *°§#	−13.1 (−13.8–−9.5) *§#	−19.1 (−22.8–−17.4) *#	−31.7 (−32.9–−30.7) *			
PO_2 (mmHg)	PRE	NaOH	138.0 (136.0–139.0) #	137.0 (137.0–143.0) #	137.5 (136.0–146.0)	141.5 (137.0–153.0)	0.231	0.460	**0.002**
		O_2	144.0 (141.0–162.0)	143.0 (140.0–159.0)	143.5 (138.0–156.0)	143.0 (139.0–154.0)			
	POST $	NaOH	125.0 (120.0–130.0)§#	130.5 (128.0–140.0) #	148.5 (142.0–157.0)	161.5 (159.0–169.0)	**<0.001**	**<0.001**	0.700
		O_2	595.5 (591.0–602.0) *§#	608.5 (603.0–623.0) *#	616.0 (611.0.–6260) *#	648.0 (632.0–654.0) *			
	Difference	NaOH	−13.0 (−16.0— −11.0)§#	−6.5 (−9.0–−3.0) §#	9.0 (6.0–11.0) #	18.0 (14.0–21.0)	**<0.001**	**<0.001**	0.105
		O_2	451.5 (429.0–461.0) *§#	455.5 (445.0–471.0) *§#	462.5 (453.0–477.0) *#	497.5 (487.0–508.0) *			
K^+ (mEq × L^{-1})	PRE	NaOH	4.1 (4.0–4.4)	4.1 (4.1–4.5)	4.2 (4.1–4.4)	4.2 (4.1–4.5)	0.127	0.594	0.299
		O_2	4.1 (3.9–4.2)	4.0 (4.0–4.2)	4.0 (4.0–4.2)	4.1 (4.0–4.2)			
	POST	NaOH	4.1 (4.0–4.3)	4.1 (4.0–4.4)	4.1 (4.0–4.3)	4.1 (4.0–4.4)	0.265	0.709	0.363
		O_2	4.1 (3.9–4.2)	4.0 (4.0–4.2)	4.0 (4.0–4.1)	4.0 (3.9–4.2)			
	Difference	NaOH	0.0 (0.0–0.1)	0.1 (0.0–0.1)	0.1 (0.1–0.1)	0.1 (0.1–0.1)	**0.009**	0.337	0.86
		O_2	0.0 (0.0–0.0) *	0.0 (0.0–0.0) *	0.0 (0.0–0.0) *	0.0 (0.0–0.1) *			
Na^+ (mEq × L^{-1})	PRE	NaOH	143.0 (142.0–144.0)	143.0 (143.0–144.0)	143.5 (142.0–145.0)	143.5 (143.0–144.0)	**0.038**	0.233	0.973
		O_2	139.0 (138.0–143.0) *	139.0 (139.0–143.0) *	139.5 (138.0–144.0) *	139.5 (138.0–145.0) *			
	POST	NaOH	141.0 (139.0–142.0)	140.0 (140.0–142.0)	140.5 (140.0–141.0)	141.5 (140.0–142.0)	0.407	0.524	0.096
		O_2	139.0 (138.0–143.0)	138.5 (137.0–143.0)	139.0 (138.0–143.0)	138.5 (137.0–143.0)			
	Difference	NaOH	−2.0 (−3.0–−2.0)	−3.0 (−3.0–−2.0)	−3.0 (−4.0–−2.0)	−2.0 (−3.0–−2.0)	**<0.001**	0.215	**0.012**
		O_2	0.0 (0.0–0.0) *#	−1.0 (−1.0–0.0) *	−1.0 (−1.0–−1.0) *	−1.0 (−1.0–−1.0) *			

Variable		Ventilation	Flow (L × min^{-1})				*p* Vent.	*p* Flow	*p* Int.
			100	250	500	1000			
Ca^{++} (mEq × L^{-1})	PRE	NaOH	1.3 (1.3–1.4)	1.4 (1.3–1.4)	1.4 (1.3–1.4)	1.4 (1.3–1.4)	0.755	0.854	0.769
		O_2	1.4 (1.2–1.4)	1.3 (1.2–1.4)	1.3 (1.2–1.4)	1.3 (1.2–1.4)			
	POST	NaOH	1.2 (1.1–1.3)	1.2 (1.1–1.2)	1.2 (1.2–1.3)	1.2 (1.2–1.3)	**0.066**	0.110	**<0.001**
		O_2	1.4 (1.2–1.4) *§#	1.3 (1.2–1.4) *§#	1.3 (1.2–1.3)	1.3 (1.2–1.3)			
	Difference [$]	NaOH	−0.1 (−0.1–−0.1)	−0.2 (−0.2–−0.1)	−0.1 (−0.1–−0.1)	−0.1 (−0.1–−0.1)	**<0.001**	**0.032**	**0.002**
		O_2	0.0 (0.0–0.0) *§#	0.0 (0.0–0.0) *§#	0.0 (0.0–0.0) *	−0.1 (−0.1–−0.1) *			
Cl^{-} (mEq × L^{-1})	PRE	NaOH	111.5 (111.0–113.0)	111.5 (111.0–113.0)	111.5 (111.0–113.0)	111.5 (110.0–113.0)	0.232	0.529	0.529
		O_2	111.0 (111.0–112.0)	111.0 (111.0–112.0)	111.0 (110.0–112.0)	111.0 (110.0–112.0)			
	POST	NaOH	114.0 (114.0–115.0)	114.5 (114.0–115.0)	114.0 (114.0–115.0)	114.0 (114.0–115.0)	**0.002**	**0.042**	**0.002**
		O_2	111.5 (111.0–113.0) *#	111.0 (111.0–113.0) *#	112.0 (111.0— 113.0) *#	112.5 (112.0–114.0) *			
	Difference	NaOH	2.5 (2.0–3.0)	3.0 (2.0–3.0)	2.5 (2.0–3.0)	2.5 (2.0–3.0)	**0.007**	**0.002**	**0.001**
		O_2	0.5 (0.0–1.0) *#	0.0 (0.0–1.0) *§#	1.0 (1.0–1.0) *#	2.0 (1.0–2.0)			
Lac (mEq × L^{-1})	PRE [$]	NaOH	1.4 (0.5–2.3)	1.4 (0.5–2.4)	1.3 (0.5–2.3)	1.4 (0.5–2.5)	0.180	0.361	0.614
		O_2	1.1 (0.4–2.5)	1.2 (0.4–2.6)	1.1 (0.4–2.6)	1.1 (0.4–2.5)			
	POST [$]	NaOH	1.4 (0.5–2.3)	1.5 (0.5–2.3)	1.4 (0.5–2.4)	1.4 (0.5–2.4)	0.197	0.459	0.850
		O_2	1.0 (0.4–2.6)	1.1 (0.4–2.6)	1.2 (0.4–2.6)	1.1 (0.4–2.5)			
	Difference	NaOH	0.0 (0.0–0.0)	−0.1 (−0.1–0.1)	0.1 (0.0–0.1)	0.0 (0.0–0.0)	1.000	0.297	0.922
		O_2	0.0 (0.0–0.0)	0.0 (−0.1–0.0)	0.0 (0.0–0.1)	0.0 (0.0–0.0)			
Hb (g × dL^{-1})	PRE	NaOH	6.45 (5.50–8.20)	6.80 (5.30–8.20)	6.70 (5.30–8.30)	6.70 (5.20–8.10)	0.643	0.641	0.511
		O_2	6.55 (5.50–8.30)	6.60 (5.30–8.20)	6.55 (5.30–8.40)	6.55 (5.40–7.90)			
	POST	NaOH	6.60 (5.50–8.30)	6.70 (5.40–8.20)	6.75(5.40–8.30)	6.60 (5.30–8.20)	0.547	0.083	0.893
		O_2	6.55 (5.50–8.40)	6.60 (5.30–8.20)	6.60 (5.30–8.50)	6.55 (5.40–7.90)			
	Difference	NaOH	0.05 (0.00–0.10)	0 (−0.10–0.00)	0.05 (0.00–0.10)	0.05 (0.00–0.10)	**0.025**	0.661	0.154
		O_2	0.00 (−0.10–0.00) *	0.00 (0.00–0.00) *	0.00 (0.00–0.10) *	0.00 (0.00–0.00) *			
HCO_3^{-} (mmol × L^{-1})	PRE	NaOH	30.1 (29.5–32.2)	30.2 (29.3–31.8)	30.3 (29.4–31.7)	29.8 (29.0–31.8)	0.050	0.508	0.165
		O_2	28.3 (27.6–29.9) *	28.2 (27.6–29.8) *	28.1 (27.5–30.4) *	28.5 (28.2–30.2) *			
	POST	NaOH	25.7 (23.3–29.1)	25.9 (23.2–28.1)	26.4 (23.2–29)	26.3 (23.7–29.7)	0.577	**0.043**	**0.003**
		O_2	28.0 (27.2–28.6) §#	27.5 (26.7–28.6) #	27.0 (26.3–28.2)	26.6 (26.1–27.2)			
	Difference	NaOH	−4.4 (−6.3–−2.4) #	−4.5 (−6.8–−2.4) #	−4.2 (−6.2–−1.3)	−3.9 (−5.7–−1.7)	**0.018**	**0.003**	**<0.001**
		O_2	−0.3 (−0.5–−0.2) *§#	−0.8 (−0.9–−0.6) *§#	−1.3 (−1.7–−1) *#	−2.1 (−2.8–−1.4)			

Variable		Ventilation	Flow (L × min^{-1})				*p* Vent.	*p* Flow	*p* Int.
			100	250	500	1000			
plasma TCO_2 (mmol × L^{-1})	PRE	NaOH	31.9 (31.4–34.1)	32.0 (31.1–33.6)	32.1 (31.3–33.5)	31.7 (30.9–33.6)	0.051	0.476	0.194
		O_2	30.1 (29.5–31.8)	30.1 (29.4–31.5)	30.0 (29.4–32.3)	30.3 (30.1–32.0)			
	POST	NaOH	26.0 (23.6–29.5)	26.3 (23.5–28.4)	26.7 (23.6–29.3)	26.7 (24.1–30.1)	0.258	**0.009**	**<0.001**
		O_2	29.7 (28.9–30.1) §#	29.1 (28.1–30.0) #	28.3 (27.4–29.5) #	27.5 (26.9–28.1)			
	Difference	NaOH	−5.9 (−7.8–−3.9) #	−6 (−8.3–−4.0) #	−5.7 (−7.6–−2.8)	−5.3 (−7.1–−3.3)	**0.006**	**<0.001**	**<0.001**
		O_2	−0.5 (−0.6–−0.3) *°§#	−1.1 (−1.3–−0.9) *§#	−1.9 (−2.2–−1.7) *#	−3.0 (−3.8–−2.3)			
$\dot{V}CO_2$ (mL × min^{-1})		NaOH	65.3 (43.3–86.7) #	67.0 (44.3–92.2) #	63.5 (31.6–84.5)	59.1 (36.4–79)	**0.006**	**<0.001**	**<0.001**
		O_2	5.4 (3.7–6.7) *°§#	12.5 (10.5–14.6) *§#	20.7 (18.6–24.9) *#	33.6 (26.1–42.6)			

Table 1: Abbreviations: pCO_2, partial pressure of carbon dioxide; pO_2, partial pressure of oxygen; Na^+, sodium; K^+, potassium; Ca^{++}, calcium; Cl^-, chloride; Lac, Lactate; Hb, haemoglobin; HCO_3^-, bicarbonate, TCO_2,total CO_2 content, $\dot{V}CO_2$, amount of carbon dioxide removed by the membrane lung. Data are expressed median (IQR); Differences were computed as POST values–PRE values. p: p values of two-way ANOVA RM or two-way ANOVA RM on ranks ($) for NaOH vs. O2 comparison (p Ventilation), Flow effect (p Flow) and interaction (p int.); Post-hoc analysis with Bonferroni or Tukey corrections: * $p < 0.05$ vs. NaOH;° $p < 0.05$ vs. 250 mL/min; § $p < 0.05$ vs. 500 mL/min; # $p < 0.05$ vs. 1000 mL × min−1

Efficiency Test

Blood gas analyses of PRE and POST blood with NaOH and oxygen are reported in Table 1. pCO_{2PRE} was stable throughout the entire test, 59.6 (58.9–60.4) mmHg. Increasing oxygen flows showed increasing CO_2 removal, both as delta pCO_2 across the membrane lung and $\dot{V}CO_2$, see Figure 3. Conversely, all NaOH flows showed similar CO_2 removal, except for a lower $\dot{V}CO_2$ at 1000 mL/min compared to 100 and 250 mL/min. When comparing $\dot{V}CO_2$ achieved with liquid and gaseous ventilation, liquid ventilation achieved significantly higher CO_2 removals for 100, 250, and 500 mL/min of flow. On the contrary, while the median value was higher also for 1000 mL/min, this difference did not reach statistical significance.

Blood pH_{POST} increased, according to the pCO_2 reduction, reaching values as high as 7.987 with NaOH at 250 mL/min. pO_{2PRE} was stable around 141.0 (137.0–147.0) mmHg both during NaOH and oxygen steps while pO_{2POST} increased up to 470.5 (452.3–507.0) mmHg only during oxygenation use, while it remained unchanged during liquid ventilation. Blood electrolytes and lactate concentrations were stable throughout the experiment.

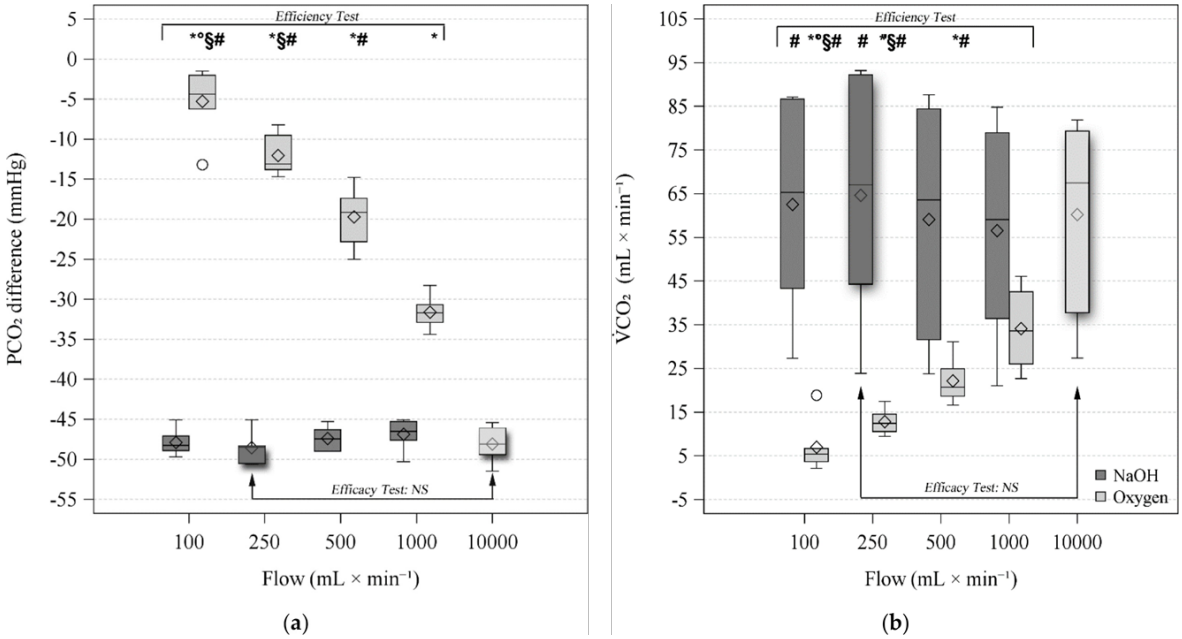

Figure 3: Figures display the distribution of data by using a rectangular box plot and whiskers, the bottom and top edges of the box indicate the intra-quartile range (IQR) between the first and third quartiles (the 25th and 75th percentiles). The diamond marker inside the box indicates the mean value. The line inside the box indicates the median value. Whiskers indicate the range of values outside of the intra-quartile range but at a distance lower than the upper and lower fences (±1.5 × IQR) Dots represent outliers (observations that are more extreme than the upper and lower fences). Dark grey represents NaOH at 100 mmol/L concentration. Light grey represents Oxygen. Efficiency test statistical analysis: Two-way ANOVA RM. * $p < 0.05$ vs. NaOH; ◦ $p < 0.05$ vs. 250 mL/min; § $p < 0.05$ vs. 500 mL/min; # $p < 0.05$ vs. 1000 mL/min. Efficacy test statistical analysis: Paired t-test between NaOH at 100 mmol/L concentration and 250 mL/min sweep flow and oxygen at 1000 mL/min sweep flow (boxes highlighted by outside shadow and arrows).(a) pCO_2 (partial pressure of carbon dioxide) difference (POST values–PRE values) distribution according to different sweep flows of NaOH and Oxygen. (b) . $\dot{V}CO_2$ (Carbon dioxide transfer across the membrane lung) distribution according to different sweep flows of NaOH and Oxygen.

Efficacy Tests

In agreement with the highest $\dot{V}CO_2$ and delta pCO_2, NaOH 250 mL/min was selected as the most performant NaOH flow and compared with 10 L/min of oxygen in the efficacy test. Table 2 reports blood gas analyses of PRE and POST blood. Both delta pCO_2 and $\dot{V}CO_2$ were similar, suggesting similar extracorporeal CO_2 removal (Figure 3, shadowed boxes)

Variable		Ventilation		
		NaOH 250 mL × min^{-1}	O_2 10,000 mL × min^{-1}	*p*
pH	PRE	7.351 (7.333–7.359)	7.328 (7.322–7.355)	**0.032**
	POST	7.987 (7.977–8.077)	7.966 (7.921–8.013)	**0.020**
	Difference	0.643 (0.624–0.718)	0.627 (0.599–0.685)	0.094
PCO_2 (mmHg)	PRE	59.5 (59–59.7)	60 (59.3–60.5)	0.254
	POST	10.5 (10.3–11.1)	11.5 (10.8–13.9)	0.106
	Difference	−48.5 (−50.5–−48.3)	−48.1 (−49.4–−46.1)	0.522
PO_2 (mmHg)	PRE $	137 (137–143)	139 (137–165)	0.625
	POST	130.5 (128–140)	661.5 (649–677)	**<0.001**
	Difference	−6.5 (−9–−3)	518.5 (509–536)	**<0.001**
K^+ (mEq × L^{-1})	PRE	4.1 (4.1–4.5)	4.2 (4–4.4)	0.611
	POST $	4.1 (4–4.4)	4.1 (4–4.3)	0.438
	Difference	0.1 (0–0.1)	0.1 (0–0.1)	1.000
Na^+ (mEq × L^{-1})	PRE	143 (143–144)	142 (141–145)	0.516
	POST	140 (140–142)	139.5 (139–143)	1.000
	Difference	−3 (−3–−2)	−2 (−2–−2)	0.102
Ca^{++} (mEq × L^{-1})	PRE	1.4 (1.3–1.4)	1.3 (1.3–1.4)	0.927
	POST	1.2 (1.1–1.2)	1.2 (1.1–1.3)	0.413
	Difference	−0.2 (−0.2–−0.1)	−0.1 (−0.1–−0.1)	0.067
Cl^- (mEq × L^{-1})	PRE $	111.5 (111–113)	111.5 (111–112)	0.813
	POST	114.5 (114–115)	115 (114–115)	1.000
	Difference	3 (2–3)	3 (2–3)	0.611
Lac (mEq × L^{-1})	PRE $	1.4 (0.5–2.4)	1.3 (0.5–2.5)	0.375
	POST	1.5 (0.5–2.3)	1.2 (0.4–2.5)	0.233
	Difference	−0.1 (−0.1–0.1)	0 (−0.1–0)	1.000
Hb (g × dL^{-1})	PRE	6.80 (5.30–8.20)	6.55 (5.50–8.40)	0.499
	POST	6.70 (5.40–8.20)	6.55 (5.40–7.90)	0.590
	Difference	0.00 (−0.10–0.00)	0.00 (0.00–0.00)	0.363
HCO_3^- (mmol × L^{-1})	PRE	30.2 (29.3–31.8)	29.4 (28.7–30.6)	0.205
	POST	25.9 (23.2–28.1)	25.1 (23.1–28.1)	0.652
	Difference	−4.5 (−6.8–−2.4)	−4.6 (−5.7–−1.8)	0.185
plasma TCO_2 (mmol × L^{-1})	PRE $	32 (31.1–33.6)	31.3 (30.6–32.5)	0.313
	POST	26.3 (23.5–28.4)	25.5 (23.5–28.4)	0.695
	Difference	−6 (−8.3–−4)	−6.1 (−7.1–−3.4)	0.191
$\dot{V}CO_2$ (mL × min^{-1})		67 (44.3–92.2)	67.4 (37.8–79.4)	0.191

Table 2: Abbreviations: pCO_2, partial pressure of carbon dioxide; pO_2, partial pressure of oxygen; Na^+, sodium; K^+, potassium; Ca^{++}, calcium; Cl^-, chloride; Lac, Lactate; Hb, hemoglobin; HCO_3^-, Bicarbonate, TCO_2, total CO_2 content, $\dot{V}CO_2$, amount of carbon dioxide removed by the membrane lung. Data are expressed median (IQR); Differences were computed as POST values–PRE values. p: p values of Paired t-test or Wilcoxon Signed Rank Test ($) for NaOH (250 mL × min−1) vs. O_2 (10,000 mL × min−1) comparison.

Discussion

This in-vitro study shows that continuous infusion (from 100 to 1000 mL/min) of highly concentrated sodium hydroxide solutions into the gas side of conventional polypropylene oxygenators is feasible, despite pH values of the sweeping solution above 12. At low sweep flows, alkaline liquid ventilation showed significantly higher CO_2 removal capacity than conventional gaseous ventilation. However, the maximum CO_2 removal efficiency achieved through liquid ventilation was not superior to the one achieved with 10 L/min of sweep gas flow.

The working hypothesis underlying this study was to exploit the high CO_2 absorbing capacity of NaOH solutions. Indeed, in our experimental context, the concentration of NaOH was always significantly higher than the amount of CO_2 extracted from the ML. The pCO_2 of the alkaline sweep fluid was persistently very close to 0 mmHg, as the added CO_2 was instantly hydrated and dissociated to bicarbonate and carbonate. This allowed to keep the pCO_2 close to zero and thus optimize the transmembrane pCO2 gradient, favoring the efficiency of extracorporeal CO_2 removal.

Indeed, a solution containing 10 mEq of NaOH could absorb 200 mL of CO_2 while maintaining pCO_2 close to zero. On the contrary, the same amount of CO_2 added to 10 L of gas would result in a pCO_2 around 15 mmHg, therefore reducing the blood-gas CO_2 gradient.

However, the data showed that increasing NaOH flow did not lead to a linear increase in CO_2 removal. Instead, for NaOH flows greater than 250 mL/min there was an unexpected reduction in CO_2 removal. This reduced efficiency could depend on the density of the sodium hydroxide solution and the mechanics of the membrane lung. Therefore, a clinical application of alkaline liquid ventilation does not seem exploitable using the current technology. The technical complexity and safety profile require further evaluations, although the present tests have recorded no damage to the membrane lung.

Another important difference between gaseous and liquid ventilation needs to be discussed. Although the oxygenation capacity of low-flow devices using conventional gaseous ventilation is limited by the amount of blood reaching the ML, a certain amount of oxygen is added to the blood. On the contrary, the NaOH infusion does not oxygenate the extracorporeal blood, limiting its potential clinical application to patients with isolated hypercapnic respiratory failure, i.e., able to oxygenate properly through their native lungs.

Although devices with higher CO_2 extraction capacity resulted more effective[64–66], numerous studies confirm the ability of $ECCO_2R$ to achieve physiological targets. Nevertheless, the clinical application of $ECCO_2R$ is still limited and no conclusive indications have been identified mainly because of safety concerns[67,68]. Indeed, a consistently high rate of complications has been reported,

mostly related to hemolysis, bleeding, and thrombosis. In this context, the present study aim was to achieve a highly efficient $ECCO_2R$ technique to ensure a clinical efficacy with limited extracorporeal blood flows, potentially enabling regional anticoagulation[69,70]. The tested technology, which was not developed for alkaline liquid ventilation, did not meet such expectations. However, we cannot exclude that a dedicated device could achieve more satisfying results.

This study presents several limitations. First, we could not perform any gas analysis of the sodium hydroxide solution. The CO_2 extraction capacity was estimated both as differences in pCO_2 and TCO_2 between the blood samples upstream and downstream of the artificial lung[71]. $\dot{V}CO_2$ showed higher variability than pCO_2, as shown in Figure 3, possibly due to the baseline different blood composition. Indeed, we can speculate that this phenomenon may be explained by the wide range in haemoglobin concentrations (Table 1), which affects the ML $\dot{V}CO2$[72]. Secondly, the alkaline liquid ventilation was tested only in vitro and for a limited time consequently we cannot exclude different effects and safety issues in vivo scenarios. Thirdly, we only tested one type of polypropylene membrane lung. Further tests with different devices may be required.

The role of Hematocrit during extracorporeal CO2 Removal an in vitro evaluation

Background

A previously described, low-flow extracorporeal CO_2 removal ($ECCO_2R$) devices have been used in patients with moderate acute respiratory distress syndrome and acute exacerbations of chronic obstructive pulmonary disease to remove the excess CO_2, while maintaining lung protective or noninvasive ventilation[73–76]. $ECCO_2R$ devices operate on analogous principles to extracorporeal membrane oxygenation, but at blood flow rates below 1 L/min[77] as their primary objective is removing CO_2 rather than oxygenation.

CO_2 is transported into the blood in three different forms: dissolved, as bicarbonates or as carbaminic compounds (see paragraph carbon dioxide removal). Hemoglobin plays an important role in CO_2 transport and as consequence in $\dot{V}CO_2$. The mechanisms for CO_2 removal, related to Hematocrit (HCT), are three: the classical Bohr and Haldane shifts involving intraerythrocytic hemoglobin[78], the total surface area available for HCO_3^-/Cl^- exchange across the red cell membrane[79], and the red cell surface area that passes through the capillary bed. Inside the red blood cells, oxygenation of reduced hemoglobin (Hb) results in the liberation of a large number of Bohr protons, which help drive the dehydration of H_2CO3 under the influence of carbonic anhydrase[80] and enhance CO_2 elimination.

In 1985, Bidani and Crandall, demonstrate, using a computation model that a decrease in HCT results in a decrease in $\dot{V}CO_2$[81].

In 2020, May et al. studied the effects of the relationship between HCT and the $\dot{V}CO_2$ of a membrane lung during a low-flow $ECCO_2R$ in an in vitro setting[72], on the basis of previous evidence reported in animal studies during periods of anemia[82]. Unfortunately, the complexities of animal studies make isolating the artificial lung $\dot{V}CO_2$–HCT relationship challenging; therefore, in vitro studies seem to be more appropriate to investigate this topic.

In this study, we tested a low flow $ECCO_2R$ in vitro setting device able to modify haematocrit through a hemodiafilter, in order to verify the effects of anaemia during dilution phases and to verify and evaluate this system as a potential strategy to increase $\dot{V}CO_2$ during concentration phases, keeping the inlet pCO_2 and the sweep gas flow constant.

Materials and Methods

In vitro circuit design

An in vitro setting (Figure 1) was built to simulate a patient undergoing extracorporeal CO_2 removal, and to allow different steps of hemoconcentration or hemodilution (Figure 2 and 3).

A closed-loop circuit was assembled with 3/8 and 1/4 inch polyvinylchloride class IV medical tubes (Medtronic, Minneapolis, USA), one 4 L reservoir (VHK 71000 venous hardshell cardiotomy reservoir, Getinge, Sweden), one polypropylene oxygenator membrane gas exchanger (Quadrox-i Small adult HMO 50000, Getinge, Sweden) and one polymethylpentene hollow fiber oxygenator (Sorin Lilliput2 ECMO, Livanova, United Kingdom).

According to the step of the experiment, a Hemodiafilter (AV1000S, Fesenius Medical Care, Bad Homburg, Germany) and different numbers of peristaltic pumps (Multiflow Roller Pump Module H10 series, Stöckert Shiley, München, Germany and PD 5206 Pump Drive, Heidolph Instruments GmbH and Co, Schwabach, Germany) were used to vary the haematocrit concentration, as shown in figure 1. The study was divided into five steps: hematocrit baseline (0%), hematocrit +10%, hematocrit +20%, hematocrit -10%, and hematocrit -20%.

The circuit was primed with about 3 L of swine blood collected at a local abattoir during usual slaughtering processes in compliance with CE regulations (1069/2009). MultiBic® solution (Fresenius Medical Care Italia, Palazzo Pignano, Italy) was added to achieve a total volume of about 4 L. Sodium Heparin 25000 I.U. (Pfizer Italia S.r.l Latina, Italy), ACD 300 mL (Fresenius Kabi Italia, Isola Della Scala, Italy) and cefazolin 1 g (Teva Italia, Milano, Italy) were added to the blood. Five different samples of swine blood were tested and for each sample two measurements for each step were recorded.

A continuous dialysis was set to clear lactate so as to keep it below 2.5 mmol/L during the entire experiment. Moreover, dialysis was used in the first phase of the experiment to reach the target baseline hematocrit, reported in Table 1. The dialysis unit was arranged in the first section of the circuit so as not to interfere with the experiment. MultiBic® solution with potassium 4 mmol/L acted as dialysate, running at 500ml/h through a dialysator (Fx 100, Fresenius Medical Care, Bad Homburg, Germany). Two peristaltic pumps were used to perform dialysis: one for waste and dialysate (Agila MC Volumat, Fresenius Kabi, Le Grand Chemin, France) and one for blood (PD 5206 Pump Drive, Heidolph Instruments GmbH and Co, Schwabach, Germany).

Downstream of the reservoir, the first gas exchanger was ventilated with a gas mixture of air and CO_2, in order to maintain a constant PCO_2 of 50±2 mmHg at the inlet of the second oxygenator

throughout all experiments. The second oxygenator was employed to remove CO_2 using oxygen sweep gas flow at a rate of 5 L/min.

Circuit accesses for blood sampling were positioned: downstream the first gas exchanger to verify the starting hematocrit and pCO_2; upstream (PRE) and downstream (POST) the second hollow fiber oxygenator to check variations in hematocrit and blood gas analysis.

All the in-vitro treatments were performed keeping a constant, 250 mL/min blood flow at the blood inlet port of the oxygenator.

The blood temperature was kept stable at 37°C through heat exchangers connected to the membrane lungs.

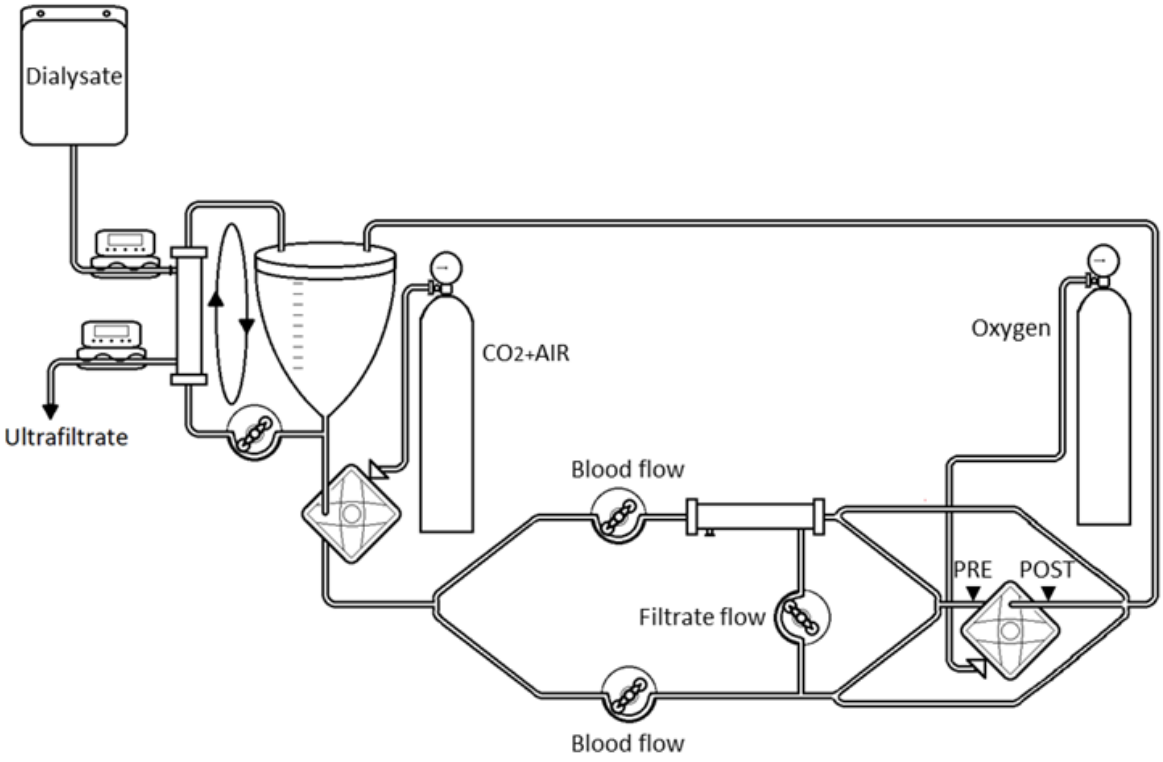

Figure 1: A complete circuit scheme as assembled during the study

Concentration and dilution

Concentration was obtained by activating a peristaltic pump which pushed the filtrate through the hemodiafilter along the circuit. The flows of blood and filtrate were set so as to reach the target hematocrit while maintaining blood flow at the oxygenator blood inlet port at 250 mL/min. Filtrate was added into the main blood flow downstream the oxygenator and reached the reservoir, as showed in figure 2.

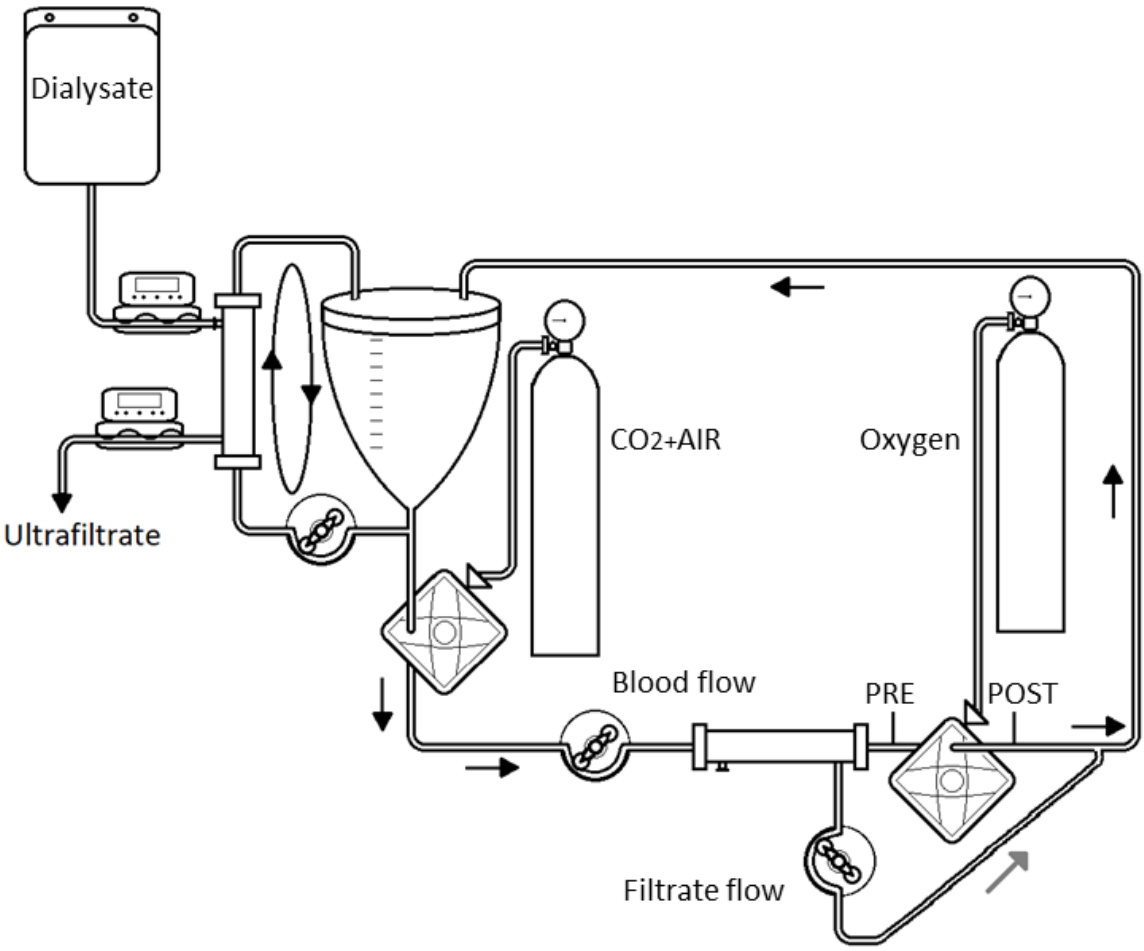

Figure 2: A simplified version of the circuit with the parts of the system used during the concentration phases: black arrows show the flow direct to the membrane lung, Grey arrow shows the filtrate flow that bypass the membrane lung during concentration phases; withdrawal ports are reported as PRE and POST.

Dilution was achieved by separating the main blood flow into two branches: a main blood branch, and a secondary branch running through the hemodiafilter. The obtained filtrate was then mixed to the main blood branch before flowing into the oxygenator. Here too, the resulting diluted blood flew into the inlet port of the oxygenator at 250 mL/min. Downstream the oxygenator the two branches flew together to reservoir, as showed in figure 3.

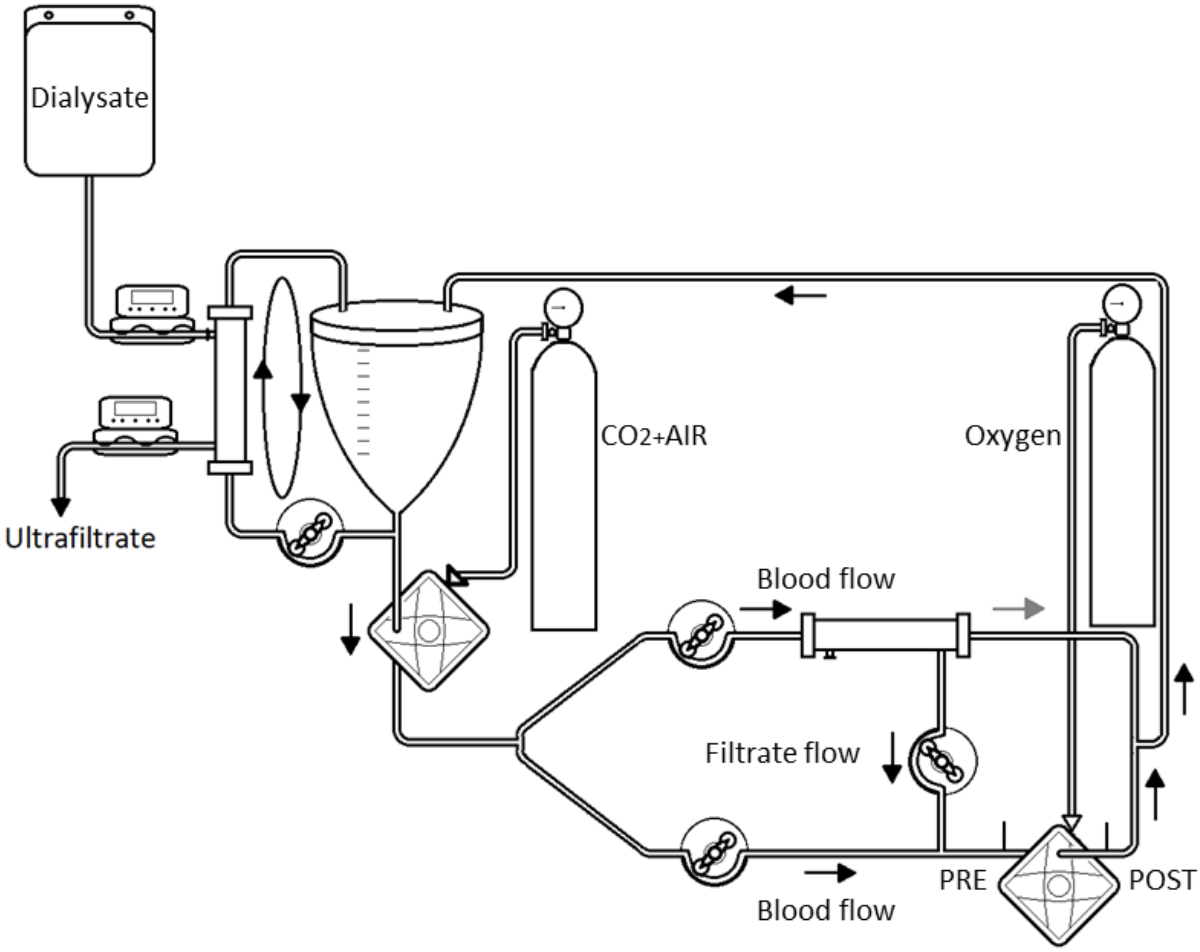

Figure 3: A simplified version of the circuit with the parts of the system used during the dilution phases: black arrows show the flow that is direct to the membrane lung, grey arrow shows the flow concentrate blood flow that bypass the membrane lung during dilution phases; withdrawal ports are reported as PRE and POST.

Experimental design

Baseline was defined as the haematocrit measured after circuit priming and lactate clearance. Four different Haematocrit percentages (treatments) were compared with the baseline.

Five different swine blood samples were tested and for each the order of the treatments was randomized; only the baseline steps (two for each blood) were performed always as first and at half of the experiment.

Variable treatments will assume values according to the different percentage of HCT evaluated (dilution treatments -20%, -10%; concentration treatments +10%, +20%); the membrane lung will assume variable effect PRE and POST.

A WMA-4 gas analyser (PP Systems, Amesbury, MA) was used to measure the CO_2 concentration of the exhaust sweep gas.

This was a within subject study design related to membrane lung effect and treatments with replicates. Before to compare the effect of treatments compared to baseline, HCT has been analysed as continuous variable to verify the effect on $\dot{V}CO_2$. Moreover, the inlet pCO_2 that has been kept during the experiment in range 50±2 mmHg, has been compared to normalized pCO_2, according to the formula used by Golob et al. to verify the effect of these variations[83].

Statistical analysis

Data were represented as mean and standard deviation. The repeated measure data were analyzed using the 'mean response profile' method[84] through generalized estimating equations (GEE) by employing identity link function. GEE standard errors were calculated with a sandwich estimator. We used the compound symmetry as correlation structure selected by correlation information criterion[85].

The linear predictor of GEE regression model was build using membrane lung effect and treatments variables with their interactions. The null hypothesis is that the difference of response variables between the different treatments was constant over time. This was verified using the multivariate Wald test, for testing Time * Treatment interaction in the GEE model. Profile likelihood Confidence intervals (CIs) at 95% confidence level were computed. The univariate Wald test was performed to evaluate the statistical significance of each GEE-estimated parameter. Post-hoc interaction constrast were performed using marginals means with Tukey adjustment.

Confidence intervals (CIs) were at 95% and 2-sided p values were calculated. A p value of < 0.05 was considered statistically significant. All analyses and graphs were carried out using an R software (version 3.2.2).

Results

A summary of all the parameters recorded during the experiment has been reported in table 1. All variables are presented as mean and standard deviation; Wald test has been used to verify the effect of HCT variations and that of the membrane lung (PRE vs. POST) and their interactions. According with study design, we reported different HCT% variations starting from different baseline, categorized as reported in table1.

Variable		Treatment Δ HCT %							
		-20	-10	0	10	20	*p* ΔHCT	*p* pre vs post	*p* Int.
HCT		16.8 (±2.3)	26.52 (±2.1)	35.5 (±1.86)	44.74 (±1.76)	53.94 (±2.4)			
pH	PRE	7.43 (±0.04)	7.43 (±0.04)	7.39 (±0.04)	7.41 (±0.02)	7.41 (±0.02)	<0.01	<0.01	<0.01
	POST	7.96 (±0.01)	7.92 (±0.05)	7.81 (±0.06)	7.76 (±0.06)	7.72 (±0.04)			
pCO2 (mmHg)	PRE	50.48 (±1.39)	49.48 (±1.8)	50.32 (±0.98)	49.58 (±0.69)	50.15 (±1.02)	<0.01	<0.01	<0.01
	POST	13.75 (±1.01)	14.59 (±1.21)	15.74 (±1.64)	16.91 (±2.48)	17.45 (±1.75)			
pO_2 (mmHg)	PRE	146.4 (±0.97)	145.1 (±2.47)	143.4 (±4.09)	143.3 (±2.87)	142.2 (±3.05)	<0.01	<0.01	<0.01
	POST	607.3 (±29.25)	627.3 (±17.91)	596.5 (±74.03)	637.1 (±42.36)	659.3 (±22.9)			
K^+ (mEq/L)	PRE	4.15 (±0.05)	4.14 (±0.07)	4.12 (±0.1)	4.11 (±0.1)	4.16 (±0.13)	<0.01	<0.01	<0.01
	POST	4.10 (±0.05)	4.08 (±0.04)	4.01 (±0.1)	4.05 (±0.1)	4.16 (±0.13)			
Na^+ (mEq/L)	PRE	141.8 (±1.81)	141.7 (±1.76)	141.2 (±2.04)	141.5 (±1.77)	142.5 (±1.43)	<0.01	<0.01	<0.01
	POST	140.6 (±1.95)	139.8 (±1.98)	138.8 (±1.81)	139.2 (±1.87)	139.7 (±1.25)			
Ca^{++} (mEq/L)	PRE	1.23 (±0.06)	1.22 (±0.06)	1.12 (±0.2)	1.13 (±0.18)	1.15 (±0.14)	0.014	<0.01	<0.01
	POST	1.13 (±0.06)	1.14 (±0.07)	1.06 (±0.2)	1.08 (±0.19)	1.09 (±0.15)			
Cl^- (mEq/L)	PRE	109.1 (±2.51)	109.4 (±2.75)	109.1 (±3.24)	109.3 (±2.83)	109.1 (±3.03)	<0.01	<0.01	<0.01
	POST	110.1 (±2.13)	111.1 (±2.99)	111.3 (±3.16)	112.0 (±3.05)	112.4 (±3.40)			
Lac (mEq/L)	PRE	1.09 (±0.48)	1.07 (±0.48)	1.42 (±0.53)	1.28 (±0.39)	1.37 (±0.52)	<0.01	0.73	<0.01
	POST	1.06 (±0.46)	1.09 (±0.46)	1.40 (±0.53)	1.33 (±0.40)	1.31 (±0.46)			
Hb (g/dL)	PRE	5.39 (±0.78)	8.50 (±1.03)	11.46 (±0.61)	14.59 (±0.60)	17.65 (±0.79)	<0.01	0.038	<0.01
	POST	5.41 (±0.79)	8.42 (±0.89)	11.44 (±0.65)	14.56 (±0.61)	17.61 (±0.68)			
HCO_3^- (mmol/L)	PRE	30.9 (±2.1)	30.3 (±2.05)	28.4 (±2.7)	28.9 (±1.5)	29.2 (±1.2)	<0.01	<0.01	<0.01
	POST	30.8 (±2.3)	27.9 (±1.6)	23.1 (±2.4)	22.0 (±1.0)	20.8 (±0.5)			
plasma TCO_2 (mmol/L)	PRE	32.4 (±2.1)	31.8 (±2.0)	29.9 (±2.7)	30.5 (±1.5)	30.7 (±1.2)	<0.01	<0.01	<0.01
	POST	31.2 (±2.3)	28.3 (±1.6)	23.6 (±2.4)	22.6 (±1.0)	21.4 (±0.6)			
VCO_2 (mL/min)		31.0 (±4.8)	37.3 (±5.7)	42.5 (±6.3)	44.9 (±6.6)	48.7 (±7.5)	<0.01		

Table1: Data are reported as mean and standard deviation (SD). Variable are divided according to treatments, HCT variations and PRE - POST according to the membrane lung side.

No differences have been reported in Inlet pCO_2 when was compared between baseline and treatments. Compared to baseline, the treatment with -20% Delta HCT obtained a reduction in pCO_2 from PRE to POST of -2.15 mmHg, while the +20% Delta HCT treatment gave a decrement of 1.88 mmHg. No significant variations were found between baseline and treatment with -10% Delta HCT (estimate -0.31, p 0.71). The pCO_2 distribution pre and post different treatments is showed in Figure 4.

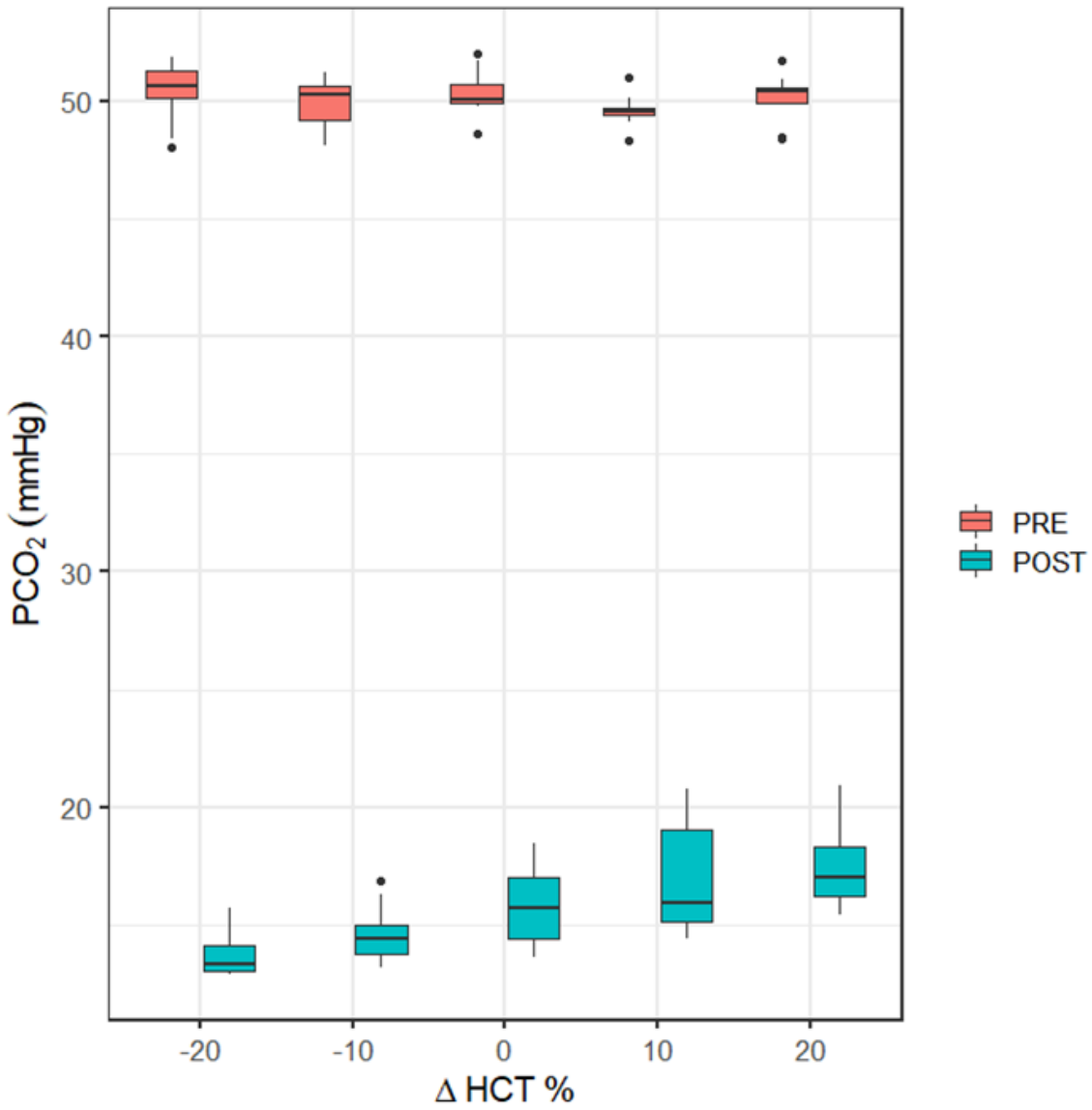

Figure 4: pCO_2 (partial pressure of carbon dioxide) distribution, PRE and POST values according to different HCT variations by using a rectangular box plot and whiskers; the bottom and top edges of the box indicate the interquartile range (IQR) between the first and third quartiles (the 25th and 75th percentiles). The line inside the box indicates the median value. Whiskers indicate the range of values outside of the intra-quartile range but at a distance lower than the upper and lower fences (±1.5 × IQR). Dots indicate outliers.

The GEE model considering HCT as continuous variable showed a significant association between HCT and $\dot{V}CO_2$. In particular, the estimated intercept was 24.52 (95% C.I. 22.07-26.97) $p<0.01$ and the slope was 0.46 (95% C.I. 0.385-0.538) with marginal $R^2=0.596$. In light of this, each increase of one unit of HCT% determines a linear increase of 0.46 ml/min in $\dot{V}CO_2$ (figure 5).

The sensitivity analysis showed closer results refitting pCO_2 using normalized pCO_2 (intercept 24.34, slope 0.46)

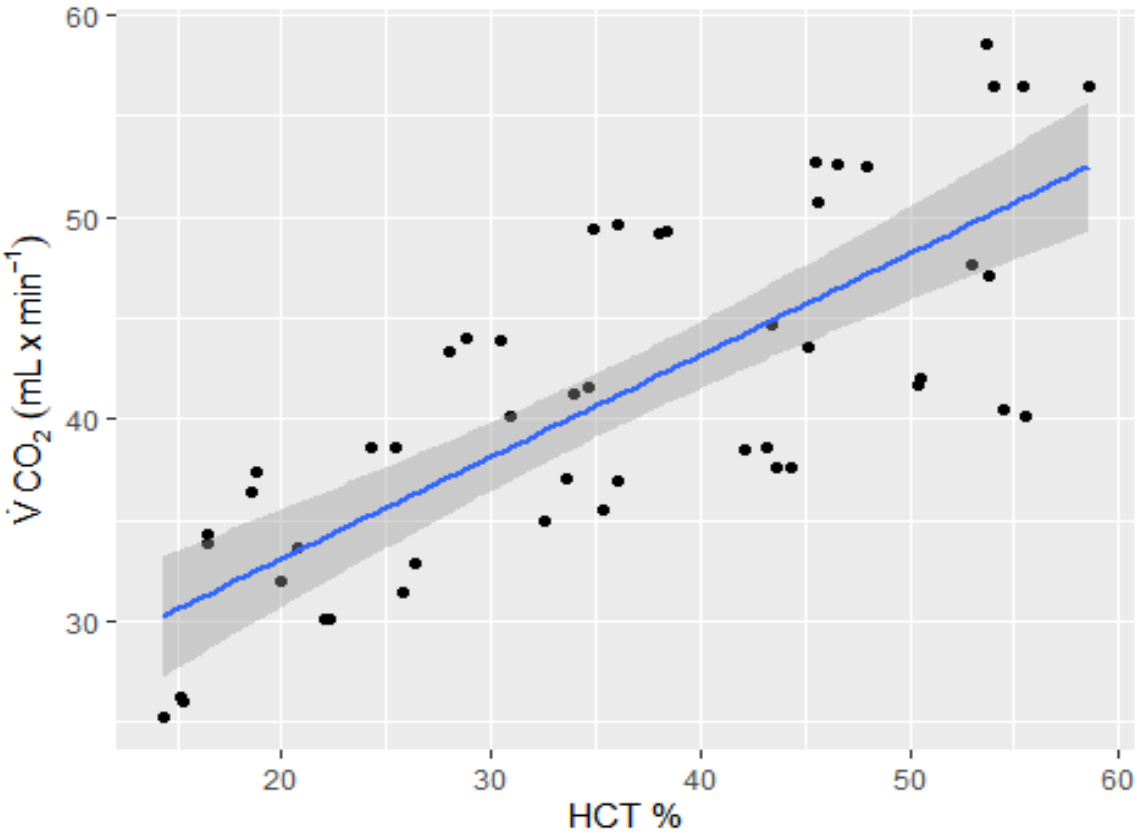

Figure 5: Linear distribution between $\dot{V}CO_2$ and HCT. Dots represent the observed points; blue line, GEE model regression line R=0.596.

According with study design, we categorized different HCT% variations starting from different baseline, as reported in table 1.

The $\dot{V}CO_2$ was our primary outcome. As reported in Figure 6 and table 2, $\dot{V}CO_2$ decreased during the dilution steps and an increased during the concentration steps compared to baseline. This difference was always significant between all the treatments, as reported in table 2 and table 3. The maximal increase compared to baseline has been recorded at steps +20% Delta HCT, with an increment of 6.23 mL/min.

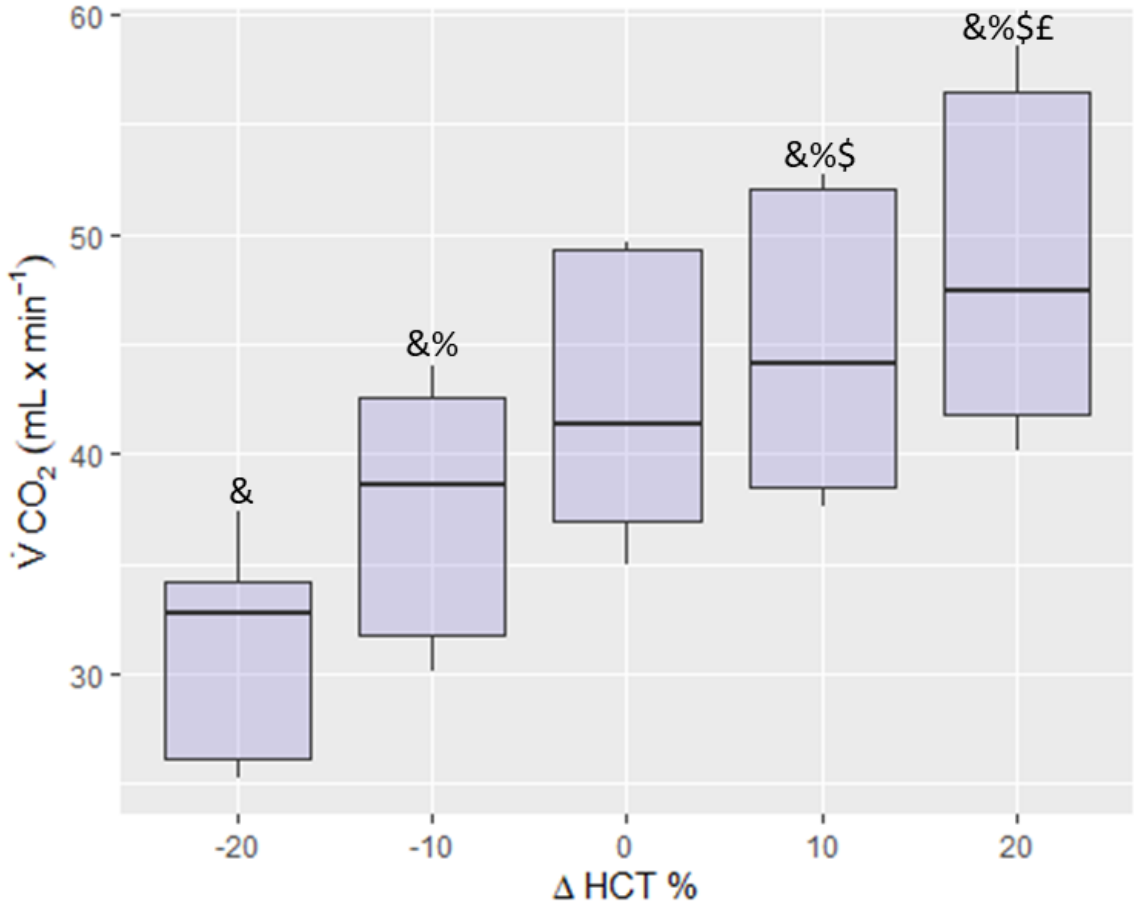

Figure 6: The distribution of $\dot{V}CO_2$ according to different HCT variations by using a rectangular box plot and whiskers; the bottom and top edges of the box indicate the interquartile range (IQR) between the first and third quartiles (the 25th and 75th percentiles). The line inside the box indicates the median value. Whiskers indicate the range of values outside the interquartile range but at a distance lower than the upper and lower fences (±1.5 × IQR). &) p<0.01 vs. 0 (baseline); %) p<0.01 vs. -20; $) p<0.01 vs. -10; £) p<0.01 vs. 10.

	Intercept			Treatment				Post vs. Pre			Interaction between treatment and Post vs. Pre			
	Estimate	CI 95%	p		Estimate	CI 95%	p	Estimate	CI 95%	p		Estimate	CI 95%	p
pH	7.39	7.37 – 7.41	<0.01	-20 vs. 0	0.03	0.02 – 0.05	<0.01	0.41	0.38 – 0.45	<0.01	-20 vs. 0	0.15	0.12 – 0.18	<0.01
				-10 vs. 0	0.03	0.01 – 0.05	<0.01				-10 vs. 0	0.07	0.05 – 0.1	<0.01
				10 vs. 0	0.01	0.00 – 0.03	0.01				10 vs.. 0	-0.06	-0.07 – -0.05	<0.01
				20 vs. 0	0.01	0.00 – 0.03	0.10				20 vs. 0	-0.10	-0.12 – -0.08	<0.01
pCO2 mmHg	50.32	49.72 – 50.91	<0.01	-20 vs. 0	0.16	-1.15 – 1.47	0.81	-34.58	-36.02 – -33.13	<0.01	-20 vs. 0	-2.15	-3.73 – -0.56	<0.01
				-10 vs. 0	-0.55	-2.26 – 0.58	0.24				-10 vs. 0	-0.31	-1.95 – 1.33	0.71
				10 vs. 0	-0.74	-1.45 – -0.02	0.05				10 vs. 0	1.91	1.42 – 2.39	<0.01
				20 vs. 0	-0.17	-1.26 – 0.92	0.76				20 vs. 0	1.88	0.49 – 3.26	<0.01
pO2 mmHg	143.4	140.5 – 146.2	<0.01	-20 vs. 0	3.0	0.17 – 5.82	0.38	453.1	417.7 – 488.4	<0.01	-20 vs. 0	7.8	-20.68 – 36.28	0.59
				-10 vs. 0	1.7	-0.92 – 4.32	0.2				-10 vs. 0	29.1	-14.55 – 72.75	0.19
				10 vs.. 0	-0.1	-1.9 – 1.7	0.91				10 vs. 0	40.7	0.43 – 80.96	0.04
				20 vs. 0	-1.2	-3.09 – 0.69	0.21				20 vs. 0	64.0	32.47 – 95.52	<0.01
K^+ mEq/L	4.12	4.05 – 4.18	<0.01	-20 vs. 0	0.03	-0.04 – 0.10	0.44	-0.11	-0.12 – -0.09	<0.01	-20 vs. 0	0.06	0.01 – 0.1	<0.01
				-10 vs. 0	0.02	-0.05 – 0.09	0.58				-10 vs. 0	0.05	0.00 – 0.09	0.04
				10 vs.. 0	-0.01	-0.02 – 0.00	0.26				10 vs.. 0	0.05	0.02 – 0.07	<0.01
				20 vs. 0	0.04	-0.00 – 0.08	0.06				20 vs. 0	0.03	-0.01 – 0.07	0.18

	Intercept			Treatment				Post vs. Pre			Interaction between treatment and Post vs. Pre			
	Estimate	CI 95%	p		Estimate	CI 95%	p	Estimate	CI 95%	p		Estimate	CI 95%	p
Na^+ mEq/L	141.2	140 – 142.4	<0.01	-20 vs. 0	0.6	0.08 – 1.11	0.02	-2.4	-2.72 – -2.07	<0.01	-20 vs. 0	1.2	0.84 – 1.55	<0.01
				-10 vs. 0	0.5	-0.05 – 1.05	0.07				-10 vs. 0	0.5	0.02 – 0.98	0.04
				10 vs. 0	0.3	-0.29 – 0.89	0.32				10 vs. 0	0.1	-0.22 – 0.42	0.55
				20 vs. 0	1.3	0.13 – 2.46	0.02				20 vs. 0	0.4	-1.04 – 0.24	0.22
Ca^{++} mEq/L	1.11	0.97 - 1.25	<0.01	-20 vs. 0	0.11	0.02 – 0.21	0.15	-0.05	-0.06 – -0.05	<0.01	-20 vs. 0	-0.04	-0.05 – -0.03	<0.01
				-10 vs. 0	0.1	0.01 – 0.2	0.28				-10 vs. 0	-0.02	-0.03 – -0.02	<0.01
				10 vs. 0	0.02	-0.002 – 0.04	0.08				10 vs. 0	0.002	-0.003 – 0.007	0.51
				20 vs. 0	0.03	0.00 – 0.07	0.04				20 vs. 0	-0.003	-0.16 – 0.01	0.65
Cl^- mEq/L	109.1	106.4 – 111.7	<0.01	-20 vs. 0	0.00	-0.61 – 0.62	1	2.2	1.98 – 2.41	<0.01	-20 vs. 0	-1.2	-1.79 – 0.6	<0.01
				-10 vs. 0	0.3	-0.14 – 0.74	0.18				-10 vs. 0	-0.5	-0.98 – -0.02	0.04
				10 vs. 0	0.2	-0.15 – 0.55	0.26				10 vs. 0	0.5	0.02 – 0.98	0.04
				20 vs. 0	0.00	-0.48 – 0.48	1				20 vs. 0	1.1	0.45 – 1.74	<0.01
Lac mEq/L	1.42	1.05 – 1.78	<0.01	-20 vs. 0	-0.33	-0.57 - -0.08	<0.01	-0.2	-0.06 – 0.02	0.38	-20 vs. 0	-0.01	-0.16 – 0.14	0.89
				-10 vs. 0	-0.35	-0.55 - -0.14	<0.01				-10 vs. 0	0.04	0.01 – 0.09	0.17
				10 vs.. 0	-0.14	-0.24 - -0.03	<0.01				10 vs. 0	0.07	0.02 – 0.11	<0.01
				20 vs. 0	-0.05	-0.29 - -0.19	0.69				20 vs. 0	-0.04	-0.28 – 0.2	0.74

	Intercept			Treatment				Post vs Pre			Interaction between treatment and Post vs Pre			
	Estimate	CI 95%	p		Estimate	CI 95%	p	Estimate	CI 95%	p		Estimate	CI 95%	p
Hb g/dL	11.46	11.02 – 11.89	<0.01	-20 vs. 0	-6.07	-6.49 – -5.64	<0.01	-0.02	-0.06 – 0.02	0.38	-20 vs. 0	0.04	-0.01 – -0.09	0.13
				-10 vs. 0	-2.96	-3.46 – -2.45	<0.01				-10 vs. 0	-0.06	-0.23 – 0.11	0.51
				10 vs. 0	3.13	2.93 – 3.32	<0.01				10 vs. 0	-0.01	-0.08 – 0.06	0.79
				20 vs. 0	6.19	5.92 – 6.45	<0.01				20 vs. 0	-0.02	-0.2 – 0.16	0.83
HCO_3^- (mmol/L)	28.4	27.16 – 29.63	<0.01	-20 vs. 0	2.52	1.47 – 3.57	<0.01	-5.24	-5.73 - -4.75	<0.01	-20 vs. 0	6.03	4.51 – 7.56	<0.01
				-10 vs. 0	1.89	0.91 – 2.88	<0.01				-10 vs. 0	2.87	2.43 – 3.31	<0.01
				10 vs. 0	0.57	0.01 – 1.13	0.04				10 vs. 0	-1.65	-2.27 – -1.04	<0.01
				20 vs. 0	0.81	0.17 – 1.46	0.01				20 vs. 0	-3.11	-3.79 – -2.43	<0.01
Plasma TCO_2	29.94	28.71 – 31.17	<0.01	-20 vs. 0	2.53	1.47 – 3.58	<0.01	-6.3	-6.82 - -5.79	<0.01	-20 vs. 0	5.96	4.46 – 7.46	<0.01
				-10 vs. 0	1.87	0.88 – 2.85	<0.01				-10 vs. 0	2.86	2.45 – 3.27	<0.01
				10 vs. 0	0.55	0.00 – 1.09	0.04				10 vs. 0	-1.59	-2.22 – -0.97	<0.01
				20 vs. 0	0.81	0.19 – 1.43	0.01				20 vs. 0	-3.05	-3.75 – -2.35	<0.01
VCO2 mL/min	42.5	37.26 – 47.74	<0.01	-20 vs. 0	-11.47	-14.15 – -8.8	<0.01							
				-10 vs. 0	-5.17	-6.55 – -3.81	<0.01							
				10 vs. 0	2.43	1.94 – 2.92	<0.01							
				20 vs. 0	6.23	5.04 – 7.42	<0.01							

Table 2: Estimated GEE regression coefficients and relative 95% confidence interval based on membrane lung effect and treatments variables with their interactions.

At dilution step -20%, 6 measurements were outside the range of measurement of our blood gas analyzer and were lost due to pH values >8. Compared to the treatment delta 0, all the dilution treatments had an increment in pH values from pre to post of 0.15 for treatment Δ -20%, and of 0.07 for treatment Δ -10%. On the other hand, all concentration treatments caused a decrease in pH: -0.06 for Δ 10% and -1 for Δ 20%. Complete data are reported in table 2 and displayed graphically in figure 7.

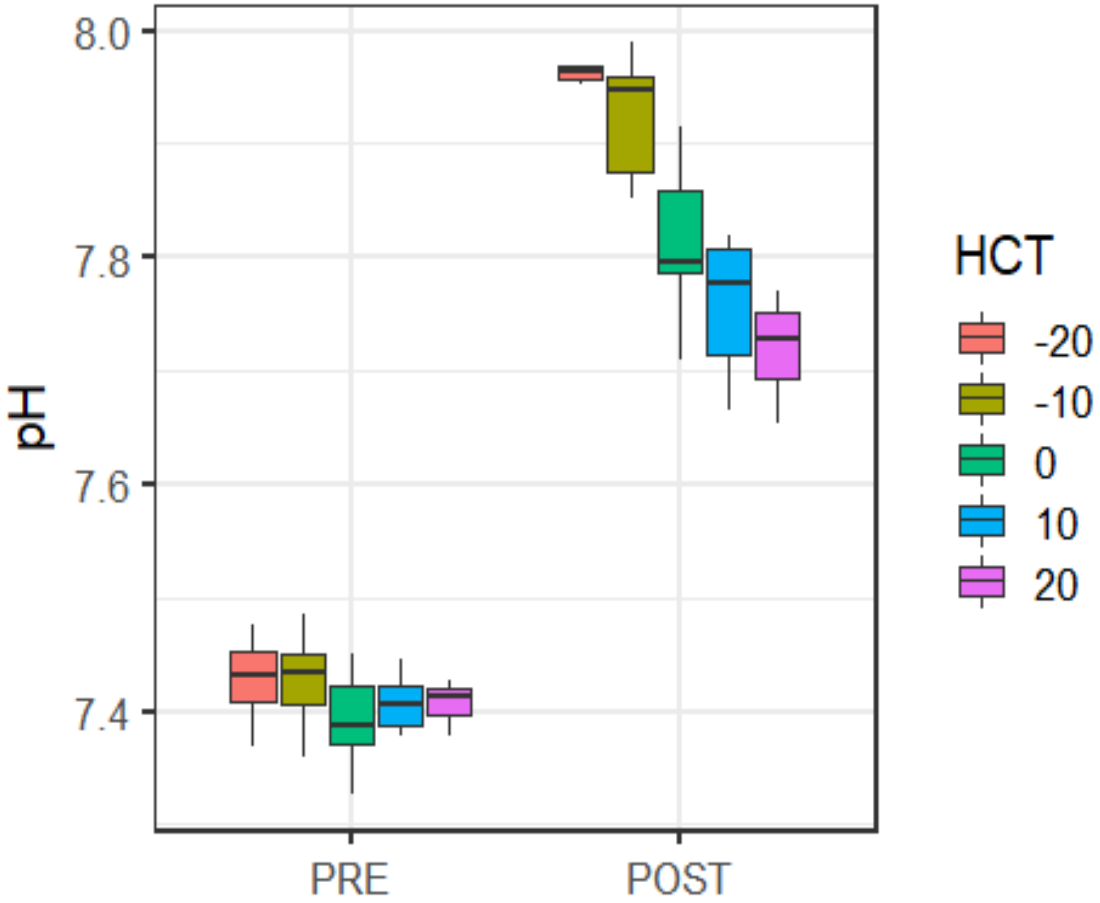

Figure 7: pH distribution at HCT variations according to PRE and POST values by using a rectangular box plot and whiskers; the bottom and top edges of the box indicate the inter-quartile range (IQR) between the first and third quartiles (the 25th and 75th percentiles). The line inside the box indicates the median value. Whiskers indicate the range of values outside of the intra-quartile range but at a distance lower than the upper and lower fences (±1.5 × IQR).

No differences were found in oxygenation, expressed as pO_2, when comparing baseline to the dilution treatments. On the other hand, the +20% Delta HCT treatment had an increase from pre to post of 64 mmHg when compared to baseline (figure 8, table 2).

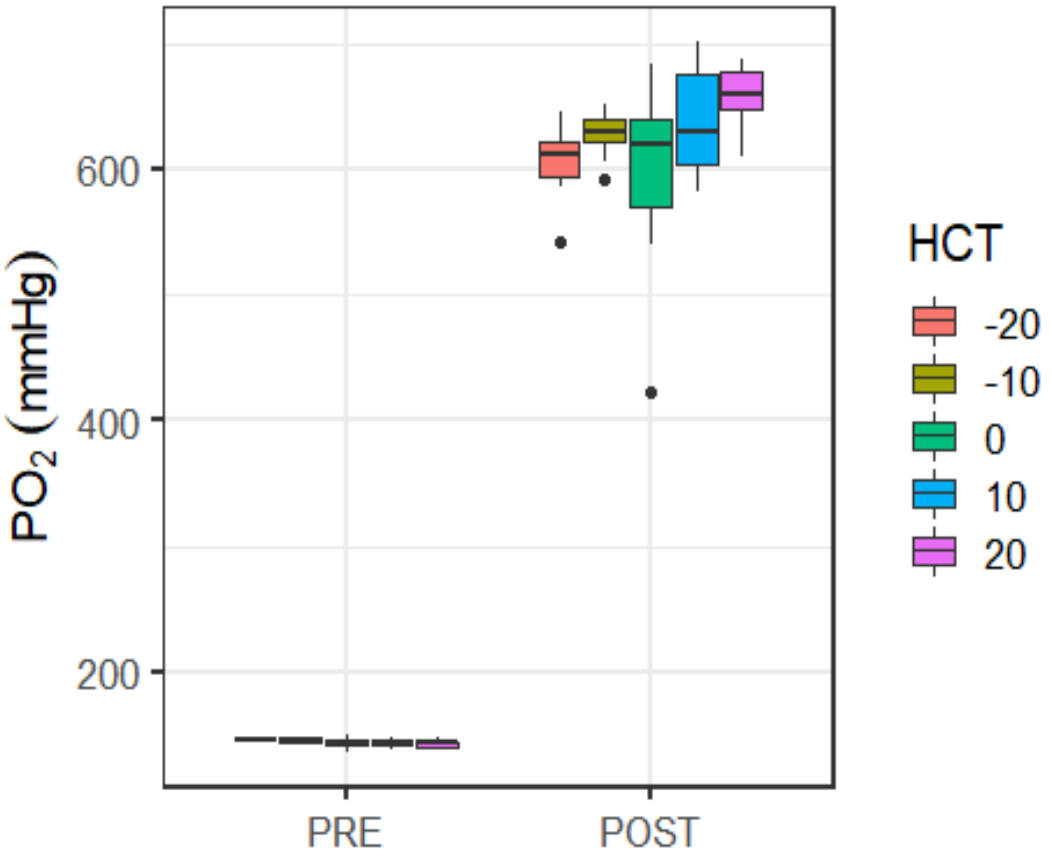

Figure 8: pO_2 distribution at HCT variations according to PRE and POST values by using a rectangular box plot and whiskers; the bottom and top edges of the box indicate the interquartile range (IQR) between the first and third quartiles (the 25th and 75th percentiles). The line inside the box indicates the median value. Whiskers indicate the range of values outside of the interquartile range but at a distance lower than the upper and lower fences (±1.5 × IQR). Dots indicate outliers.

In line with the effect of our setup, Haemoglobin (Hb) variations have been recorded in all the steps and compared to the treatment baseline (see Table 2 and Figure 9). Compared to baseline, all dilution treatments obtained a decrease in Hb values upstream the membrane lung, which was of -6.07 mg/dL for treatment Δ -20%, and of -2.96 mg/dL for treatment Δ -10%. On the other hand, an increment has been recorded for all concentration treatments: 3.13mg/dL for Δ +10%, and 6.19 mg/dL for Δ +20%.

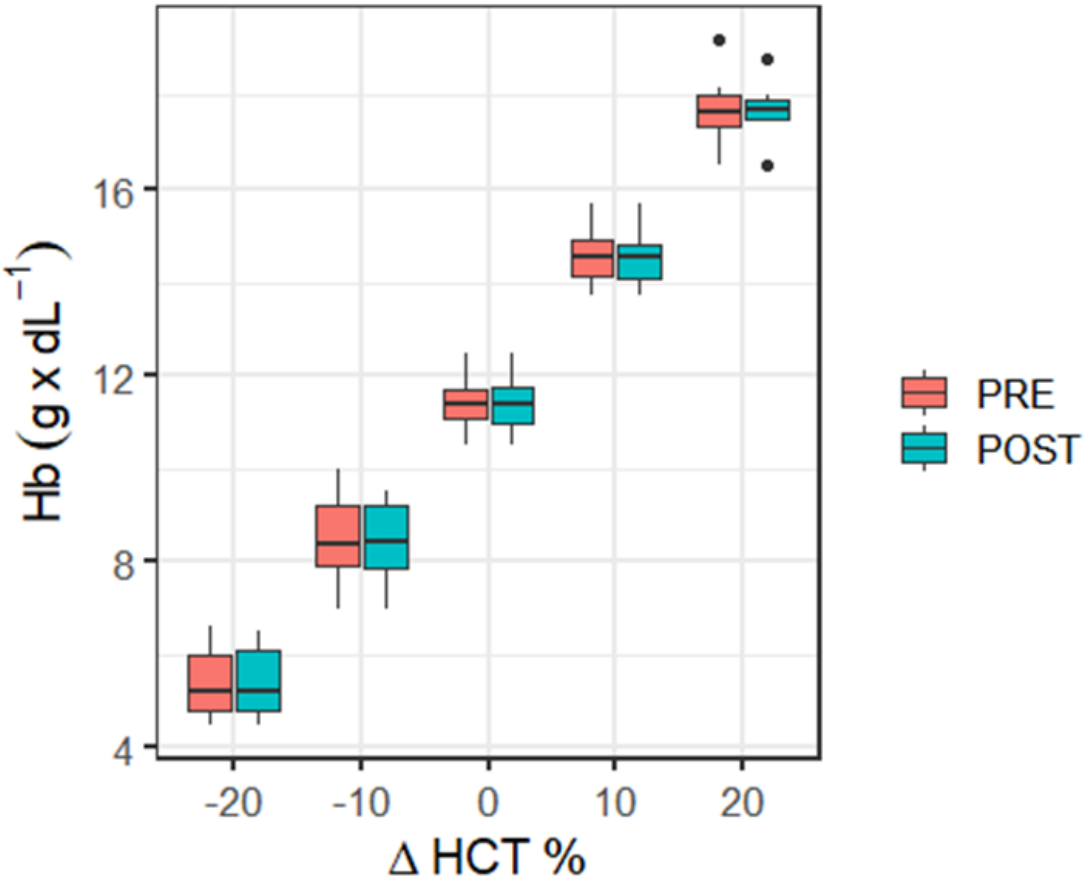

Figure 9: Haemoglobin (Hb) distribution , PRE and POST values, according to different HCT variations by using a rectangular box plot and whiskers; the bottom and top edges of the box indicate the interquartile range (IQR) between the first and third quartiles (the 25th and 75th percentiles). The line inside the box indicates the median value. Whiskers indicate the range of values outside of the interquartile range but at a distance lower than the upper and lower fences (±1.5 × IQR). Dots indicate outliers.

Bicarbonate ion concentration ([HCO_3^-]) was calculated from pH and pCO_2 modifying the Henderson-Hasselbalch equation[59]. The trend for bicarbonate ion concentrations is reported in figure 10. Compared to baseline, the dilution treatments had a decrease in bicarbonate concentration from pre to post of 6.03 mmol/L for treatment Δ -20%, and 2.87 mmol/L for treatment Δ -10%. On the other hand, an increment has been recorded for all concentration treatments: -1.65 mmol/L for Δ +10%, and -3.11 mmol/L for Δ +20%.

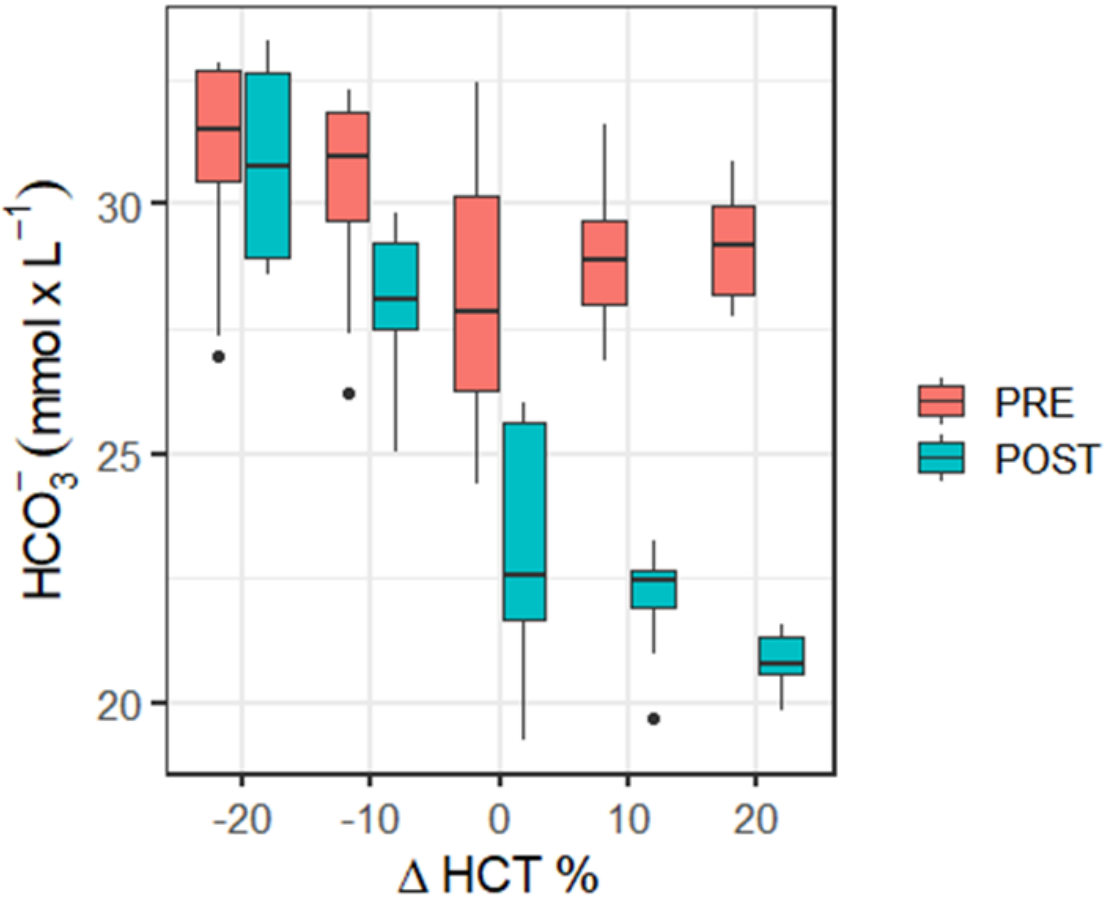

Figure 10: Bicarbonates ion concentrations distribution, PRE and POST values, according to different HCT variations by using a rectangular box plot and whiskers; the bottom and top edges of the box indicate the interquartile range (IQR) between the first and third quartiles (the 25th and 75th percentiles). The line inside the box indicates the median value. Whiskers indicate the range of values outside of the interquartile range but at a distance lower than the upper and lower fences (±1.5 × IQR). Dots indicate outliers.

Plasma carbon dioxide content PRE and POST membrane lung (expressed in mmol/L) was calculated according to the method published by Douglas et al.[84]. The trend of CO_2 content in plasma (TCO_2) is shown in figure 11 and the effect of haematocrit variations between pre and post membrane lung has been reported in table 2.

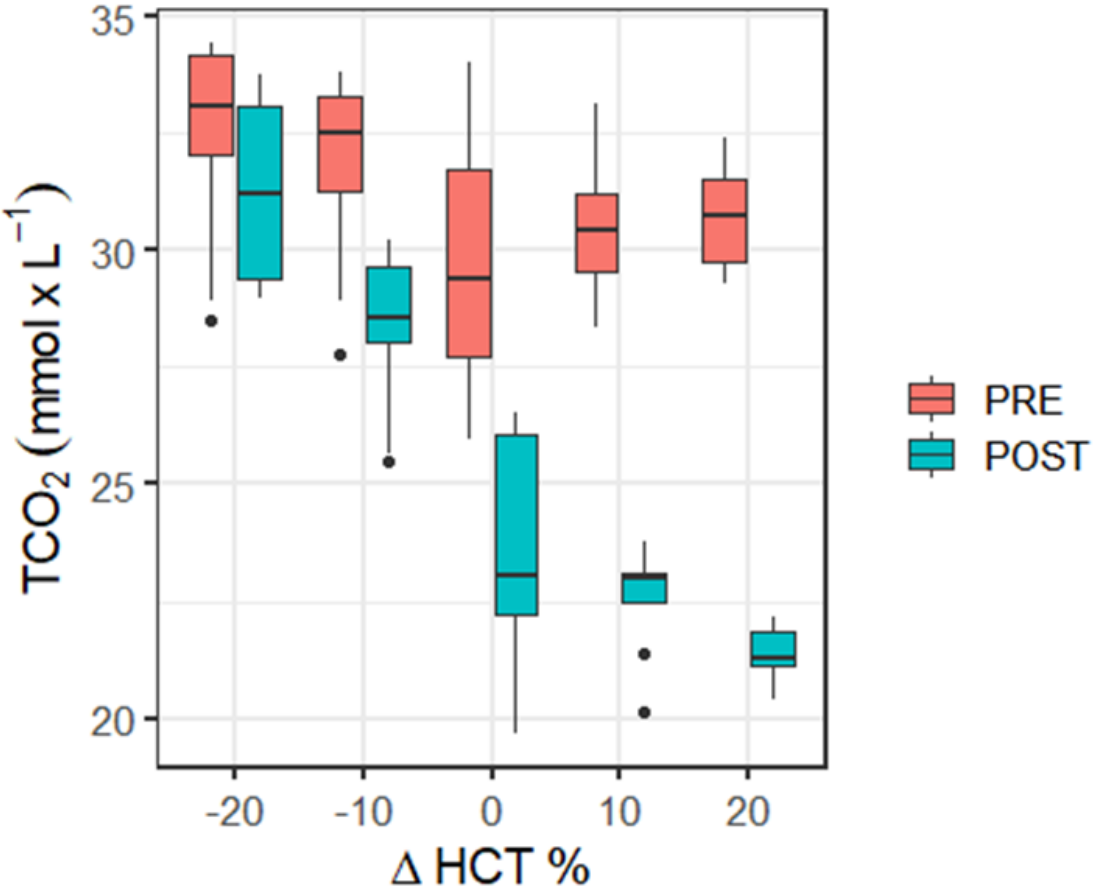

Figure 11: Plasma CO_2 content (TCO_2) distribution, PRE and POST values, according to different HCT variations by using a rectangular box plot and whiskers, the bottom and top edges of the box indicate the interquartile range (IQR) between the first and third quartiles (the 25th and 75th percentiles). The line inside the box indicates the median value. Whiskers indicate the range of values outside of the interquartile range but at a distance lower than the upper and lower fences (±1.5 × IQR). Dots indicate outliers.

The electrolytes chloride, sodium, potassium and calcium had the same trend reported in a previous in vitro experiment by our group (Vivona). POST chloride concentrations were higher than PRE values, while sodium concentrations were lower. Moreover, a simultaneous decrease in potassium and calcium POST concentrations was observed. The electrolytes trend is presented in figure 12 and their variations compared to the baseline are reported in table 2.

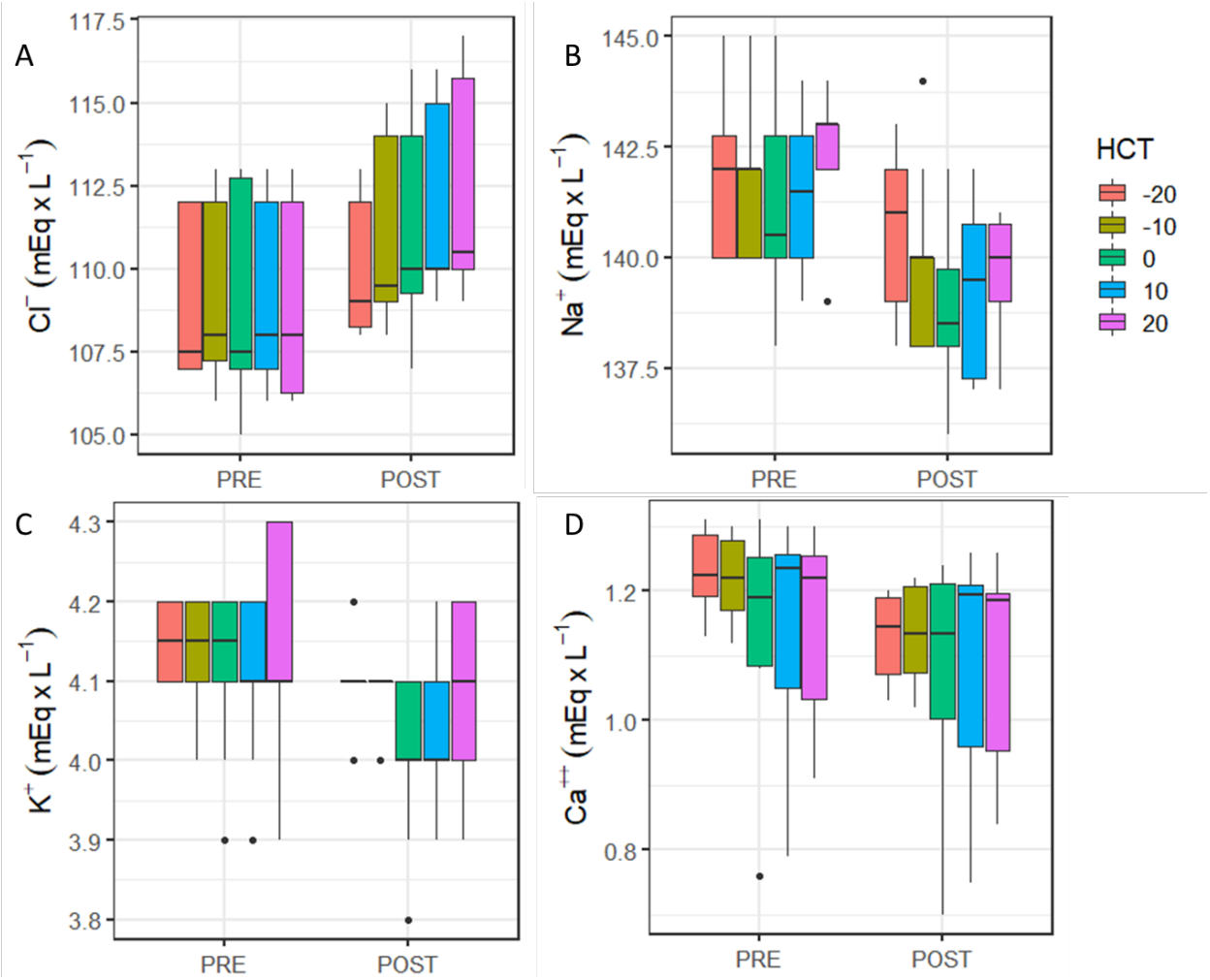

Figure 12: Electrolytes distribution (Cl^-, chloride, Panel A; Na^+, sodium, Panel B, K^+, potassium, Panel C; Ca^{++}, calcium, Panel D) at HCT variations according to PRE and POST values by using a rectangular box plot and whiskers; the bottom and top edges of the box indicate the interquartile range (IQR) between the first and third quartiles (the 25th and 75th percentiles). The line inside the box indicates the median value. Whiskers indicate the range of values outside of the interquartile range but at a distance lower than the upper and lower fences (±1.5 × IQR). Dots indicate outliers.

Lactate had no stable trend during the experiment. Only for treatment Δ+10% (table 2) differences Pre and Post membrane lung were found upon comparison with baseline.

Variable	Contrast interaction between treatment and Post vs. Pre	Estimate	p	Variable	Contrast interaction between treatment and Post vs. Pre	Estimate	p
pH	-20 vs. 0	0.151	<0.01	Hb g/dL	-20 vs. 0	0.04	0.12
	-10 vs. -20	-0.073	<0.01		-10 vs. -20	-0.1	0.22
	10 vs. -10	-0.143	<0.01		10 vs. -10	0.05	0.66
	20 vs. 10	-0.038	<0.01		20 vs. 10	-0.01	0.87
pCO2 mmHg	-20 vs. 0	-2.15	<0.01	HCO_3^- mmol/L	-20 vs. 0	6.04	<0.01
	-10 vs. -20	1.84	<0.01		-10 vs. -20	-3.17	<0.01
	10 vs. -10	2.22	0.01		10 vs. -10	-4.53	<0.01
	20 vs. 10	-0.03	0.96		20 vs. 10	-1.46	<0.01
pO2 mmHg	-20 vs. 0	7.8	0.59	Plasma TCO_2 mmol/L	-20 vs. 0	5.97	<0.01
	-10 vs. -20	21.3	0.07		-10 vs. -20	-3.11	<0.01
	10 vs. -10	11.6	0.29		10 vs. -10	-4.46	<0.01
	20 vs. 10	23.3	0.04		20 vs. 10	-1.46	<0.01
K^+ mEq/L	-20 vs. 0	0.06	<0.01	Cl^- mEq/L	-20 vs. 0	-1.2	<0.01
	-10 vs. -20	-0.01	0.55		-10 vs. -20	0.7	0.03
	10 vs. -10	0.00	1		10 vs. -10	1	<0.01
	20 vs. 10	-0.02	0.51		20 vs. 10	0.6	0.02
Na^+ mEq/L	-20 vs. 0	1.2	<0.01	Lac mEq/L	-20 vs. 0	-0.01	0.9
	-10 vs. -20	-0.7	<0.01		-10 vs. -20	0.05	0.47
	10 vs. -10	-0.4	0.06		10 vs. -10	0.03	<0.01
	20 vs. 10	-0.5	0.18		20 vs. 10	-0.11	0.37
Ca^{++} mEq/L	-20 vs. 0	-0.046	<0.01	VCO2 mL/min	-20 vs. -10	-6.3	<0.01
	-10 vs. -20	0.018	<0.01		-20 vs. 10	-13.91	<0.01
	10 vs. -10	0.030	<0.01		-20 vs. 20	-17.71	<0.01
	20 vs. 10	-0.005	0.28		-10 vs. 10	-7.61	<0.01
					-10 vs. 20	-11.41	<0.01
					10 vs. 20	-3.8	<0.01

Table 3: Interaction contrast comparing the effects between treatments. Post-hoc interaction constrast performed using marginals means with Tukey adjustment.

Discussion

The factors affecting the $\dot{V}CO_2$ of a membrane lung are sweep gas and blood flow rates, and inlet pCO_2 of the blood[86,87]. In our in vitro study, we kept inlet pCO_2 stable, blood flow at membrane lung at 250 mL/min, and sweep gas flow at 5 L/min according with membrane lung characteristics. As far as we know, the setup we developed has been the first evaluation of a continuous extracorporeal in vitro design able to increase HCT and to evaluate the effect on $\dot{V}CO_2$. We showed that variations in HCT corresponded to variations in $\dot{V}CO_2$.Specifically, in our study, an increase of HCT by 20% determined a rise in $\dot{V}CO_2$ of 15% compared to treatment baseline. Considering HCT as a continuous variable and maintaining inlet pCO_2 stable, it was possible to calculate the linear distribution and the slope related to $\dot{V}CO_2$. Our results are in line with those obtained by May et al., who also demonstrated that HCT affects $\dot{V}CO_2$ at membrane lung[72]. To avoid any bias, a sensibility test using normalized pCO_2 was used to verify our data. In our setup, we also aimed at reducing the effect of sweep gas flow rate on. CO_2 removal. At a low flow rate of sweep gas, CO_2begins to accumulate within the sweep gas itself as it passes through the membrane lung. This reduces the overall CO_2removal ability of the device, as the gradient driving $CO_2$from the blood to the sweep gas diminishes[72]. Therefore, in our arrangement, we used the maximum sweep gas flow rate tolerated by our membrane lung (Sorin Lilliput2 ECMO, Livanova, United Kingdom), which was 5 L/min[88]. Our dilution technique was achieved with a hemodiafilter, and the aim of our setup was to have a closed loop circuit where only the blood components of the same subject ran. We chose this more physiological arrangement in order to avoid the use of other fluids. In fact, previous evidences showed that different hemodilution fluids (saline, plasma, PBS) had no effect on $\dot{V}CO_2$[72,89]. Arazawa et al. demonstrated that the buffering capacity of plasma proteins is not significant enough to accommodate for the reduction, or absence, of HCT within an artificial lung. This is because of the CO_2 carrying capacity of plasma being substantially due to the chloride shift, which requires the presence of the erythrocytes to occur[89]. Starting from this knowledge, we created a device that successfully increases the $\dot{V}CO_2$ of the membrane lung just by rising the value of the HCT. As a proof of concept, we were also able to show that lower HCTs determine lower $\dot{V}CO_2$ values. This study has several limitations. To guarantee a constant blood flow of 250 mL/min at membrane lung, we had to vary the speeds of several peristaltic pumps, which is not easily reproducible. Furthermore, flow was not continuously measured, but only verified at the beginning and at the end of each experiment. We therefore could not control for shifts in the pumps mechanics nor for deterioration of the tubing. Moreover, the clinical application of our design is not straightforward. To achieve target haematocrit, we needed the flow rate of whole blood to reach 400 mL/min, but usual $ECCO_2R$ devices may run at even higher blood flows, still obtaining appropriate decarboxylation. This makes our set up a proof of concept more than a reliable device immediately transferable to the clinics.

Conclusion

In the past three years of work, we conducted a series of experiments on extracorporeal life support to overcome some of the limitations of the technique currently available.

Firstly, we analysed a novel technique for regional anticoagulation. We were able to demonstrate that the interposition of ion exchange resins in an extracorporeal circuit allowed for an effective, simple and free from complications regional anticoagulation.

Secondly, we devised a method to quantify recirculation flow (RF) during veno-venous ECMO. Testing different blood flows and cardiac outputs, our thermodilution technique could detect recirculation and quantify the RF with accuracy and precision.

Thirdly, we experimented with the possibility of liquid ventilation. In this proof of concept study, we showed that continuous infusion of alkaline, highly concentrated sodium hydroxide solutions into the gas side of conventional oxygenators is feasible and obtains CO_2 extraction.

Lastly, we studied the effect of haematocrit (HCT) variations on the rate of CO_2 removal in low-flow $ECCO_2R$. We showed that an increase of HCT determines a rise in $\dot{V}CO_2$ compared to treatment baseline.

Overall, starting from physiology, we tackled some open issues of extracorporeal life support. Our results are promising and expand the fund of knowledge on extracorporeal techniques. The next steps will require further studies in order to move our findings from the bench to the bedside, improving the currently available devices for organ support in intensive care units.

Bibliography

1. Hill, J. D. *et al.* Prolonged extracorporeal oxygenation for acute post-traumatic respiratory failure (shock-lung syndrome). Use of the Bramson membrane lung. *N. Engl. J. Med.* **286**, 629–634 (1972).
2. Noah, M. A. *et al.* Referral to an Extracorporeal Membrane Oxygenation Center and Mortality Among Patients With Severe 2009 Influenza A(H1N1). *JAMA* **306**, 1659–1668 (2011).
3. Peek, G. J. *et al.* Efficacy and economic assessment of conventional ventilatory support versus extracorporeal membrane oxygenation for severe adult respiratory failure (CESAR): a multicentre randomised controlled trial. *The Lancet* **374**, 1351–1363 (2009).
4. Combes, A. *et al.* Extracorporeal Membrane Oxygenation for Severe Acute Respiratory Distress Syndrome. *N. Engl. J. Med.* (2018) doi:10.1056/NEJMoa1800385.
5. Biscotti, M., Sonett, J. & Bacchetta, M. ECMO as bridge to lung transplant. *Thorac. Surg. Clin.* **25**, 17–25 (2015).
6. Gaffney, A. M., Wildhirt, S. M., Griffin, M. J., Annich, G. M. & Radomski, M. W. Extracorporeal life support. *BMJ* **341**, c5317–c5317 (2010).
7. Conrad, S. A. *et al.* The Extracorporeal Life Support Organization Maastricht Treaty for Nomenclature in Extracorporeal Life Support. A Position Paper of the Extracorporeal Life Support Organization. *Am. J. Respir. Crit. Care Med.* **198**, 447–451 (2018).
8. Lectures in Respiratory Physiology by Dr. John B. West, M.D., Ph.D. - University of California San Diego. https://meded.ucsd.edu/ifp/jwest/resp_phys/acknowledgements_credits.html.
9. Riley, R. L. & Cournand, A. Ideal alveolar air and the analysis of ventilation-perfusion relationships in the lungs. *J. Appl. Physiol.* **1**, 825–847 (1949).
10. Scaravilli, V., Zanella, A., Sangalli, F. & Patroniti, N. Basic Aspects of Physiology During ECMO Support. in *ECMO-Extracorporeal Life Support in Adults* (eds. Sangalli, F., Patroniti, N. & Pesenti, A.) 19–36 (Springer Milan, 2014). doi:10.1007/978-88-470-5427-1_3.

11. Abrams, D., Brodie, D. & Brechot, N. Identification and management of recirculation in venovenous ECMO. 7 (2015).
12. Zanella, A. *et al.* A mathematical model of oxygenation during venovenous extracorporeal membrane oxygenation support. *J. Crit. Care* **36**, 178–186 (2016).
13. Cipulli, F. *et al.* Quantification of Recirculation During Veno-Venous Extracorporeal Membrane Oxygenation: In Vitro Evaluation of a Thermodilution Technique. *ASAIO J.* **Publish Ahead of Print**, (2021).
14. Cove, M. E. & Federspiel, W. J. Veno-venous extracorporeal CO2 removal for the treatment of severe respiratory acidosis. *Crit. Care Lond. Engl.* **19**, 176 (2015).
15. Park, M. *et al.* Determinants of oxygen and carbon dioxide transfer during extracorporeal membrane oxygenation in an experimental model of multiple organ dysfunction syndrome. *PloS One* **8**, e54954 (2013).
16. Gattinoni, L., Kolobow, T., Damia, G., Agostoni, A. & Pesenti, A. Extracorporeal carbon dioxide removal (ECCO2R): a new form of respiratory assistance. *Int. J. Artif. Organs* **2**, 183–185 (1979).
17. Gattinoni, L. *et al.* Clinical application of low frequency positive pressure ventilation with extracorporeal CO2 removal (LFPPV-ECCO2R) in treatment of adult respiratory distress syndrome (ARDS). *Int. J. Artif. Organs* **2**, 282–283 (1979).
18. Mulder: ECMO and anticoagulation: a comprehensive review - Google Scholar. https://scholar.google.com/scholar_lookup?journal=Neth+J+Crit+Care&title=ECMO+and+anticoagulation:+A+comprehensive+review.&author=MMG+Mulder&author=I+Fawzy&author=MD+Lance&volume=26&publication_year=2018&pages=6-13&.
19. Esmon, C. T. The impact of the inflammatory response on coagulation. *Thromb. Res.* **114**, 321–327 (2004).
20. Mann, K. G., Butenas, S. & Brummel, K. The dynamics of thrombin formation. *Arterioscler. Thromb. Vasc. Biol.* **23**, 17–25 (2003).

21. Marasco, S. F., Lukas, G., McDonald, M., McMillan, J. & Ihle, B. Review of ECMO (extra corporeal membrane oxygenation) support in critically ill adult patients. *Heart Lung Circ.* **17 Suppl 4**, S41-47 (2008).
22. Bembea, M. M. *et al.* Variability in anticoagulation management of patients on extracorporeal membrane oxygenation: an international survey. *Pediatr. Crit. Care Med. J. Soc. Crit. Care Med. World Fed. Pediatr. Intensive Crit. Care Soc.* **14**, e77-84 (2013).
23. Malfertheiner, M. V. *et al.* Hemostatic Changes During Extracorporeal Membrane Oxygenation: A Prospective Randomized Clinical Trial Comparing Three Different Extracorporeal Membrane Oxygenation Systems. *Crit. Care Med.* **44**, 747–754 (2016).
24. Panigada, M. *et al.* Hemostasis changes during veno-venous extracorporeal membrane oxygenation for respiratory support in adults. *Minerva Anestesiol.* **82**, 170–179 (2016).
25. Thelin, S. *et al.* Heparin-coated cardiopulmonary bypass circuits reduce blood cell trauma. Experiments in the pig. *Eur. J. Cardio-Thorac. Surg. Off. J. Eur. Assoc. Cardio-Thorac. Surg.* **5**, 486–491 (1991).
26. Borowiec, J. *et al.* Heparin-coated circuits reduce activation of granulocytes during cardiopulmonary bypass: A clinical study. *J. Thorac. Cardiovasc. Surg.* **104**, 642–647 (1992).
27. Passero, B. A. *et al.* Citrate versus heparin for apheresis catheter locks: An efficacy analysis. *J. Clin. Apheresis* **30**, 22–27 (2015).
28. Buchta, C., Macher, M., Bieglmayer, C., Höcker, P. & Dettke, M. Reduction of adverse citrate reactions during autologous large-volume PBPC apheresis by continuous infusion of calcium-gluconate. *Transfusion (Paris)* **43**, 1615–1621 (2003).
29. Kato, C. *et al.* Anticoagulation strategies in extracorporeal circulatory devices in adult populations. *Eur. J. Haematol.* **106**, 19–31 (2021).
30. McNamee, J. J. *et al.* Effect of Lower Tidal Volume Ventilation Facilitated by Extracorporeal Carbon Dioxide Removal vs Standard Care Ventilation on 90-Day Mortality in Patients With

Acute Hypoxemic Respiratory Failure: The REST Randomized Clinical Trial. *JAMA* **326**, 1013–1023 (2021).

31. Wu, M.-Y. *et al.* Regional citrate versus heparin anticoagulation for continuous renal replacement therapy: a meta-analysis of randomized controlled trials. *Am. J. Kidney Dis. Off. J. Natl. Kidney Found.* **59**, 810–818 (2012).
32. James, M. F. M. & Roche, A. M. Dose-response relationship between plasma ionized calcium concentration and thrombelastography. *J. Cardiothorac. Vasc. Anesth.* **18**, 581–586 (2004).
33. Varga-Szabo, D., Braun, A. & Nieswandt, B. Calcium signaling in platelets. *J. Thromb. Haemost. JTH* **7**, 1057–1066 (2009).
34. Scaravilli, V. *et al.* Enhanced Extracorporeal CO2 Removal by Regional Blood Acidification: Effect of Infusion of Three Metabolizable Acids. *ASAIO J.* **61**, 533–539 (2015).
35. Oudemans-van Straaten, H. M. & Ostermann, M. Bench-to-bedside review: Citrate for continuous renal replacement therapy, from science to practice. *Crit. Care* **16**, 249 (2012).
36. Zanella, A. *et al.* Ion-Exchange Resin Anticoagulation (I-ERA): A Novel Extracorporeal Technique for Regional Anticoagulation. *SHOCK* **46**, 304–311 (2016).
37. Schneider, A. G., Journois, D. & Rimmelé, T. Complications of regional citrate anticoagulation: accumulation or overload? *Crit. Care Lond. Engl.* **21**, 281 (2017).
38. Strobl, K., Harm, S., Weber, V. & Hartmann, J. The Role of Ionized Calcium and Magnesium in Regional Citrate Anticoagulation and its Impact on Inflammatory Parameters. *Int. J. Artif. Organs* **40**, 15–21 (2017).
39. Forbes, C. D. & Prentice, C. R. Thrombus formation and artificial surfaces. *Br. Med. Bull.* **34**, 201–207 (1978).
40. Heilmann, C. *et al.* Acquired von Willebrand syndrome in patients with extracorporeal life support (ECLS). *Intensive Care Med.* **38**, 62–68 (2012).
41. Kindgen-Milles, D., Brandenburger, T. & Dimski, T. Regional citrate anticoagulation for continuous renal replacement therapy. *Curr. Opin. Crit. Care* **24**, 450–454 (2018).

42. Monchi, M. *et al.* Citrate vs. heparin for anticoagulation in continuous venovenous hemofiltration: a prospective randomized study. *Intensive Care Med.* **30**, 260–265 (2004).
43. Mariano, F. & Triolo, G. [Anticoagulation of extracorporeal circuit in critically ill patients]. *G. Ital. Nefrol. Organo Uff. Della Soc. Ital. Nefrol.* **24**, 34–42 (2007).
44. Kramer, L. *et al.* Citrate pharmacokinetics and metabolism in cirrhotic and noncirrhotic critically ill patients. *Crit. Care Med.* **31**, 2450–2455 (2003).
45. Davenport, A. & Tolwani, A. Citrate anticoagulation for continuous renal replacement therapy (CRRT) in patients with acute kidney injury admitted to the intensive care unit. *NDT Plus* **2**, 439–447 (2009).
46. Lewandrowski, E. L., Van Cott, E. M., Gregory, K., Jang, I.-K. & Lewandrowski, K. B. Clinical evaluation of the i-STAT kaolin activated clotting time (ACT) test in different clinical settings in a large academic urban medical center: comparison with the Medtronic ACT Plus. *Am. J. Clin. Pathol.* **135**, 741–748 (2011).
47. Patel, A. R., Patel, A. R., Singh, S., Singh, S. & Munn, N. J. Venovenous Extracorporeal Membrane Oxygenation Therapy in Adults. *Cureus* (2019) doi:10.7759/cureus.5365.
48. Palmér, O., Palmér, K., Hultman, J. & Broman, M. Cannula Design and Recirculation During Venovenous Extracorporeal Membrane Oxygenation: *ASAIO J.* **62**, 737–742 (2016).
49. Xie, A., Yan, T. D. & Forrest, P. Recirculation in venovenous extracorporeal membrane oxygenation. *J. Crit. Care* **36**, 107–110 (2016).
50. Sreenan, C., Osiovich, H., Cheung, P.-Y. & Lemke, R. P. Quantification of recirculation by thermodilution during venovenous extracorporeal membrane oxygenation. *J. Pediatr. Surg.* **35**, 1411–1414 (2000).
51. Bland, J. M. & Altman, D. G. Calculating correlation coefficients with repeated observations: Part 2--Correlation between subjects. *BMJ* **310**, 633 (1995).

52. Stetz, C. W., Miller, R. G., Kelly, G. E. & Raffin, T. A. Reliability of the thermodilution method in the determination of cardiac output in clinical practice. *Am. Rev. Respir. Dis.* **126**, 1001–1004 (1982).

53. Bland, J. M. & Altman, D. G. Agreement between methods of measurement with multiple observations per individual. *J. Biopharm. Stat.* **17**, 571–582 (2007).

54. Zou, G. Y. Confidence interval estimation for the Bland-Altman limits of agreement with multiple observations per individual. *Stat. Methods Med. Res.* **22**, 630–642 (2013).

55. Vivona, L. *et al.* Alkaline Liquid Ventilation of the Membrane Lung for Extracorporeal Carbon Dioxide Removal (ECCO2R): In Vitro Study. *Membranes* **11**, 464 (2021).

56. Karagiannidis, C. *et al.* Impact of membrane lung surface area and blood flow on extracorporeal CO2 removal during severe respiratory acidosis. *Intensive Care Med. Exp.* **5**, 34 (2017).

57. Morelli, A., Del Sorbo, L., Pesenti, A., Ranieri, V. M. & Fan, E. Extracorporeal carbon dioxide removal (ECCO2R) in patients with acute respiratory failure. *Intensive Care Med.* **43**, 519–530 (2017).

58. Austin, W. H., Lacombe, E., Rand, P. W. & Chatterjee, M. Solubility of carbon dioxide in serum from 15 to 38 C. *J. Appl. Physiol.* **18**, 301–304 (1963).

59. Constable, P. D. Total weak acid concentration and effective dissociation constant of nonvolatile buffers in human plasma. *J. Appl. Physiol.* **91**, 1364–1371 (2001).

60. Harned, H. S. & Bonner, F. T. The First Ionization of Carbonic Acid in Aqueous Solutions of Sodium Chloride. *J. Am. Chem. Soc.* **67**, 1026–1031 (1945).

61. Putnam, R. W. & Roos, A. Which value for the first dissociation constant of carbonic acid should be used in biological work? *Am. J. Physiol.-Cell Physiol.* **260**, C1113–C1116 (1991).

62. Douglas, A. R., Jones, N. L. & Reed, J. W. Calculation of whole blood CO2 content. *J. Appl. Physiol.* **65**, 473–477 (1988).

63. Barrett, N. A., Hart, N. & Camporota, L. In vivo carbon dioxide clearance of a low-flow extracorporeal carbon dioxide removal circuit in patients with acute exacerbations of chronic obstructive pulmonary disease. *Perfusion* **35**, 436–441 (2020).
64. Combes, A. *et al.* Feasibility and safety of extracorporeal CO2 removal to enhance protective ventilation in acute respiratory distress syndrome: the SUPERNOVA study. *Intensive Care Med.* **45**, 592–600 (2019).
65. Combes, A. *et al.* Efficacy and safety of lower versus higher CO2 extraction devices to allow ultraprotective ventilation: secondary analysis of the SUPERNOVA study. *Thorax* **74**, 1179–1181 (2019).
66. Goligher, E. C. *et al.* Determinants of the effect of extracorporeal carbon dioxide removal in the SUPERNOVA trial: implications for trial design. *Intensive Care Med.* **45**, 1219–1230 (2019).
67. Mauri, T., Langer, T., Zanella, A., Grasselli, G. & Pesenti, A. Extremely high transpulmonary pressure in a spontaneously breathing patient with early severe ARDS on ECMO. *Intensive Care Med.* **42**, 2101–2103 (2016).
68. Augy, J. L. *et al.* A 2-year multicenter, observational, prospective, cohort study on extracorporeal CO2 removal in a large metropolis area. *J. Intensive Care* **7**, 45 (2019).
69. Sharma, A. S., Weerwind, P. W., Bekers, O., Wouters, E. M. & Maessen, J. G. Carbon dioxide dialysis in a swine model utilizing systemic and regional anticoagulation. *Intensive Care Med. Exp.* **4**, 2 (2016).
70. Morimont, P. *et al.* Extracorporeal CO2 removal and regional citrate anticoagulation in an experimental model of hypercapnic acidosis. *Artif. Organs* **43**, 719–727 (2019).
71. Hospach, I. *et al.* In vitro characterization of PrismaLung+: a novel ECCO2R device. *Intensive Care Med. Exp.* **8**, 14 (2020).
72. May, A. G., Omecinski, K. S., Frankowski, B. J. & Federspiel, W. J. Effect of Hematocrit on the CO2 Removal Rate of Artificial Lungs. *ASAIO J. Am. Soc. Artif. Intern. Organs 1992* **66**, 1161–1165 (2020).

73. Bein, T. *et al.* Lower tidal volume strategy (≈3 ml/kg) combined with extracorporeal CO2 removal versus 'conventional' protective ventilation (6 ml/kg) in severe ARDS: the prospective randomized Xtravent-study. *Intensive Care Med.* **39**, 847–856 (2013).
74. Zimmermann, M. *et al.* Pumpless extracorporeal interventional lung assist in patients with acute respiratory distress syndrome: a prospective pilot study. *Crit. Care Lond. Engl.* **13**, R10 (2009).
75. Lund, L. W. & Federspiel, W. J. Removing extra CO2 in COPD patients. *Curr. Respir. Care Rep.* **2**, 131–138 (2013).
76. Bonin, F., Sommerwerck, U., Lund, L. W. & Teschler, H. Avoidance of intubation during acute exacerbation of chronic obstructive pulmonary disease for a lung transplant candidate using extracorporeal carbon dioxide removal with the Hemolung. *J. Thorac. Cardiovasc. Surg.* **145**, e43-44 (2013).
77. Abrams, D., Roncon-Albuquerque, R. & Brodie, D. What's new in extracorporeal carbon dioxide removal for COPD? *Intensive Care Med.* **41**, 906–908 (2015).
78. Fjw, R., Fenn, W. O. & Rahn, H. *Transport of oxygen and carbon dioxide*. (American Physiological Society Washington DC, 1964).
79. Wieth, J. O. & Brahm, J. Kinetics of bicarbonate exchange in human red cells—physiological implications. *Membr. Transp. Erythrocytes Munksgaard Cph.* 467–482 (1980).
80. Itada, N. & Forster, R. E. Carbonic anhydrase activity in intact red blood cells measured with 18O exchange. *J. Biol. Chem.* **252**, 3881–3890 (1977).
81. Bidani, A. & Crandall, E. D. Analysis of the effects of hematocrit on pulmonary CO2 transfer. *J. Appl. Physiol.* **53**, 413–418 (1982).
82. Wearden, P. D. *et al.* Respiratory dialysis with an active-mixing extracorporeal carbon dioxide removal system in a chronic sheep study. *Intensive Care Med.* **38**, 1705–1711 (2012).
83. Golob, J. F. *et al.* Acute In Vivo Testing of an Intravascular Respiratory Support Catheter. *ASAIO J.* **47**, 432–437 (2001).

84. Fitzmaurice, G. M., Laird, N. M. & Ware, J. H. *Applied longitudinal analysis*. vol. 998 (John Wiley & Sons, 2012).

85. Hin, L.-Y. & Wang, Y.-G. Working-correlation-structure identification in generalized estimating equations. *Stat. Med.* **28**, 642–658 (2009).

86. Federspiel, W. J. & Hattler, B. G. Sweep gas flowrate and CO2 exchange in artificial lungs. *Artif. Organs* **20**, 1050–1052 (1996).

87. May, A. G., Jeffries, R. G., Frankowski, B. J., Burgreen, G. W. & Federspiel, W. J. Bench Validation of a Compact Low-Flow CO2 Removal Device. *Intensive Care Med. Exp.* **6**, 34 (2018).

88. Pediatric devices - ScienceDirect. https://www.sciencedirect.com/science/article/pii/B9780128104910000096.

89. Arazawa, D. T., Kimmel, J. D., Finn, M. C. & Federspiel, W. J. Acidic sweep gas with carbonic anhydrase coated hollow fiber membranes synergistically accelerates CO 2 removal from blood. *Acta Biomater.* **25**, 143–149 (2015).